MASTER'S THESIS

Microsurgical anatomy of the parapharyngeal space.

Waidyasekara, Pasan

Award date:
2019

Microsurgical Anatomy of the Parapharyngeal Space

Pasan Sachintha Waidyasekara

Submitted in total fulfilment of the requirements of the degree of

Master of Science by Research

April 2019

Faculty of Health Sciences and Medicine

Supervisors

Professor Peter Jones

Assistant Professor Athanasios Raikos

Associate Professor Allan Stirling

Dr Samuel Dowthwaite

This research was supported by an Australian Government Research Training Program Scholarship.

Abstract

Introduction: The parapharyngeal space is an anatomically defined region, part of the seven compartments of the deep head and neck. The space is frequently entered when resecting neoplasms of the tongue base, tonsil, and parapharyngeal space. The transoral surgical approaches to gain access to these regions rose in popularity recently due to advancements in transoral robotic surgery. We aim to describe the topographical anatomy of the parapharyngeal space to facilitate safe operating in this area.

Methods: Fifteen formalin-fixed cadaveric head and neck specimens were dissected on both sides with a surgical microscope. Two specimens were sectioned sagitally and thirteen were sectioned coronally. Photographs were taken at each step of the dissection while gainig acess to and defining the neurovasculature of the parapharyngeal space. Mean measurements were made from select anatomical landmarks to neurovasculature of the parapharyngeal space.

Results: The parapharyngeal part of the lingual artery was a mean distance of 21mm from the base of tongue midline. The lingual artery was 3.5mm superior to the greater cornu of hyoid bone. The hypoglossal nerve was a mean distance of 26.3mm from the epiglottic vallecula. The apex of the tonsillar fossa was on average 16.1mm far from the internal carotid artery. The midpoint of the stylopharyngeus muscle was 2.1mm posterolaterally to the internal carotid artery. The glossopharyngeal nerve was a mean distance of 5mm from the styloid process. The styloglossus muscle midpoint was 14.6mm superior to the facial artery. The distal attachment of the stylopharyngeus and styloglossus muscle is a highly vascular area. The facial artery was 9.5mm from the oropharyngeal mucosa. The lingual nerve was 3mm from the lateral surface of the pharyngeal constrictor muscle at its parapharyngeal portion before entering the mouth.

Conclusion: Topographic observations and mean proximity distances obtained in this study may have the potential to add to the inside-to-outside anatomy of the parapharyngeal space for surgeons accessing this space via the transoral route and transoral robotic surgery. The area parallel to the base of tongue where the stylopharyngeus attach to the pharynx, and styloglossus muscle's distal attachment site at the base of tongue represents a highly vascular area supplied by branches directly from the external carotid artery, superior thyroid artery, lingual artery, and the facial artery.

Keywords
Anatomy; Parapharyngeal Space; Transoral Robotic Surgery

Declaration of originality

This thesis is submitted to Bond University in fulfilment of the requirements of the degree of Masters by Research. This thesis represents my own work towards this research degree at this university, except where due acknowledgement is made.

_____ Pasan Waidyasekara 16 April 2019

Acknowledgement

I thank my wife, Jessica, for her loving kindness. To my parents and sister for the care and support they continue to provide. To my research supervisors and all my teachers for providing the spark of inspiration and guidance.

Personal Statement

During the clinical phase of completing my Bachelor of Medicine, Bachelor of Surgery at Bond University, I developed an interest in the field of Otolaryngology - Head and Neck Surgery. It was during this time I was exposed to the utility of Transoral Robotic Surgery (TORS) for the treatment of neoplasms of the oropharynx. The combination of this new surgical technology with the development of unique standardised surgical procedures has led to a revisiting of the anatomy of the parapharyngeal space.

This research project was supervised by Professor Peter Jones, Assistant Professor Athanasios Raikos, and Associate Professor Allan Stirling from the Medical Program of Bond University and a clinical supervisor from the Gold Coast University Hospital - Dr Samuel Dowthwaite.

The aim of this research is to present original morphometric and descriptive anatomy linking the anatomy of the parapharyngeal space to oropharyngeal mucosal landmarks. I aim also to explore any anatomical variations in the area which might have significant impact in the outcomes of TORS. I hope the new information will be useful for safe surgical navigation during resection of neoplasms of the tonsil, tongue base and parapharyngeal space.

A literature review related to the anatomy relevant to TORS was performed. Dissections of mid-sagitally and coronally sectioned cadavers have been completed. Key neurovascular structural relationships to useful anatomical landmarks for TORS have been collected in the form of distance measurements and photographic observations.

By completion of this project I aim to provide new information relating distances and patterns of morphology of the parapharyngeal space structures in relation to oropharyngeal mucosal landmarks. I hope this will further our understanding of anatomy in this region and facilitate the performance of safe TORS operations.

Table of Contents

List of Tables

List of Figures and Graphs

Figures

Figure 15: **A.** Posterior view of the left parapharyngeal space. **B.** The posterior view of the right parapharyngeal space.

Figure 16: The Lingual artery and facial artery has a common origin from the external carotid artery as the linguofacial trunk. The internal carotid artery is retracted laterally to reveal the branches of the external carotid artery.

Figure 17: **A.** The relatively straight path of the internal carotid artery. **B.** An aberrant internal carotid artery

Figure 18: A right parapharyngeal space with the pharyngeal constrictor muscle partially removed posteriorly

Figure 19: A small unnamed arterial branch is given off the external carotid artery before the lingual artery branch off point

Figure 20: A right parapharyngeal space dissection. The internal carotid artery is retracted laterally to reveal the branches of the external carotid artery.

Figure 21: A left side parapharyngeal space dissection with the internal carotid artery and external carotid artery retracted laterally.

Figure 22: Right parapharyngeal space dissection with the posterior aspect of the pharyngeal constrictor muscle partially removed to reveal the oropharynx.

Figure 23: A right parapharyngeal space dissection with retraction of the internal carotid artery medially and external carotid artery laterally to reveal conceptual triangle.

Graphs

Graph 1: The graph illustrates the frequencies of the presence of the linguofacial trunk on the right side, left side and cumulative of both sides.

Graph 2: The graph represents the frequency of the presence of a tortuous parapharyngeal portion of the internal carotid artery on the right side, left side and overall sum of both sides.

Graph 3: Graph represents the frequency of the ascending palatine artery origin from facial artery or directly from the external carotid artery on the right side, left side and overall sum of both sides

Abbreviations

APA	-	Ascending pharyngeal artery
aPA	-	Ascending palatine artery
BOT	-	Base of tongue
CCA	-	Common carotid artery
CNIX	-	Glossopharyngeal nerve
CNX	-	Vagus nerve
CNXI	-	Accessory nerve
CNXII	-	Hypoglossal nerve
ECA	-	External carotid artery
FA	-	Facial artery
GCH	-	Greater cornu (horn) of hyoid bone
ICA	-	Internal carotid artery
IJV	-	Internal jugular vein
IPC	-	Inferior pharyngeal constrictor
LA	-	Lingual artery
LN	-	Lingual nerve
MPC	-	Middle pharyngeal constrictor
OA	-	Occipital artery
OP	-	Oropharynx
OPSCC	-	Oropharyngeal squamous cell carcinoma
PPS	-	Parapharyngeal space
SCC	-	Squamous cell carcinoma
SCM	-	Sternocleidomastoid muscle
SGM	-	Styloglossus muscle
SHM	-	Stylohyoid muscle
SP	-	Styloid process
SPM	-	Stylopharyngeus muscle
SPC	-	Superior pharyngeal constrictor
STA	-	Superior thyroid artery

TLM - Transoral Laser Microsurgery

TORS - Transoral Robotic Surgery

Introduction

Clinical problem

How can we improve our anatomical understanding of the parapharyngeal space (PPS) to resect benign and malignant tumours of the PPS, palatine tonsil, and base of tongue (BOT) with transoral robotic surgery (TORS)?

Head and neck cancer is the sixth most common cancer in the world, of which 95% is squamous cell cancer (SCC) and the rest is mainly adenocarcinomas of paranasal and salivary gland origin [1]. Cancers of this region of the body can involve different anatomical locations such as larynx, pharynx and oral cavity. Tumours of the PPS account for 0.5% of head and neck neoplasia [2]. About 80% of these tumours are benign and 20% malignant [3]. The incidence of head and neck cancer has been increasing with the greatest contributor for this being cancer of the oropharynx (OP) [4]. Over the last three decades human papilloma virus (HPV) associated oropharyngeal SCC (OPSCC) incidence has been increasing. From the time period of 1998 to 2004 oropharyngeal cancer incidence has increased by 225%. It is predicted that by the year 2020 the incidence of oropharyngeal cancer attributable to HPV will surpass the incidence of HPV related cervical cancer [5].

It is known that the OPSCC harbours a higher HPV viral load than SCC from any other sites of the head and neck [6]. In this group HPV is implicated in the aetiology of the neoplastic process. This subpopulation of patients with HPV positive OPSCC tend to be younger in age and do not have the classical risk factors for head and neck SCC, which are alcohol and tobacco smoke misuse. The HPV positive OPSCC group tend to present at ages 40 – 50 which is about two decades earlier than the traditional OPSCC patient seen in the past. There is a male predominance and an association with increased number of sexual partners and orogenital intercourse with HPV positive OPSCC patients [7]. In the United States the prevalence of oral HPV was three times higher in men than women. Furthermore there was a higher prevalence of HPV in smokers than non-smokers. Overall this population's disease tends to be of better prognosis compared to the HPV negative OPSCC patient population. This is due to the HPV positive OPSCC population having a decreased local /regional failure of treatment, improved progression free survival and overall survival [8]. The increasing rates of HPV positive OPSCC has become an important issue to address worldwide. Unlike HPV related cervical cancer, HPV positive oropharyngeal cancer does not have a detectable precancerous stage. This places emphasises on the importance of implementing good treatment options for those effected by the condition and further more investment on preventative strategies.

The HPV is a common sexually transmitted virus. It is a double strand DNA virus that infects stratified squamous epithelial cells. Most of the HPV associated infections are asymptomatic and clear spontaneously. HPV is associated with a number of different types of cancers which include vulvar, vaginal, cervical, penile, rectal and oropharyngeal cancers. For humans, the oncogenic high risk types of HPV include HPV 16, 18, 31, 33, 35, 39, 45, 51, 56, 58 and 59. Of this group the most virulent types are HPV 16 and 18 which are most likely to persist and progress to cancer. The mechanism for oncogenesis for HPV is mainly through the production of the oncoproteins E6 and E7 which inhibits the action of the human tumour suppressor proteins p53 and retinoblastoma protein, respectively. This in turn overall leads to uncontrolled excessive cell growth. The diagnosis can be made with DNA in situ hybridisation, polymerisation chain reaction and immunostainig for p16. The p16 is a tumour suppressor protein that is found to be expressed in high levels to control cell cycle progression in a number of different cancers. Therefore p16 is not specific for HPV and it can be positive in about 10-20% of OPSCC in the absence of HPV [5]. Thus it is considered a surrogate marker for HPV.

In 2016 the Centre for disease control and prevention estimated an annual incidence of HPV associated cancer to be 38,793. HPV 16 and 18 was associated with 63% of all HPV associated cancers of the United States. Where the most common cancers were cervical cancer (7.4/100,000) and oropharyngeal cancer (4.5/100,000) [9]. In the OP, the tongue base and the tonsil are the two major anatomical sub-sites of oropharyngeal cancer.

On the other hand HPV 6 and 11 are regarded as low risk for oncogenic potential. HPV 11 is responsible for laryngeal papillomatosis and HPV 6 is the culprit for genital warts. Recurrent respiratory papillomatosis is characterised by frequent recurring papillomas of the respiratory tract. It can be a debilitating condition for patients. HPV 6 and 11 are the main strains that are responsible for this condition. There are two main ways of acquisition of this condition. The first is through vertical transmission from mother to child during childbirth. This leads to the first peak in the prevalence of the condition in the first years of life (Juvenile onset). The second way is through sexual contact at around adulthood (adult onset). Although recurrent respiratory papillomatosis is a rare condition, its implications for the patient is of high morbidity. It can lead to hoarseness of voice quality, respiratory compromise and malignant transformation [5]. Some of these patients would require regular surgical excision or laser ablation of these lesions under general anaesthesia. It is important to recognise that although female only vaccinations can lead to a decrease in rates of

vertical transmission, the second peak at adult onset is more efficiently managed with gender neutral vaccinations.

Implications of vaccines for prevention of HPV Head and Neck cancer

Currently there are three different types of HPV vaccines available which are approved by the United States Food and Drug Administration (FDA) and European Medicines Agency. These cover from two to nine strains of HPV that are known to cause disease in humans [9]. These vaccines are recombinant virus particulates. Each vaccine contains the major capsid protein of the HPV type that it offers immunity against [10]. Cervarix is a bivalent vaccine that only covers against HPV 16 and 18. Gardasil is a quadrivalent vaccine that covers for an additional two more strains which are the low risk HPV 6 and 11 [10]. Gardasil 9 is the latest HPV vaccine available today which is a nonavalent vaccine that has additional coverage against HPV 31, 33, 45, 52 and 58 [10]. All the vaccines are approved to be administered in two to three doses for children of ages 9 and above in a gender neutral way [5].

The vaccine was initially promoted for girls but now have progressed to be promoted in a gender neutral fashion in immunisation programs of most countries for the prevention of HPV associate infections and cancer. The initial view was that by treating only females the HPV transmission will be reduced and that males would be protected by herd immunity. However, this view has two main weaknesses. One, it depends on high levels of vaccination of the female population of a particular region. It is estimated that for sufficient coverage for the male cohort, the vaccination rate for females must reach greater than 80% [5]. Second, it does not cover for the males who are not so to speak involved in sexual contact with the immunised females. A predominant group that is not covered were the group of men who have sex with men. However, with the introduction of gender neutral vaccination these two main issues can be addressed. Not only does it provide personal protection to the individual but also increases the herd immunity of that region's community.

The National Immunisation Programme Schedule of Australia promotes the HPV vaccine for girls and boys 12 to 13 years of age currently, recognising potential for the reducing the burden of HPV related disease and cancer [10]. In fact Australia was the first country to fund the HPV vaccine for both genders in 2013. In Europe, Austria was the first country to publically funded HPV vaccine in a gender neutral vaccination program in 2014. This was followed by Switzerland, Lichtenstein and Czech Republic recommending universal HPV vaccination programs. Now in Australia, Gardasil 9

has replaced Gardasil in the school based National Immunisation Programme since February 2018 in an attempt to broaden the coverage to protect against the additional oncogenic types of HPV. Overall, about 70% of oropharyngeal cancer is the result of HPV. Of this group about 60% of disease causing HPV types are protected against by the quadrivalent HPV vaccine. The nonavalent vaccine protects against a further 6% thus broadening the vaccine coverage [5].

A meta-analysis of the HPV vaccine trials have shown a great vaccine efficacy of 95% with the greatest efficacy demonstrated to be against the HPV types 16 and 18 [11]. This has led to promotion of catch up vaccination programs in several nations. In Australia and the United States, catch up vaccination is recommended up to age 26. In France and United Kingdom, the catch up vaccinations are encouraged up to age 23 and 17, respectively. The effectiveness of the vaccine for prevention of cancer can be challenging to evaluate due to the onset of cancer as an endpoint can take decades to manifest. In several Scandinavian countries (Norway, Sweden, Iceland and Denmark) post phase 3 vaccine trial termination, there will be a 10 year surveillance that will be carried out. Here the current data from the first six year follow up has been promising as it showed no HPV associated disease or cancer in the vaccinated cohort [12].

A cost-benefit analysis has shown universal vaccination to be overall positive [13]. It was estimated that to treat one patient with oropharyngeal cancer for a year having made the diagnosis was $48,000 to $80,000 United States dollars and in Canada $25, 000 Canadian dollars [13]. For vaccinating an individual, it would cost an estimated $400 in Canada [13]. The population model overall demonstrated that there would be a save of 8 to 28 million Canadian dollars over the lifetime of that population.

The prevalence of head and neck cancer and its anatomical sub-sites of occurrence is changing. Oropharyngeal cancer that is attributable for HPV is increasing in incidence and have reached an epidemic level worldwide. This makes addressing the management of oropharyngeal cancer an important contemporarily issue for clinicians. Thus new management options for those affected need to be strengthened with sufficient preclinical and clinical research. The HPV vaccination have impact in reducing the rate of HPV associated head and neck cancer. The success of this depends population wide uptake of the vaccine in a gender neutral fashion to establish herd immunity [5].

Oropharyngeal Neoplasia

Oropharyngeal neoplasia can manifest symptomatically as a sore thorat, dysphagia, odynophagia, a change in voice quality, trismus, dysarthria, a sense of restriction of the mobility of the tongue and a globus sensation. In addition to the traditional risk factors of alcohol consumption and cigarette

smoking, HPV has become an increasing culprit of disease in this anatomical region as discussed earlier. In addition to HPV, Epstei-Barr virus (EBV) is also another cancer causing virus at this anatomical site adjacent the PPS. EBV is responsible for causing lymphoepithelioma which is not as common as SCC in this region.

Considering the anatomical sub-sites of the OP, the lateral pharyngeal wall and the tonsil are the most common sub-site of the OP for cancer development. They often present as an exophytic mass or an ulcerative lesion. They have an aggressive growth potential and often present with regional neck lymph node disease in about 65% to 75% of cases [14]. The OP is also a region that gives rise to lymphoma and lymphoepitheliomas at a relatively high frequency.

The BOT is another OP sub-site that gives rise to aggressive OPSCC with a poor prognosis of estimated 65% 5-year survival for all stages. They are more aggressive than anterior tongue cancer (anterior to circumvallate papillae). There is a high rate of neck metastases at a rate of 60% unilaterally and 20% bilaterally [14]. Lymphoma accounts for about 10% to 15% of the tongue base cancers. On the other hand, primary tumours of vallecula origin are uncommon. Sometimes tongue base cancer can extend to the vallecula.

Posterior pharyngeal wall cancer is less common. Although they are considered aggressive, they have less metastatic potential than BOT cancer. Soft palate cancer is also rare. They are often discovered at an early stage due to this region being a more visible area of the OP compared to the other subsites. Thus regional metastases at discovery is between 20% to 45% of cases and the five year survival is about 70% [14]. Other less common types of OP cancer include minor salivary gland malignancies, sarcoma and metastatic disease.

The tumour, node, metastasis (TNM) classification scheme is often used in staging malignant disease of the OP and is based on the American Joint Committee on Cancer (AJCC) tumour staging by site. The staging system includes: T- the characteristic of the tumour at the site of origin which can include the size, location or both. N- The number extent of involvement of the regional lymph nodes. M- The presence or absence of distant metastatic disease.

The 8th edition of the AJCC has produced a separate staging algorithm for high risk HPV positive oropharyngeal cancers to distinguish them from oropharyngeal cancers that arise from other causes [15]. This change has come about to reflect the relative better prognosis of a HPV related OP cancer compared to a non-HPV related OP cancer. Thus there has been an overall down-staging of P16 positive OP cancer that otherwise would have an advance staging if staged only taking into account

the tumour size and lymph node status. The other most significant change made to the 8th Edition of the AJCC is the emphasis on extranodal extension (ENE) of a positive lymph node. This feature is an important characteristic when staging P16 negative and non-EBV related head and neck cancers.

For the OP, the nomenclature is denoted as follows: TX, the primary tumour location cannot be assessed. T0, there is no evidence of primary tumour. T0 nomenclature was eliminated from all of the head and neck subsite TNM staging except for the OP and nasopharynx in the latest edition of AJCC [15]. This is because now it is accepted that tumours of unknown primary that show P16 positivity have a high probability of originating from the OP, thus these are staged using the OP tumour classification for P16 positive OPSCC. Similarly unknown primary tumours that show EBV positivity are highly likely to have originated from the nasopharynx thus they are staged using the nasopharynx TNM classification system [15]. Tis, denotes carcinoma in situ. For P16 positive OPSCC, the new nomenclature does not contain Tis. The non-HPV related P16 negative OPSCC still contains the Tis. T1, the tumour's greatest dimension is 2cm or less. T2, the tumour's greatest dimension is more than 2cm, however this tumour is less than 4cm. T3, the tumour is greater than 4cm on its greatest dimension or there is extension of tumour to the lingual surface of the epiglottis. Here by convention a BOT or vallecula tumour extension to the lingual surface of the tongue is not considered invasion of the larynx. T4a is considered moderate locally advance disease with tumour extension to the intrinsic or extrinsic muscles of the tongue, larynx, medial pterygoid muscle, hard palate or mandible. T4b is defined as very advance local disease. Here the tumour invades the lateral pterygoid muscle, the pterygoid plates, the lateral nasopharynx, or skull base or encases the carotid artery [16]. For P16 postive OPSCC the T4b category has been removed in the latest 8th edition of AJCC [15]. The main reason for this is because P16 positive OPSCC is pathologically indistinguishable between the T4a and T4b stages.

The regional lymph node involvement is classified as follows for P16 negative OPSCC: NX, the regional lymph nodes cannot be determined. N0, there are no regional lymph node involvement. N1, there is an ipsilateral single lymph node metastasis. The involved lymph node is less than 3cm or less in its maximum diameter and there is no ENE. N2a, There is a single ipsilateral lymph node metastasis with the involved lymph node being between 3cm to a maximum diameter of 6cm and there is no ENE. N2b, multiple ipsilateral lymph node metastases present with none greater than 6cm in maximum dimension and no ENE. N2c, bilateral or contralateral lymph node metastases present with none greater than 6cm in maximum diameter and no ENE. N3 is regarded as metastases to a lymph node that is greater than 6cm in maximum diameter with no ENE or metastases in any lymp node or

lymph nodes with ENE. N3a, the metastatic lymph node is greater than 6cm with no ENE. N3b denotes any metastatic lymph node or lymph nodes with ENE.

In contrast, P16 positive OPSCC lymph node nomenclature was simplified due to similar hazard consistency in this group of patients [15]. In this population lymph node involvement, as long as it was ipsilateral and less than 6cm in diameter had similar survival outcomes. Thus the nomenclature includes lymph node stages from NX to N3 without subcategories. NX and N0 is the same as P16 negative OPSCC. N2, there is one or more ipsilateral lymph node metastasis with dimensions no greater than 6 cm. N2, contralateral or bilateral lymph node involvement with diameter no greater than 6 cm. N3, any lymph node metastasis larger than 6cm.

The distant metastases nomenclature is as follows: MX, distant metastasis cannot be determined. M0, there is no distant metastases. M1, there is distant metastasis present.

Parapharyngeal Neoplasia

Most neoplasia of the PPS are benign. Patients can present with dysphagia from the medial wall of the OP displacement or from a mass at the angle of the mandible. A mass effect on the pharyngotympanic tube can cause otologic symptoms such as hearing loss and otalgia. A mass effect on the sympathetic chain can result in Horner's syndrome. The damage to the sympathetic chain at this region can give rise to the ipsilateral symptoms and signs. This is marked by miosis of the eye, partial ptosis of the eyelid and anhydrosis of the forehead. The partial ptosis arises from the paralysis of the superior tarsal muscle. This is smooth muscle that is under the sympathetic innervation from the postganglionic sympathetic fibres that originate at the superior cervical ganglion. The superior tarsal muscle is involved in aiding the levator palprabrae superioris muscle to elevate the eyelid. Miosis is due to the loss of sympathetic innervation of the iris sphincter muscle that lead to uninhibited parasympathetic stimulation. Anhydrosis of the forehead is related to the loss of sympathetic innervation of the cutaneous sweat glands of this region [14].

The lower cranial nerve palsies of CN IX – CN XII can occur with PPS tumours. Involvement of the muscles of mastication can result in trismus. Salivary gland tumours mostly originate from the parotid gland. The most common type is pleomorphic adenoma [14]. Neurogenic tumours are the next most common primary tumour of the PPS. These can originate from any myelinated nerve in this region. Different types of neurogenic tumours include paraganglioma, neuroma and neurofibroma. Other less

common primary tumours of this region includes lipoma, liposarcoma, chondrosarcoma, lymphoma and meningioma. Secondary lesions in this region can be due to extension of oropharyngeal, submandibular, intracranial, base of skull or tongue base tumours. Metastatic disease from the nasopharynx are another source of secondary lesions in this region. Other mass lesions of this space can include lymphadenopathy, lymphatic malformations and branchial cleft cysts [14].

For salivary gland tumours of the PPS a similar tumour staging as described above is used from TX to T3. T4a is moderately advanced local disease where the tumour has involved the skin, ear canal, mandible and/or the facial nerve (CNVII) [16]. T4b is very advanced local disease where the tumour has extended to the skull base, pterygoid plates and/or encases the carotid artery.

Neoplasia of the OP is managed with a combination of primary surgical resection, or surgery in combination with radiotherapy or chemoradiotherapy. This is associated with high acute and chronic morbidity [8]. Traditionally the tumour of the OP were managed with chemotherapy as a single modality treatment for T1/ T2 or N0/ N1 staging tumours. Simultaneous chemoradiotherapy has become a standard for patients with more advance staging such as T3/ T4 or N2b/ N2c/ N3 [16].

Chemotherapy

Neoadjuvant or induction chemotherapy is a type of chemotherapy provided as a treatment before the local treatment strategy that may involve surgery or radiotherapy. The advantage of this method is that it may allow improved drug efficacy to target the cancer site prior to the surgery or radiotherapy by disrupting the vascular route to the area of interest [14]. Further, tumour bulk may be reduced by the induction chemotherapy treatment rounds. The downside for such therapy is that patients become quite weak and generally deconditioned. This in turn can increase the risk of complications associated with surgery or radiotherapy. It may also make surgical margin assessment difficult. Concomitant treatment involves delivering chemotherapy continuously or in set intervals simultaneously with radiotherapy. The synergy of the two modalities enables a maximum therapeutic effect against the cancer. This has been the standard for treatment of locally advance cancer of the OP. The disadvantage with this approach is that it can increase the side effects of the chemotherapeutics such as infection, malnutrition, mucositis, and strictures.

The chemotherapy agent Cisplatin treatment at week 1, 4 and 7 has been most widely evaluated and can be regarded as a standard of care. It is also often used in combination therapy, adjuvant, neoadjuvant and concomitant therapies. The common side effects of this drug is nephrotoxicity, ototoxicity, peripherial neuropathy and nausea. 5-Fluorourocil is similarly used widely in head and neck cancer treatments in combination chemotherapy regiments. Myelosupression and cardiac

toxicity are two significant common side-effects of this drug. Other common side-effects include nausea, anorexia, mucositis, diarrhoea and alopecia.

Targeted chemotherapy agents are also currently used in phase III trial settings for head and neck cancer management [17]. They are relatively new drugs that target specific molecular signatures of particular cancers. Cetuximab is a monoclonal antibody that bind to the epidermal growth factor receptor of cells thus inhibits cell division. A phase III randomised control trial had shown that cetuximab improved 3 year and 5 year survival of locally advanced head and neck SCC when administered with radiotherapy compared to radiotherapy alone [18, 19]. Diarrhoea, acneiform rash and hypomagnesemia are common side-effects of cetuximab.

Radiotherapy

Radiation therapy aims to control cancer by incapacitating its clonogenic survival. This is achieved through ionisation radiation that cause direct damage to vital elements of a cell such as its DNA and cell membranes. It can also bring about cell death in an indirect fashion by damaging cell components which in turn leads to creation of free radicals. These free radicals would then damage the important components of the cell which eventually lead to cell death. Radiotherapy can be delivered in several different treatment modalities and regiments.

Conventional fractionation is radiotherapy given in smaller intervals, usually one treatment per day for 5 weeks. It aim to deliver a radiation dose between 1.8 to 2.2 Gy [14]. Pure hyperfractionation is signified by increased rate of treatment, usually with twice a day dosing for the same duration of treatment where each dose is smaller than the dose provided in conventional fractionation. This method overall delivers more total radiation dose than conventional fractionation. It is believed that this method would decrease the late on set side effects of radiotherapy [14].

Intensity Modulated Radiation Therapy (IMRT) is a mode of radiotherapy where three-dimensional computer modelled radiation therapy is devised taking into account the position and size of the primary tumour. IMRT is delivered to the target site from numerous beam directions using a combination of several intensity modulated fields. By delivering radiation in this way the aim is to provide a high dose of radiation to the tumour bed whist avoiding damage to the uninvolved adjacent tissue. Here, the skill of the planner is important to minimize complications and increase the effectiveness of the radiation treatment [14].

Preoperative radiotherapy is offered in certain cases for reduction of tumour bulk prior to surgical treatment, thus reduce the surgical resection extent. This method however can be associated with

increased postoperative complications such as wound infection and carotid artery blowout [14]. Irradiated tissue can also make the surgical resection more difficult due to tissue fibrosis from radiation damage causing loss of the normal tissue planes. Postoperative radiotherapy in contrast, allows time for tissue healing, pathology team assessment of resections and determine risk of recurrence. Compared to preoperative radiotherapy, the dose administered postoperatively is higher and the field that is irradiated is larger.

Radiation therapy often leaves patients with the short term risk of developing wound breakdown post irradiation. Furthermore, other unfavourable outcomes long term includes problems with xerostomia (dry mouth) and neck stiffness. These can result in poor quality of life long term. There can be localised cutaneous reactions. These can result in skin dryness, erythema, hyperpigmentation, telangiectasis, subcutaneous fibrosis and desquamation. Mucositis is the inflammation of mucous membranes which can be tender. It can be quite erythematous and oedematous. It increases the risk of bacterial infections, candida and herpes simplex virus infection. Furthermore, the risk of xerostomia and dental caries make good oral hygiene an important priority for these patients. Xerostomia can often be irreversible because salivary acinar cells damage because these cells are very sensitive to radiation therapy. Radiotherapy can leave tissue hypovascular and ischaemic. This increases the risk of osteoradionecrosis of the mandible. Dental extractions after radiotherapy, combined chemotherapy, and radiation doses above 50Gy are factors that increases the risk of osteoradionecrosis [14]. There is also an increased risk of radiation induced cancer. These include salivary gland cancer, sarcoma, temporal bone cancer and leukaemia. If the irradiated region is close to the temporal bone there can be otologic complications such as otitis externa, auriculachondritis and otitis media with effusion. Dysphagia can be a result of chemoradiation from fibrosis of the irradiated region particularly the oesophagus and OP.

Radiotherapy for head and neck cancer is associated with considerable morbidity for these patients. There are currently randomised clinical trials on going to investigate the ability of novel surgical interventions vs radiotherapy and chemoradiotherapy in an effort to deescalate treatments and reduce harmful side effects of radiotherapy and chemotherapy [17, 20, 21]. With the rapid expansion of novel surgical stratergiest to treat head and neck neoplasia comes a revitalising of the basic anatomical knowledge. We hope that our current study will be able to further the anatomical knowledge of this region in a way to strengthen the head and neck surgeons confidence in the anatomy of this region and to thus contribute to increased surgical safety.

Surgery

The surgical resection of the tumours of the OP and PPS are challenging due to difficulty in accessing the anatomical site. Surgical approaches to these tumours have involved invasive operations with high morbidity. These invasive approaches often involve a facial scar, long term tracheostomy, percutaneous gastrostomy tube feeding and risk of long term dysphagia.

Recent advances in surgical techniques and technology has allowed surgery to be an integral part of the combined modality treatment approach for OPSCC. Some of these surgical technique advances include transoral laser microsurgery (TLM) and TORS. Furthermore there are currently clinical trials being conducted that are exploring treatment de-intensification comparing such new surgical modalities to current standard of care with chemotherapy or chemoradiotherapy especially for early stage cancer of the OP [17, 21, 22]. A summary of the three major clinical trials that are ongoing currently are discussed below.

A phase II Randomized Trial for Early-stage Squamous Cell Carcinoma of the Oropharynx: Radiotherapy vs TORS (ORATOR) is a multicenter trial which was commenced in June 2012 across centers in Canada and one center in Australia [20, 22]. The study is currently on going and is estimated to conclude in June 2021. It has enrolled 68 adult participants with early stage OPSCC. This included T1 and T2 tumour stages and nodal stages N0, N1 and N2. The study population were randomized to the control arm which received radiotherapy or chemoradiotherapy followed by salvage surgery for persistent disease. The experiment arm underwent TORS and neck dissection. The study's primary outcome is the quality of life at one year post treatment. The secondary outcomes assessed include overall survival at postoperative year three and five, disease free survival, toxicity and swallow function.

Another randomized clinical trial based in the United States of America is currently being conducted to look at the efficacy of TORS in advance stage HPV positive OPSCC treatment [17]. Phase II Randomized Trial of Transoral Surgical Resection Followed by Low-Dose or Standard-Dose IMRT in Resectable p16 Positive Locally Advanced Oropharynx Cancer (Eastern Cooperative Oncology Group E3311 trial) was commenced August 2013 and estimated to complete on February 2023. The study has recruited 511 adult participants who have HPV infection positive stage III, IVa and IVb OPSCC. There is four experimental arms in this study for which the study population is randomised into. The first group underwent transoral surgery only. In this study tranoral surgery included TORS and TLM. The second group underwent transoral surgery followed by low dose IMRT five days per week for five weeks. The third group underwent transoral surgery then completed standard dose

IMRT for five days per week for six weeks. The final group were allocated for transoral surgery followed by standard dose IMRT and chemotherapy. In this final group the cisplatin was administered intravenous for 60 minutes or intravenous carboplatin over 30 minutes for seven rounds at set interval dates while receiving radiotherapy [17]. The primary outcomes assessed in this study are the progression free survival rate, accrual rate, and risk distribution. Another important primary outcome measured is the rate of postoperative bleeding and positive surgical margins. Secondary outcomes monitored in the aforementioned study are the incidence of adverse effects, overall survival, and swallow function before and after treatment, voice quality before and after treatment, and overall patient reported quality of life changes after treatment.

'A study ssessing the best of radiotherapy vs best of surgery in patients with oropharyngeal carcinoma' is a phase III Randomised Multicentre Trial (EORTC 1420-HNCG-ROG Trial) is being currently conducted in Europe [21]. The study commenced on November 2017 and is currently actively enrolling patients. So far they have recruited 170 adult patients with OPSCC with a TNM stage of T1 or T2, N0, M0. This study is estimated to complete in May 2026. The patients are randomized to receive radiotherapy or surgery. The radiotherapy group will receive IMRT. The surgery group will receive transoral surgery which includes TLM, TORS and conventional transoral surgery. The primary outcome of this study is to note the change in the MD Anderson Dysphagia Inventory (MDADI) [23] score at the set time intervals of 4, 5, 6, 9 and 12 months after randomization.

Radiological imaging of the head and neck is an important investigation that aids in treatment planning. Computer Tomography (CT) scan of the head, neck and chest is often the first choice of imaging for a patient who presents with an oropharyngeal cancer. The chest is included in the study to investigate for distant metastasis. CT scan is useful for deducing the extent of tumour, involvement of major vessels of the head and neck and lymphadenopathy. Often a Magnetic Resonance Imaging study of the head and neck is useful for more precise delineation of soft tissue involvement. It is particularly useful for checking for perineural involvement. Due to the majority of the PPPS being occupied by soft tissue, in order to clearly visualised these structures an MRI would be more preferable.

Surgical resection of OPSCC has typically required combination of various transcervical, transfacial and transmandibular approaches. The choice of approach is dictated by the location and extent of tumour size to allow the best exposure for adequate oncologic resection. These procedures are often

associated with the need for tracheostomy and prolonged functional rehabilitation of the upper aerodigestive tract.

The transcervical approach is suitable for large tumours of the BOT and palatine tonsil. The mandible and lower lip is not incised. Some patients can experience numbness of the chin. In this instance the OP can be reached with a transoral floor of mouth incision. Overall this approach allows poor exposure.

A mandibulectomy is performed if the tumour involves the mandible or multiple sites of tumour requiring a larger composite resection. This is approached from the midline with a lip splitting incision or further laterally along the mandible. The procedure carries a risk of palate extrusion and malocclusion. On the other hand, mandibulotomy spares the mandible. The incision can be made in a stepwise way to aid in repair of the mandible with a rigid fixation.

The lateral pharyngotomy approach is used to access posterior pharyngeal wall and for accessing small BOT tumours. The pharynx is entered between the superior laryngeal nerve and hypoglossal nerve (CNXII). This procedure conserves the mandible and the lower lip. However the exposure created by this approach is small. The transhyoid pharyngotomy can be utilised to access small posterior pharyngeal wall and BOT tumours which do not extend towards the direction of the palatine tonsil superiorly [14]. Further the vallecula should be free of disease. This is because the incision is made to enter the pharynx above the hyoid bone or through the bone leading to enter at the vallecula. This approach also conserves the mandible and the lower lip. The disadvantage of this approach is that the exposure achieved with the approach is limited.

Surgery remains the main standard of treatment for most neoplasia of the PPS [24]. Preoperative imaging with Computer Tomography (CT) or Magnetic Resonance Imaging (MRI) is vital for planning the surgical approach. The key features that needs to me evaluated with imaging is the position of the internal carotid artery (ICA) and internal jugular vein (IJV) relative to the tumour, the involvement of the skull base, and the vascularity of the tumour. Due to the higher contrast resolution and soft tissue differentiation, MRI is more preferable than CT for the investigation of PPS tumours [24]. Overall it is important to take into consideration the radiological findings, the surgical approach that gives the best exposure of the operating field, the ability to preserve key neurovascular structures, ability to provide a minimal aesthetic impairment, and the surgical teams experience when addressing the management of these tumours. Ultrasound guided fine needle aspiration cytology is useful in obtaining a preoperative tissue diagnosis on non-vascular origin tumours.

Certain PPS tumours may require transfacial and transmandibular approaches. Depending on position of the lesion, a transcervical, combined transcervical-submandibular, or a transparotid approach can be taken. These approaches involve a cervical incision and disruption of neuromuscular planes of the neck. Most often preoperative imaging is mandatory for surgical planning for a PPS mass.

The trancervical approach allows access to the PPS via a transverse incision made at the level of the hyoid bone. The exposure here can be increased by performing a mandibulotomy. The transvervical approach provides a fairly good cosmesis overall. The styloid process and the muscles that attach to it can be excised to gain better exposure to the superior portion of the PPS [24]. The transcervical submandibular approach allows access to the PPS via the dissection of the submandibular triangle. The exposure here can also be improved with a mandibulotomy. Transparotid approach combined with the submandibular approach can be utilised for excision of deep lobe parotid tumours. Here the exposure is improved with extending the incision to the submandibular region and the tumour removed via the parotidectomy incision. Infratemporal fossa and craniofacial approaches can give access to tumours of the PPS that are located near or involve the base of skull.

The transparotid approach carries the risk of injury to the CNVII. Depending on the extent of damage to the CNVII, reconstruction can be achieved with direct end to end anastomosis of the nerve or nerve grafting with used of the greater auricular nerve [24]. Other complications include infection, haematoma, trismus, recurrence, seroma and salivary fistula formation. Most of these resolve in two to three weeks. Fluid can be aspirated or the wound can be probed to release the fluid. Then a pressure dressing can be applied.

First bite syndrome is a complication where parotid pain occurs after the first bite of a meal. This is due to the loss of sympathetic innervation of the myoepithelial cells of the parotid glad. This leads to a denervation hypersensitivity of these cells which is responsible for the symptoms. Frey's syndrome is another complication that can occur from the disruption of the parotid gland during access to the PPS. The condition is also known as gustatory sweating. Patients experience sweating and erythema of the operated side face when having their meals. The symptom onset can occur delayed up to 5 years after the procedure [14]. This occurs due to the auriculotemporal nerve being injured during the procedure. This nerve carries parasympathetic postganglionic nerve fibres from the otic ganglion that innervates the parotid gland. With injury to the auriculotemporal nerve an aberrant innervation of the sweat glands of the skin by the post ganglionic parasympathetic fibers are responsible for the symptoms. The risk of the occurrence of the condition can be reduced by placement of dermal grafts

or allografts between the parotid tissue and the skin flap. The use of a thick skin flap can also reduce the risk. The condition can be managed medically with anticholinergic and antiperspirant preparations. Botox injections are also used for treatment of gustatory sweating. There are surgical management options also such as tympanic neuronectomy. The tympanic branch of the glossopharyngeal nerve (CN IX) can be excised via a tympanotomy approach. However, the results of this method of managing Frey's syndrome is controversial with a high incidence of recurrence [14]. Another surgical solution for the problem is the introduction of facia lata or dermis as a sheet between the parotid gland tissue and the skin. For patients with severe symptoms who had failed management with all other strategies may undergo radiotherapy as a treatment.

These procedures are often of long duration under general anaesthesia which may take six to twelve hours or more depending on the complexity of the approach and need for microvascular reconstruction. This can increase risk of complications associated with prolonged anaesthesia such as myocardial infarction, pulmonary gas exchange abnormalities and acute renal failure for these patients. The hospital stay after such invasive surgical approaches are lengthy, often being a week or longer. It usually requires intensive postoperative upper aerodigestive rehabilitation during the inpatient stay and further close speech pathology team follow up as an outpatient. Some lesions of the PPS can be accessed transorally, especially with novel surgical technologies such as TORS, eliminating the need for these invasive approaches.

In a tertiary hospital experienced in the treating PPS tumours, a treatment algorithm was developed to incorporate TORS as a surgical option [24]. Well circumscribed neoplasms which have a clear division plane from neurovascular bundles and lateral displacement of the ICA on preoperative imaging were regarded as ideal for undergoing resection via TORS. In our current study we hope to expand on the anatomical knowledge base further clarifying the point of clear cleavage planes from the neurovascular bundles. It is important to revisit the anatomical planes and the topography of the PPS neurovasculature to further delineate these relationships in a meaningful way to be utilised by surgeons performing TORS. Furthermore distance relationships from the key neurovasculature to the OP sub-sites would be another way to add further light into the relevant anatomy for TORS safely and efficiently to address tumours of the PPS.

Reconstruction

Reconstruction is often necessary after large amount of tissue bulk removal in OPSCC and PPS tumour resection. Primary closure is a good reconstruction method as it is associated with good speech and swallow functional outcomes [14]. In order to avoid stenosis or stricture, a tension free

closure is desired. Split thickness skin grafts also have favourable functional outcomes while resurfacing the ablated area. The disadvantage with the split thickness skin graft is the lack of tissue bulk.

Pedicled regional flaps give tissue bulk to the reconstruction region. They can be deployed in a relatively shorter operating time. However it does compromise the functional outcomes of speech and swallow. There is a limited range of mobility and risk of distal necrosis is high. The pectoralis major regional pedicle myocutaneous flap is a relatively reliable pedicled flap. It is the most commonly used regional pedicle flap for head and neck reconstruction. The main arterial supply to this flap is from the thoracoacromial artery's pectoral branch [14]. It has good reach to the head and neck region. It can be performed as a single staged procedure and it is relatively easy to harvest. If the mandible needs reconstruction this pedicled flap can be harvested with the fifth rib. It is commonly used in the reconstruction of internal and external defects of the OP, oral cavity and hypopharynx. There is potential deformity of the breast in women as a result of harvesting the pectoralis major pedicled flap.

The trapezius muscle allows for three versatile myocutaneous pedicle flaps. These flaps are generally thin, flat and can be deployed in a single stage. They are commonly used for the reconstruction of the OP, hypopharnx and the posterior face. There can be significant donor site morbidity associated with the trapezius flaps. They can lead to significant upper limb weakness. The donor site may need a skin graft for closure. The relative limited arc of rotation of these flaps can make them awkward for positioning. The upper trapezius pedicled flap is based on three angiosomes. It gains its main arterial supply from the occipital artery and paraspinal perforator arteries. The middle of the flap is provided by the transverse cervical artery. Branch of the thoracoacromial artery also supplies the lateral region of this flap. The lateral island trapezius flap is based on the superficial branches of the transverse cervical artery. The lower trapezius island flap gains its arterial supply from the dorsal scapular artery and the descending branches of the transverse cervical artery. This flap is used often for the reconstruction of the side of the face and auricular region [14].

The latissimus dorsi regional pedicle flap is another myocutaneous flap than can be used for similar reconstructions as the pectoralis major pedicle flap. It has a significant amount of tissue bulk and skin available for reconstruction of the head and neck. Further, it has great reach up to the vertex of scalp if needed. It also has the potential to be used as a bilobed skin islands if needed providing good versatility. The harvesting of the flap requires patient repositioning during the operation to the lateral decubitus position. The donor site morbidity is significant for seroma formation with this pedile flap

harvesting. In certain patients with large body habitus, it may be unsuitable to use due to the flap becoming too bulky. The flap is based on the thoracodorsal artery and its comitant veins which allows a pedicle length of about 15cm [14].

Sternocleidomastoid pedicle flap is a myocutaneous flap. Its blood supply is based on the perforator branches of the occipital artery for its superior portion. The perforating branches of the posterior auricular, superior thyroid and thyrocervical arteries supply the middle and inferior portions of this flap. The great advantage of this pedicle flap is that the donor site is quite closely located to the defect that requires reconstruction. It is used for the reconstruction of the oral cavity, lateral OP and parotid defects. The flap can be raised with the clavicle's periosteum to repair defects of the trachea and larynx. However, the vascular supply to this flap is overall quite weak. The platysma muscle limits the role of the skin perforators. The vascular supply and the accessory nerve (CNXI) limits its ability to be rotated to a certain degree.

The platysma myocutaneous pedicled flap is another flap which is in close proximity to its donor site from the defect site. The flap overall consists of thin supple skin. Its blood supply is inconsistent and is usually from the perforator branches of the facial artery (FA) and random perforator branches from the external carotid artery (ECA). The flap is commonly used for pharyngeal wall reconstruction although it has a risk of infection due to poor blood supply [14].

In addition to the above mentioned myocutaneous pedicled flaps the temporoparietal and deltopectoral flaps are fasciocutaneous flaps that can be used in head and neck reconstruction. The temporoparietal fascia pedicle flap's arterial supply is from the superficial temporal artery. It is a technically easy flap to access and close the donor site primarily. There is risk of damaging the temporal branch of the CNVII which can lead to morbidity associated with incomplete ipsilateral eye closure. This fasciocutaneous flap is used for reconstructing defects over the ear cartilage, orbit, anterior skull base, upper and mid third of the face and oral cavity.

The deltopectoral pedicled flap is another fasciocutaneous flap where the fascia is derived from the pectoralis major muscle. The arterial supply for this flap is via the first perforating branches of the internal thoracic artery. The flap is used for reconstruction of the OP, hypopharynx and oral cavity. The flap's blood supply is reliably strong and large amount of donor tissue is available for reconstruction. The main disadvantage of the deltopectoral pedicled flap is the need for a second stage operation for detachment which needs to be performed around six to eight weeks later. Further, the donor site most likely would also require a skin grafting procedure [14].

Microvascular free tissue transfer is another useful option for reconstruction post OPSCC and PPS oncologic surgery. They provide adequate tissue bulk. However they do compromise swallow and speech function. The radial forearm free flap is the most commonly used free flap for the reconstruction of the head and neck. This free flap can be harvested as a fasciocutaneous or osseocutaneous free flap along with the radius bone. Its main arterial supply is the radial artery. The free flap can be harvested relatively quickly with a long pedicle of about 20cm and there is about 10cm of bone also available. It is ideal for an area that requires a thin flap to cover a defect. It can also be shaped into a tube to reconstruct defects of the pharynx. The donor site often requires a skin graft. If bone is also harvested there is a risk of pathological fractures. The harvested bone in this instance is not able to accept endosseous implants as only 30-40% of the circumferential of bone is available for harvest [14]. Furthermore another disadvantage is that to harvest this flap one would have to sacrifice a main artery that supplies the hand.

The lateral forearm free flap is a fasciocutaneous flap. Harvesting this flap leaves only a small area of donor site defect. It can also involve a portion of the humerus bone if required. It is a free flap that is relatively easy to harvest. Similar to the radial free flap, the lateral forearm free flap is a thin flap that can be used for the reconstruction of moderate to large defects. It too can be shaped into a cylinder for pharyngeal reconstructions. The main arterial supply to this flap is from the profunda brachii artery and posterior radial collateral artery. The posterior cutaneous nerves and venae comitantae of the artery is also harvested. One down side of this free flap is that it has a short pedicle. Another disadvantage is that there can be a risk of sensory loss on the extensor aspect of the forearm.

The scapular free flaps are versatile osseocutaneous free flaps. This free flap is based on the circumflex scapular artery and its horizontal cutaneous branch [14]. The high versatility of this free flap is because it can be harvested together with the latissimus dorsi muscle or serratus anterior muscle with its blood supply as needed. The scapular free flap allows for about 8cm to 14cm of bone along the lateral border of scapular for harvest [14]. The scapular tip flap is ideal for angle of mandible reconstruction [25]. The skin from this region is similar in colour and texture to the face skin which allows a favourable aesthetic reconstruction. The free flap can be developed into two skin paddles if required. The free flap can also be used for mandibular reconstruction. The donor site morbidity from harvesting the scapular free flap can be significant because it involves the detachment of the shoulder girdle. The volume of bone that is available is relatively small. The patient needs to be repositioned in the lateral decubitous position for harvesting this flap.

The fibular osseocutaneous free flap is ideal for mandibular reconstruction. This free flap's arterial supply is from the peroneal artery. The peroneal vein and the lateral cutaneous nerve of the peroneal nerve is also transferred in this free flap. About 40cm of bone being available with this free flap allows it to be adequate for filling large bony defects. Segmental osteotomies can possible due to adequate segmental periosteal blood supply. However, the blood supply to the skin paddle of this free flap can be unreliably weak [14]. The donor site may need a skin graft depending on the size of the harvested free flap.

The iliac crest represents a region where primary bone flap or osseomyocutaneous free flaps can be harvested from. About 3cm to 4cm of muscle and about 14 cm of bone is available for reconstruction [14]. The cancellous bone from here allows endosteal implants and for overall good reconstruction of the mandible. The free flap can be useful for filling large surgical defects such as when needing to reconstruct the hemi-tongue or floor of mouth. The donor site surgical scar is in an area that can be easily concealed with clothing. The vascular transfer of this free flap includes the deep circumflex iliac artery and vein. In certain large flaps this may involve superficial circumflex artery anastomosis as well. The abdominal adipose tissue bulk and obligatory retention of muscle makes this a quite bulky free flap that is difficult to be thinned. The dissection to harvest this flap can be extensive. This often leaves the patient with a painful donor site, hip paresthesia and a temporary hip weakness. There is also a risk of abdominal herniation.

The rectus abdominis myocutaneous free flap can be used for the reconstruction of the tongue, maxilla, orbit and skull base [14]. This free flap is composed of two dominant pedicles which are inferior epigastric artery and superior epigastric artery along with their perforator branches. It allows versatility in flap design. There is a large amount of soft tissue available. The vascular pedicles have a long length. There is a risk of ventral herniation of bowel at the donor site. This is especially true when the free flap is obtained below the arcuate line.

The lateral thigh fasciocutaneous free flap is ideal for large regions that required skin with intact sensation. It is commonly used for pharynx and tongue reconstruction. The neurovascular transfer of this free flap includes profunda femoris artery's third perforator and the lateral femoral cutaneous nerve [14]. The donor site can be closed primarily after harvesting this flap. It can be technically difficult to harvest this flap. Occasionally there can be hair which make it somewhat unfavourable to use as a free flap. Further, there is a risk of seroma formation at the donor site. The anterolateral thigh free flap offer similar advantages and disadvantages to the lateral thigh flap. The skin thickness is slightly less than the lateral thigh flap.

The jejunum can be used as a visceral free flap for the reconstruction of lengthy defects of the pharynx and oesophagus. The arterial supply to this free flap is via the superior mesenteric arcade. This visceral free flap withstands radiation treatment well and most patients will be able to tolerate a soft diet post operatively [14]. It has a similar diameter to the oesophagus making the extrathoracic oesophagus reconstruction quite favourable with this visceral free flap. On the down side, to harvest this flap a laparotomy is required. The jejunal free flap only tolerates a short warm ischemic time relative to other free flaps. If the length of free flap is left too long during the reconstruction, the patients can experience postoperative dysphagia.

The gracilis muscle free flap is an ideal reconstruction option for the face, more specifically for facial reanimation. Its shape is of a thin sheet of muscle which make it a good option for the use in facial reanimation of the paralysed face. The neurovasculature that is transferred with this flap includes the adductor artery which is a branch of the profunda femoris artery, the associated venae comitantes and the anterior branch of the obturator nerve [14].

A wide variety of reconstruction options are available for the modern head & neck and reconstructive surgeon to fill the defect caused by open oropharyngeal and PS oncologic surgery. Each option chosen carries its own advantages and disadvantages. The surgical morbidity associated with the open ablative procedures and reconstructions are significant. TORS thus minimises these because most of the resections done via TORS are favourable for healing via secondary intention [14]. This method of healing also gives a better oncological outcome and better postoperative swallow function compared to pedicled regional flaps and microvascular free flap reconstructions. Thus the investment in further study in safe TORS procedures are important for providing the best care for patients undergoing such oncologic procedures. In our current anatomical study we hope to provide more anatomical insights that may facilitate such TORS procedures. We aim to achieve this through further clarifying the topography and relative distances between important neurovasculature and anatomical landmarks of the PPS.

Transoral Robotic Surgery

Transoral surgical approaches have been historically used back in the early 20th century even with high risk of vascular injury. Furthermore the approach involved the threat of damage to key nerves and high chance of tumour spillage, mainly due to the limitations of adequate visualisation [24]. In the 1960s, with advances in anaesthesia, the transcervical approaches were increasingly utilised [26, 27]. The transoral approach has regained interest due to the advent of TLM and more recently TORS. The first human TORS clinical trial involved three patients who underwent resection of their BOT

neoplasms in 2005 [28]. The United States FDA approved the application of TORS in otolaryngology-head and neck surgery in 2009 and since then its role in the management of tumours of the upper aerodigestive tract has been expanding [8].

TORS provides another modality to access lesions of the upper aerodigestive tract and PPS through the oral cavity. It requires an understanding of the head and neck topography from the medial to lateral direction, or the otherwise known as the inside to outside perspective. The technique allows a minimally invasive approach to tumours that otherwise require extensive surgical approaches. TORS has the ultimate goal of providing the best oncological outcome while reducing the treatment associated morbidity [8]. Often after TORS procedures, healing is promoted by secondary intention without approximation of the wound edges. This allows for the optimum functional outcomes of swallowing and speech [14]. Prospective follow up studies and a retrospective large cohort analysis studies have shown TORS for OPSCC is associated with decreased rates of tracheostomy, gastrostomy tube placement, decreased duration of hospital stay, and decreased operation time compared to conventional surgery [26-28].

Currently the Da Vinci Robotic Surgical System (Intuitive Surgical, Sunnyvale, California) is used in the field of head and neck surgery. The setup of the robotic surgical system include the surgical cart and the robotic arm docking system than is deployed at the patient's side. The robotic arm docking system has three laterally placed arms for instruments. There are 8mm and 5mm robotic arms with numerous variety of miniaturised traditional surgical tools available for use during a procedure. The central arm holds the endoscope that has two integrated video cameras. This allows the surgeon to view images in three-dimensions at the console. The console is set up away from the patient's bed side in the same theatre. Where he or she is able to move and twist the robotic arms by the patient side by manipulating the handles at the console. The assistant sits at the head of the bed and the scrub nurse at the left of the patient. The robotic arms are placed transorally into position to begin the procedure. The average set up times for a TORS case is about 9 minutes and it can range from 2 to 22 minutes [32].

TORS provides a 3-dimensional magnified view with angled telescopes allowing for a superior view of the areas of the pharynx that are otherwise difficult to visualise with other available modalities. High precision of resections are achieved with increased freedom of robotic arm movement, scalability of movements of the hands to the robotic arm, and tremor filtration function. Furthermore, the en-bloc resectability of lesions with TORS as opposed to piecemeal resection with TLM has made TORS the more superior modality to address tumours of the upper aerodigestive tract [8, 28]. The

high magnification and precision offered by the TORS instruments can lead to delicate dissections with avoidance of tumour fragmentation and capsular disruption.

The TORS radical tonsillectomy was described by Weinstein et al. in a phase I clinical trial for patients with carcinoma of the tonsil [32]. There were 27 patients enrolled in the prospective study with six months of follow up. There were no mortalities and 96% of patients returned to normal diet with no gastrostomy tube placement. The procedure set up included the oroendotracheal intubation and a Crow-Davis mouth gag (Karl-Storz, Heidleburg, Germany) was placed to expose the pharynx. The patients were extubated at the end of the procedure if there was no epiglottic oedema. In the case of laryngopharyngeal oedema at the end of the procedure patients were treated with steroids and intubated for one to three days. The mean duration for this procedure was 1 hour and 43 minutes with a rage from 26 minutes to 3 hours and 56 minutes [32].

The TORS for BOT neoplasms were introduced in an experimental procedure publication by O'Malley et al. [28]. In this study three cadavers, two live canines and three human subjects with BOT carcinoma were operated on with the Da Vinci surgical robot (Intuitive Surgical, Sunnyvale, California). The set up was similar to the setup of a TORS radical tonsillectomy case [32]. The 8mm robotic arms were utilised to complete the operation which included the forceps, hook and spatula cautery instruments were used for the robotic. In this study the robotic set up time ranged from 7 minutes to 28 minutes [28]. The procedure time ranged from 1 hour and 31 minutes to 2 hours and 11 minutes.

O'Malley et al., have published their initial clinical outcomes for TORS for PPS neoplasms in a prospective study of 10 patients in the year 2010 [33]. In this study they operated on benign neoplasms and achieved complete local clearance of disease in all patients with no significant complications. There were no patients with bone erosion or carotid artery encasement included in this study. There was a mean follow up period of 29.9 months. Complications included a pharyngeal dehiscence in two patients and a conversion to an open procedure in one patient. The patients who experienced the pharyngeal dehiscence were all managed conservatively. They were fed with a nasograstric tube for 3 weeks and had complete healing of the surgical wound bed. The hospital stay for the patients ranged from one day to five days maximum.

For PPS procedure the patients were positioned and the surgical set up was done in a similar way to the other above mentioned TORS procedures. The patient was intubated with a wire-enforce endotracheal tube and the tube was secured to the contralateral side nasolabial fold with a suture. The

endotracheal tube was further secured under the contralateral tongue, sutured to the lateral edge of the tongue and the anterior tonsillar pillar of the non-operating side. The access within the oral cavity was further improved with the use of a Crow-Davies mouth retractor (Karl-Storz, Heidleburg, Germany). For the surgical arms, a 5mm Maryland dissector and a monopolar spatula cautery was used. For this procedure the average set up time for the surgical robot was 4 minutes and 27 seconds with a range from 1 minute and 50 seconds to 10 minutes and 50 seconds. The mean total TORS procedure time take for the PPS tumour operations was 1 hour and 48 minutes with a range from 35 minutes to 2 hours and 32 minutes.

Complications and contraindications for TORS

Post-operative haemorrhage is a potential complication of TORS procedures, although overall it has been minimal (3 to 7% of cases) [34, 35]. There has been reported incidences of haemorrhage needing return to theatre for local control, sometimes requiring external neck exploration and tracheostomy [35, 36]. In a multicentre retrospective survey, post-operative haemorrhage was identified as the most common complication of TORS (62 patients, 3.1%) [35]. In the aforementioned study 77% of post-operative haemorrhage cases required return to theatre for haemorrhage control transorally, 16% by transcervical ligation and 8% required emergency tracheostomy. Chu et al recommended that in the event of uncontrolled bleeding or tumour spillage during TORS, the procedure should be converted to a transcervical approach [24]. They also concluded that the size of the tumour should not be a factor to contraindicate TORS. In their experience well circumscribed large tumours have been removed via TORS with relative ease when the tumour does not invade or medially displacing the IJV or ICA.

With the open procedures the rates of postoperative haemorrhage are lower compared to the transoral approach. In a retrospective review of oropharyngeal cancer patients undergoing the lateral pharyngotomy approach to the OP, no patients had postoperative haemorrhage [37]. The most common complication for the lateral pharyngotomy group was the development of pharyngocutaneous fistula which was experienced by 20% of patients. In another study of patients who had surgical treatment for PPS tumours via open surgery, postoperative haemorrhage did not occur in any of their cases [38]. In this group Horner's syndrome was experienced by 25% of patients. The next significant complication was development of temporarily paralysis of the lower lip related to the neuropraxia of the marginal branch of the CNVII. A large retrospective review of 99 patients with PPS tumours treated with the conventional open surgery (expect for one patient who had purely transoral surgery) in the Netherlands reported their haemorrhage frequency as 3.6% [39]. In this study they reported a short term CNVII palsy rate of 28.1%. The most common long term complications

were first bite syndrome (16.4%) followed by Frey's Syndrome (7.3%). The advantage with the open approach over the traditional transoral surgery of the PPS and OP is that the open approach offers improved visualisation and access for surgical instrumentation which in turn allows the surgeon to control haemorrhage early and ligate vessels that they anticipate as being high risk of bleeding.

With the exception of the carotid artery, haemorrhage from arteries such as the FA, lingual artery (LA) and tonsillar branch of FA were managed with clip application. Prophylactic transcervical ligation of arteries during the primary procedure has shown a trend towards decreased post-operative haemorrhage [36]. This suggest that proximal control of vessels may reduce the risk of postoperative haemorrhage. Proximal vessel control with TORS requires detailed knowledge of the topography of these vessels as it would be encountered from the oropharyngeal aspect. Knowledge about the estimated distances to anticipate key vessels is also beneficial.

It is useful to study the parapharyngeal arterial supply to understand where vessels can be anticipated to lie intraoperatively within the PPS. Furthermore, when resecting advanced tumours of the OP, invasion into the PPS can be encountered. In a single institutional review of OPSCC resection via TORS, the PPS was entered into in 24% of patients [40]. All patients had no evidence of PPS extension of tumour on preoperative evaluation. Thus, overall it is important to understand and anticipate the PPS vasculature during oropharyngeal and parapharyngeal tumour resection. Measurements from the oropharyngeal mucosa to the PPS key neurovasculature is a possible area for further investigation. Expansion of the knowledge here through this current study may be beneficial for reducing in adverted injury to the key vascular structures. Knowing the topographic relations and distance measurement to key lower cranial nerves may reduce morbidity associated with injury to these structures during TORS.

Regarding neural injury from TORS procedures, Chia et al., reported CNXII and lingual nerve (LN) injury in 1% and 0.6% of cases, respectively [35]. During TORS radical tonsillectomy achieving a far lateral margin can bring the surgeon close to the LN. In a recent large retrospective review of 99 patients with PPS tumours treated with conventional open surgery there were no cased of LN injury reported [39]. Another smaller retrospective observational study of open surgery for PPS tumours also had no patients experiencing a LN injury [38]. It is possible that the improved visualisation in these quite invasive procedures along with well-established anatomical knowledge of the lateral to medial approach of the PPS by the surgeons help them avoid injury to the LN in traditional open surgery of the PPS. The CNXII can be at risk during lateral tongue base resection and resection of the inferior border of the tongue base. The inferior border is of particular interest as that is where the

lingual neurovascular bundle is formed with CNXII and LA [41]. The topography of CNXII within the PPS is important when these BOT tumours are resected with adequate margins and when they extend to the PPS.

A better understanding of nerve position relative to oropharyngeal landmarks may aid localisation and avoid injury. The foramen caecum at the BOT, vallecula, and palatine tonsil's superior pole are readily identifiable landmarks within the OP to make deductions on anatomical correlations to the PPS structures.

Contraindications for TORS currently have been suggested by the pioneers of this technique. They are however relative, contemporary and not absolute. With development of our understading of the inside to outside anatomy of the parapharyngeal space and advancement of surgical techniques and technologies, these contraindications will continue to change and some factors may no longer be contraindications. The current contraindications advised by Weinstein et al serve as expert advice to make the TORS for oropharyngeal cancers technically feasible for the surgeon and safe for the patient [32]. They serve to reduce vascular complications faced during and after TORS, generate reproducible good functional outcomes, and to achieve adequate negative margins to avoid adjuvant therapy thus avoiding the morbidity associated with such treatments.

Several contraindications for TORS of the OP exist with regard to the PPS and OP vasculature. Once such contraindication is the retropharyngeal carotid artery associated with the ipsilateral carotid arterial system. Another is the presence of a midline BOT or vallecula tumour that would increase the risk of injury to both LAs. Tumours that are intimately associated with the ICA or carotid bulb that would result in exposure of the artery during dissection is another contraindication. Furthermore, primary tumours or metastatic lymph nodes that are encasing the carotid artery should not be resected via TORS [32].

When considering the conservation of functional aspects of the upper aerodigestive tract post operatively, the following tumours should not be resected with TORS: if resection requires excision of more than half of the deep musculature of the BOT, resections that would involve more than half of the posterior pharyngeal wall, and tumours that require entire epiglottis and more than half the BOT.

From an oncological perspective patients with advanced oropharyngeal cancer (T4b) should not undergo TORS [32]. On clinical examination, tonsillar cancers that demonstrate fixation to the posterolateral prevertebral fascia is another contraindication. Patients with neck disease that is

deemed not surgically resectable, cancers that produce trismus and the presence of multiple distant metastases should not undergo TORS.

Certain general patient conditions may also contraindicated the use of TORS as a treatment option. Any medical condition that prevents the patient from stopping antiplatelet or anticoagulant medications should avoid TORS. The haemorrhage risk in these patients would be too high. Any medical conditions that carry an unacceptably high mortality and morbidity for having a general anaesthetic or going through the postoperative recovery period should be cautioned against TORS. Cervical spine conditions or trismus related to any other reason that hinders with proper patient positioning or limits surgical access for TORS may render the patient an unsuccessful candidate for this minimally invasive procedure.

Training and Cost Effectiveness of TORS

The training is required to perform TORS. The primary training facility has been the University of Pennsylvania where the inventors of TORS have remained the primary post-graduate teachers of TORS worldwide. Now there are several postgraduate TORS training programmes around the world that is providing teaching regarding the technical expertise of TORS with the aid of cadaveric dissection in robotic training labs [32]. Currently in most countries there is a sacristy of standardised training and credentialing for robotic surgery in the field of otolaryngology- head and neck surgery [42]. Thus most otolaryngologist rely considerably on the guidance of industry. The Robotic Task Force had drafted recommendations to the American Academy of Otolaryngology- Head and Neck Surgery on training and credentialing. Since then there has been more detailed recommendations [42].

In United States of America a study group collected information on training and credentialing for TORS in academic and community hospitals demonstrated that the system had three common major components. These include preclinical didactic training, proctored surgical cases and necessities for the maintenance of privileges [42]. All centres required the completion of didactic training. This included instruction time of about eight hours, a minimum of three hours of operating time with the robotic console on animal models or cadavers or completion of a simulator training programme. Some institutions also required the observation of at least one TORS case. Following this the surgeons were required to undertake a minimum number of supervised cases which range from two to ten cases. All institutions also had monitoring of the surgeons' robotic case load to maintain their privileges in performing TORS. In most centres in the USA the minimum requirement was two to five cases per year, one centre required 10 cases per year and another required 25 cases over two years [42]. Currently there are no readily available information for the public regarding the credentialing and the

training a particular surgeon has undertaken in TORS in the USA [42]. Thus the public are reliant of the information provided by individual surgeons.

It is important to incorporate both preclinical and clinical components for the training of surgeons in TORS. It is also important to tailor these training curricula to the graduate and postgraduate surgeons accordingly. Graduates have a better chance at following a structured curriculum, gaining graduated responsibility while training. This structure does not translate well for the postgraduate surgeon. The reason being, they may have limitations in personal and practise finances, hospital resources, lack of mentorship and time restrictions.

Ideally all surgeons who are about to undertake TORS training should have access to reviewing a head and neck surgery specific robotic procedure video library as part of the didactic training. Overall an ideal training curriculum should also include didactic sessions on patient selection, management of these patients in the perioperative setting, the transoral anatomy, intraoperative troubleshooting, complications, and how to manage them. These should be supplemented with access to hands on TORS training with cadaveric or animal models. The findings of our current study on the PPS microsurgical anatomy would potentially be useful for surgeons who are completing their preclinical didactic sessions on preparing to gain competence. It could also possibly benefit the currently practising TORS surgeons to refine their anatomy of the PPS in a way to enhance their confidence in conducting TORS.

For graduates, the preclinical training should have didactic teachings of the functioning of the robotic surgical system, technical overview of the robot, functional aspects of the system, and troubleshooting tips. The above can perhaps be achieved with training modules that can be completed online by the graduate. There after surgical skills can be refined with practising procedures on an animal model and cadavers in a robotic laboratory. TORS specific tasks on positioning the patient, robotic console and robotic arms set up for procedures, and performance of TORS procedures in a graduated fashion with the supervision of an expert.

The clinical training for graduates would begin with observation of TORS cases. Then progress to assisting at the bedside under the supervision of the operating surgeon. At this stage the graduate should gain proficiency in the following: being able to anticipate the steps undertaken by the operating surgeon, adequate retraction of tissue to gain good exposure of the areas of interest, grasp and move the robotic arms to stop collisions, grasping and cauterising tissue, and deliver real time reporting to the operating surgeon. Management of a case during an intraoperative or postoperative

emergency should also be part of this training. Thus this would lead to the development of a solid foundation on the way to becoming a proficient operating TORS surgeon. Next the graduate can progress to the completion of TORS procedures in a step by step graduated manner as an operating surgeon under the supervision of an expert. The following operations can be undertaken in this order as a step-wise graduation from technically simple to increasing in complexity of procedures: starting with benign tonsillar pathology excision, lingual tonsillectomy, radical tonsillectomy, hemi-tongue base resection, and finally supraglottic laryngectomy [42].

For postgraduate surgeons who are seeking to undertake TORS training should do so in the aim of making TORS another option for addressing the type of cases they undertake as a part of their normal day to day case load. Thus the postgraduate surgeon should already be proficient in the other surgical options for treating the disorders that are treated with TORS such as neoplasms of the BOT, palatine tonsil and PPS. More specifically, they should be familiar in the open and endoscopic approaches to treating these conditions. TORS should not be undertaken in the hopes of becoming a super specialist, rather it should supplement the current experience of the postgraduate surgeon. This way TORS would be another tool in their armamentarium for treating their everyday patients.

The preclinical training for the postgraduate surgeon would be similar to a graduate's training. Making material available to complete as online modules for the preclinical fundamental components would benefit the busy already practising surgeon. Access to view a TORS video library should also be an important feature of the didactic component of training. It is imperative for the postgraduate surgeon to have a mentor in close geographical proximity. The clinical components of TORS training for postgraduates need to be more structured to account for the limited time available for them to acquire the skills. The timeframe for the clinical phase would be shorter thus the training aspects here would have to be more compressed. The technical aspects of assisting in TORS would still apply for the postgraduate surgeon. This would have to be followed by surgical cases performed as the principle surgeon. This period should be proctored by an expert proficient in TORS for the initial few cases.

For credentialing the graduates Gross et al., recommends applicants to already have gained privileges in equivalent surgery via open or endoscopic approaches, the residency or fellowship director to provide a letter of confirmation of completing TORS training, evidence of completing the didactic component of training, evidence of performing a minimum of ten TORS cases as an assistant and another ten cases performed as the principle surgeon [42].

For postgraduate surgeons, credentialing would similarly require the applicant surgeon to be already practising oncologic surgery of the head and neck via endoscopic or open methods, evidence of completion of didactic training, evidence of the applicant observing at least four TORS cases performed by an expert and evidence of the applicant performing a minimum of two cases independently while being supervised by an expert [39]. In Australia there is no graduate TORS training programme yet. All surgeons have gained competency in TORS as postgraduates via attending a course or completing a fellowship program that offers TORS training. The Australian Society of Otolaryngology- Head and Neck Surgery (ASOHNS) have set out clear guidelines for these surgeons to maintain their TORS privileges. For a surgeon to maintain accreditation in TORS they have recommended a minimum of 20 robotic operations per year, from this at least ten should be performed as the principle operating surgeon [43].

Maintenance of the privileges gained to performing TORS should be ideally monitored at the practising institution level. The aspects that should be monitored for ongoing credentialing of TORS privileges should include: clinical performance, TORS case volume, and complication rates. Appropriate peer review of these factors should ensure that the case load and complication rates are equivalent to open or endoscopic approach complication rates [42].

The surgeons acting as proctors of TORS should be able to fulfil the following criteria as been adapted from the Society of Urological Robotic Surgeons: they should be an expert in transoral endoscopic and TORS having performed a minimum of 20 TORS cases, the patient should give inform consent for the presence of the proctor in the theatre, the proctor may have privileges to assist during surgery, the role of the proctor during an emergency should be clearly established, be present in the operating theatre for the entire duration of the case, and the proctor should check with their indemnity provider whether additional malpractice insurance is required for undertaking such a role [42].

TORS is becoming popular in Australia and New Zealand, where an online survey sent through speciality membership databases demonstrated that 43.6% of head and neck surgeons have used TORS [43]. The most commonly performed TORS procedure for them was radical tonsillectomy then followed by BOT resections. TORS was least commonly used for obstructive sleep apnoea (OSA). In our study we aimed to focus on the anatomy of the PPS as it would relate to the two most common TORS procedures performed currently: the radical tonsillectomy and BOT resections.

In the survey of the Australian and New Zealand otolaryngologist, their opinion of the challenges for adopting TORS include the high cost, limited access to the robotic surgical system, and the scarcity

of training opportunities [43]. The off label use of TORS has been reported in the OSA, thyroidectomy, neck dissection, and paediatric otolaryngology. These procedures at this stage are not approved by the United States FDA currently. It is advisable for the novice surgeon to not undertake these procedures in his or her early stages of performing TORS [42]. There may be considerable medico-legal malpractice issues in events of a patient adverse outcome in these instances. In Krishnan et al's study there were no surgeons performing robotic thyroid surgery, six surgeons performed robotic OSA surgery, and only one performed robotic surgery in the paediatric setting across Australia and New Zealand [43]

The treatment of OP cancer with TORS has been shown to be associated with decreased hospital related costs and an overall treatment related cost of care compared to non-TORS methods of treatment [44, 45]. The cost of da Vinci robotic Surgical System (Intuitive Surgical, Sunnyvale, California) installation in Australia is estimated to cost AUD $3.25 million. The maintenance of the robotic system cost about AUD $100,000 per year and each case would carry a disposable cost of AUD $2000 [43]. In a retrospective review of treatment of 3573 patients with OP cancer in the United States of America, the patients who had undergone TORS had significantly lower likelihood of receiving adjuvant chemoradiation, postoperative gastrostomy placement and tracheostomy [45]. Overall this was associated with a decrease in a mean incremental treatment cost by USD $22, 724. This has implications in the future for health care reform in all areas of the world that are implementing TORS as a method for addressing neoplasia of the head and neck. It shows the potential that TORS has to benefit a health care system in providing a high value outcome with a reduction of consumption of health care resources. We hope that our study may also play at least a small role in furthering this value by offering the surgeons more anatomical knowledge to strengthen their ability undertake operations in this complex area. In most regions of the world health care resources are scarce and it is becoming more important for health care reformers to adopt a value based medical system. TORS has the potential to add to a value based health care system because its ability to reduced treatment intensification which is the current focus of investigation in three randomized control trials on going currently [17,20,21].

Traditionally the oncological surgery of the OP would be followed by postoperative radiotherapy. In certain subsites of the upper aerodigestive tract such as the larynx, non-operative management result in improved outcomes in speech and swallowing. However, the organ preservation option can also be associated with high levels of treatment related morbidity in the early and late stages of treatment [45]. This includes long-term dysphagia and dependence on gastrostomy. In Motz et al.'s

retrospective cross-sectional analysis study postoperative radiotherapy and chemotherapy were significantly associated with dysphagia post treatment, gastrostomy, tracheostomy and weight loss. Gastrostomy and/ or tracheostomy were significant factors that contributed to high treatment related costs. The mean incremental cost related to gastrostomy and tracheostomy during treatment was USD $14334 and USD $54606, respectively [45]. Furthermore, the highest treatment related cost were related to adjuvant therapy. Undergoing postoperative radiotherapy and chemoradiotherapy were associated with a mean incremental cost of USD $89001 and USD $113634 [45].

The treatment deintensification potential of TORS is currently under the investigation of the Eastern Cooperative Oncology Group E3311 clinical trial which is a multicentre randomised control trial, ORATOR trial and EORTC trial. [20-22]. It is possible that if these studies demonstrate the evidence supporting treatment deintesification, there may be further expansion of TORS technology development, indications for robotic surgery in the head and neck, and be considerable healthcare cost saving at the same time. With the TORS technology likely to keep expanding, the surgical anatomy knowledge of the areas ventured by such surgical technology will also need to be revisited and expanded. We hope the anatomical findings of our study would contribute to another small step towards improved safety and care for patients undergoing TORS.

Embryology

The embryological development of the pharynx is key for understanding the relationship of PPS contents and adjacent pharyngeal structures. Embryological remnants during development may manifest as anatomical variations at the PPS.

Pharyngeal arches

The pharyngeal arches are formed during the fourth week of embryonic life (**Figure 1**). These are outpouchings of the proximal foregut that begin at day 27 and complete their formation between day 31 and 35 of gestation [46]. The inner surface is lined by epithelium of endodermal origin. Squamous cell carcinomas of the OP arise from this epithelial layer. The outer surface is derived from ectoderm. The core of each pharyngeal arch is composed of mesenchyme derived from para-axial and lateral plate mesoderm. Neural crest cells also migrate to each pharyngeal arch core contributing to the formation of the facial skeleton, thymus, middle ear ossicles and elements of the teeth. Each arch has its own cranial nerve innervation and blood supply. By day 30 of development, afferent and efferent roots of the trigeminal (CNV) and vagus (CNX) cranial nerves are also present [46].

The first pharyngeal arch contributes to the formation of the mandible, maxilla and muscles of mastication. The mandible and medial pterygoid muscle form the lateral border of the PPS. The CNV's mandibular and maxillary divisions are the chief nerve supply to structures derived from the first pharyngeal arch. Thus, the LN's origin is from the first pharyngeal arch. This nerve is at risk when tumours that involve medial pterygoid muscle need resection.

The second pharyngeal arch gives rise to the styloid process, stylohyoid ligament, posterior belly of digastric muscle, upper part of body of hyoid, and lesser cornu of hyoid [47, 48]. The CNVII derives from the second pharyngeal arch and supplies all the muscles derived from the second pharyngeal arch [47]. The CNVII is often at risk of injury when approaching PPS tumours from transcervical approaches.

The third pharyngeal arch gives rise to the stylopharyngeus muscle (SPM) which is innervated by the nerve of the third pharyngeal arch – the glossopharyngeal nerve (CNIX). It contributes to the formation of the greater cornu of hyoid (GCH) and lower body of hyoid. GCH is the inferior border of the PPS.

The fourth pharyngeal arch contributes to the formation of the pharyngeal constrictors. The buccopharyngeal fascia that line the lateral surface of this musculature is the medial border of the PPS. Dissection through this fascia is sometimes required to achieve an adequate surgical margin when resecting certain tumours of the OP. The superior laryngeal nerve of the CNX is the nerve of

the fourth pharyngeal arch. The sixth pharyngeal arch contributes to structures beyond the PPS: the larynx and its intrinsic muscles.

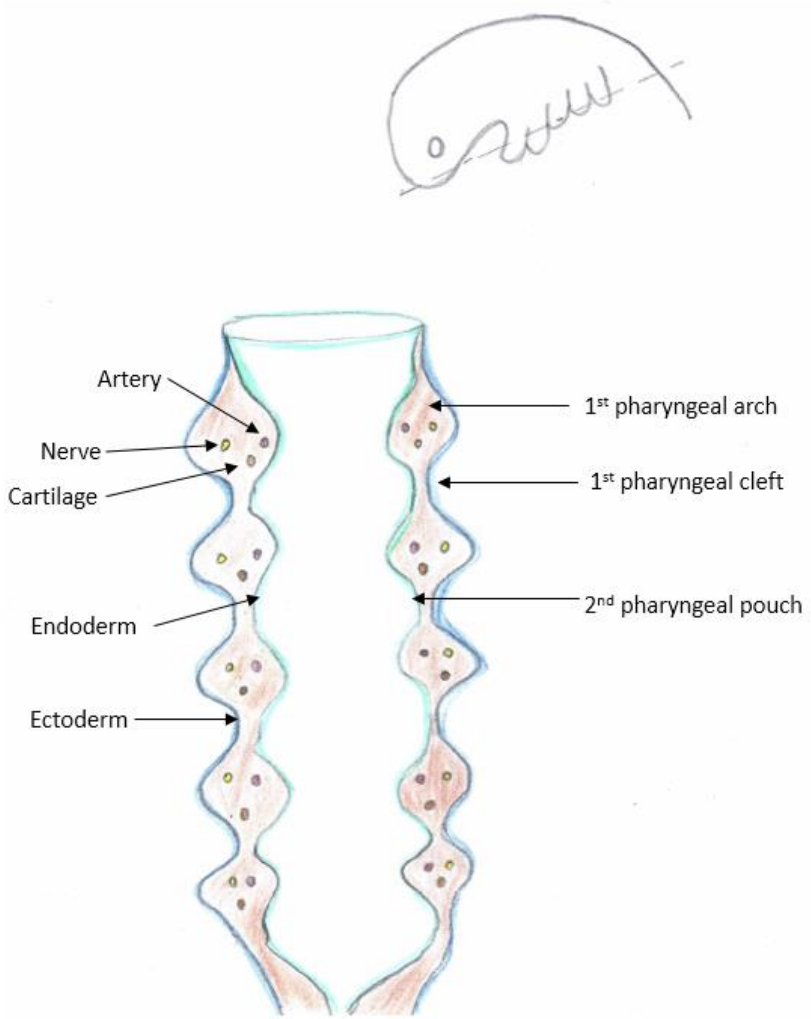

Figure 1 Each pharyngeal arch is composed of a core of embryonic mesenchyme and receives its own arterial and nerve supply. Endoderm lines the internal aspect while ectoderm lines the outer surface. Pharyngeal clefts appear externally with corresponding pharyngeal pouches forming internally.

Development of the arterial supply

Each pharyngeal arch receives an aortic arch (term for the vascular supply of pharyngeal arch) as its blood supply. The aortic arches branch from the distal truncus arteriosus- the aortic sac. Distally the aortic arches terminate at each left and right dorsal aorta (**Figure 2**). Each arch forms successively starting from the first being most cranial. The primitive vessels move to the head at day 38 [46]. During development these are modified and parts progressively regress, sometimes leaving remnants that survive through adult life in the final form.

The maxillary artery is formed from the remnant of the first aortic arch which regresses by day 27 of embryonic life [447. The common carotid artery (CCA) and the proximal internal carotid artery (ICA) are formed from the third aortic arch. The ICA is formed from the distal portion of the dorsal aorta.

ICA tortuosity can sometimes occur due to incomplete descent of the dorsal aortic root at eight weeks of development [49]. These variations in infancy have been reported to occur at a frequency of 5-10% [50, 51]. Such tortuosity can bring the ICA near the pharyngeal wall thus increasing the risk of vascular injury during transoral oropharyngeal surgery. The external carotid artery (ECA) is a branch from the third aortic arch. The vascularisation of the pharynx is complete by day 38 [46].

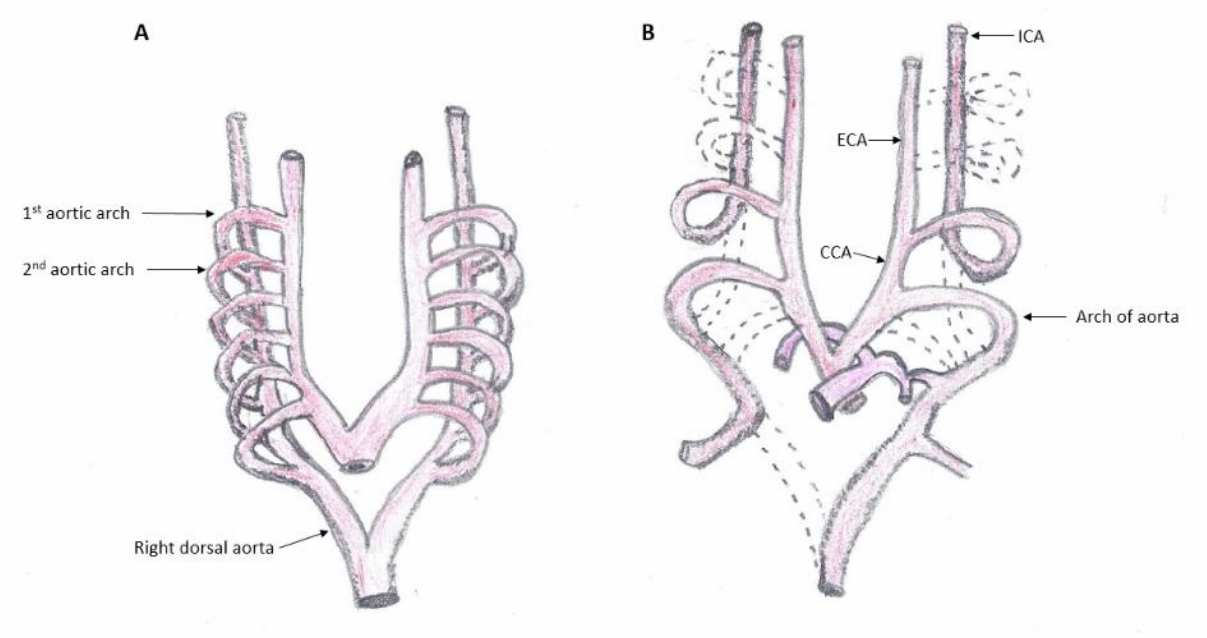

Figure 2 A. The aortic arch system where each aortic arch contributes to the arterial supply to a pharyngeal arch. **B.** The aortic arch system after transformation to the final vascular pattern. The dotted lines represent regressed components. Abbreviations: **ICA** internal carotid artery, **ECA** external carotid artery, **CCA** common carotid artery.

Pharyngeal pouches

Human embryos have four pairs of pharyngeal pouches that form synchronously when the pharyngeal arches form (**Figure 1**). The pouches are infoldings of endoderm of the proximal foregut. The tonsillar fossa is a remnant of the second pharyngeal pouch. The second pharyngeal pouch endoderm divides and invades the surrounding mesenchyme tissue. The pouch is invaded by the mesenchyme to form the primordial palatine tonsil which appears at day 56 [46, 47]. Lymphatic tissue infiltrates the tonsil during the third and fifth week of gestation. Lymphocytes are present in the palatine tonsil at 13 weeks [46]. The epithelium of the palatine tonsil is a source of OPSCC and the role of HPV infection is implicated in most of these tumours although the pathogenesis is currently not established [6].

Pharyngeal clefts

The fourth week embryo contains four pairs of pharyngeal clefts (**Figure 1**). These are infoldings of externally lining ectoderm. The first cleft gives rise to the external auditory canal and tympanic membrane. Proliferation of secondary arch mesenchyme causes overlap with the second, third and

fourth pharyngeal arches. This results in the coalescence of the second, third and fourth pharyngeal clefts forming a cervical sinus that is lined by ectoderm which disappears with further development.

A branchial fistula forms when the second pharyngeal arch fails to fuse with the third and fourth pharyngeal arches. This leaves a tract between the lateral cervical sinus and the outer surface. Most fistulas are found anterior to the sternocleidomastoid muscle. The most common location of a cervical cyst is below the angle of the mandible. Some fistulas can form in the preauricular region. Sometimes a tract of the branchial fistula can be present between the ECA and the ICA within the parotid tissue [52]. Rarely, internal branchial cysts can form when the communication is formed between the pharyngeal clefts and the pharyngeal pouches, connecting lateral cervical cysts to the pharynx by means of a narrow tract. Most pharyngeal communications are found at the tonsillar fossa.

The primordium of the parotid gland appears between day 42 and 48 [46]. It continues its growth over the next seven days, with branching of the parotid gland into primordial cell cords and is completed at 10 weeks. Further differentiation of the parotid gland is completed between 14 to 20 weeks [46]. The gland forms the posterolateral border of the PPS.

Development of the tongue

The primordium of tongue appears between day 35 and day 40 of development [46]. The anterior two thirds are derived from lateral lingual swellings of the first pharyngeal arch. Thus, the nerve supply to this area is from the mandibular division of CNV. The posterior one third is formed from the second, third and fourth pharyngeal arches. The tissue from the second pharyngeal arch is overtaken by the third pharyngeal arch. The posterior one third of the tongue receives its taste and general sensory innervation from the CNIX.

The most posterior part of the tongue and the epiglottis is derived from the fourth pharyngeal arch thus the sensory innervation of this area is from the superior laryngeal nerve. The tongue muscles are derived from occipital somites of the suboccipital myotome. As they migrate towards their final position, they drag with them their nerve supply- CNXII. The transposition of tongue occurs at day 56 of development [46]. This explains the path of the CNXII as it travels through the PPS inferiorly and anteriorly to innervate the tongue.

CNXII is at risk of injury during TORS BOT resections. Achieving an adequate lateral margin of these lesions sometimes involve dissection towards the PPS [53]. An understanding of the adjacent myofascial planes of the operative field and the neurovasculature of the PPS is useful for safe resection of these lesions.

Anatomy

Boundaries of the parapharyngeal space

The PPS is an inverted pyramid shaped potential space of the head and neck (**Figure 3**). It is continuous with the retropharyngeal space medially which is between the prevertebral facia and the buccopharyngeal fascia of the pharynx. The PPS extends from the base of skull superiorly to the GCH inferiorly. Posteromedially it is bounded by the prevertebral facia, and anteromedially by buccopharyngeal fascia of the superior pharyngeal constrictor muscle [53, 54]. Anteriorly the space is bound by the pterygomandibular raphe [53]. The lateral border is delined by the ramus of mandible and medial pterygoid muscle. The posterolateral border is formed by the deep lobe of the parotid gland.

The medial pterygoid muscle has a superficial and deep head. The superficial head of the medial pterygoid muscle originates from the medial surface of the lateral pterygoid plate. The deep head originates from the pyramidal process of the palatine bone. It has a vertical orientation and inserts onto the medial surface of the mandibular ramus. It mirrors the externally positioned masseter muscle. It is innervated by an anterior division branch of the mandibular division of the trigeminal nerve. Its function is to elevate, protrude and medialise the mandible as in when chewing.

PPS is divided into the prestyloid and poststyloid spaces by the styloid diaphragm. The styloid diaphragm is a fibrous sheath that contains attachments of the posterior belly of digastric, stylohyoid (SH), styloglossus (SGM), stylopharyngeus (SPM) muscles and stylomandibular ligament [48]. The stylohyoid ligament extends from the styloid process to the lesser cornu of hyoid. Gunn et al., showed that the stylohyoid ligament is an important landmark for transoral surgery, as it is positioned between SPM and SGM [55]. The study demonstrated transoral anatomy through endoscopic cadaveric dissection of the lateral oropharyngeal wall, BOT and PPS. The aforementioned study did not include any information on distances from the OP to the PPS structures which is a potential area of further study.

The OP is the region that is medial to the PPS. Much of the important neurovasculature of the PPS traverse this space through to the OP and oral cavity region. The OP anterior boundary is the junction between the hard palate and the soft palate superiorly. The circumvallate papillae also mark the

anterior boundary of the OP. The inferior limit of the OP is conceptually regarded as the region of the pharynx that is at the level the posterior wall of the pharynx that is bound between the aforementioned limits. The nasopharynx and the laryngopharynx are the regions of the pharynx superior and inferior to these limits, respectively. Sub-sites of the oropharynx that can be involved in neoplasia include BOT, inferior surface of the soft palate including the uvula, lateral and posterior pharyngeal wall, pharyngeal tonsils, palatopharyngeal arch, palatoglossal arch, and glossotonsillar sulci.

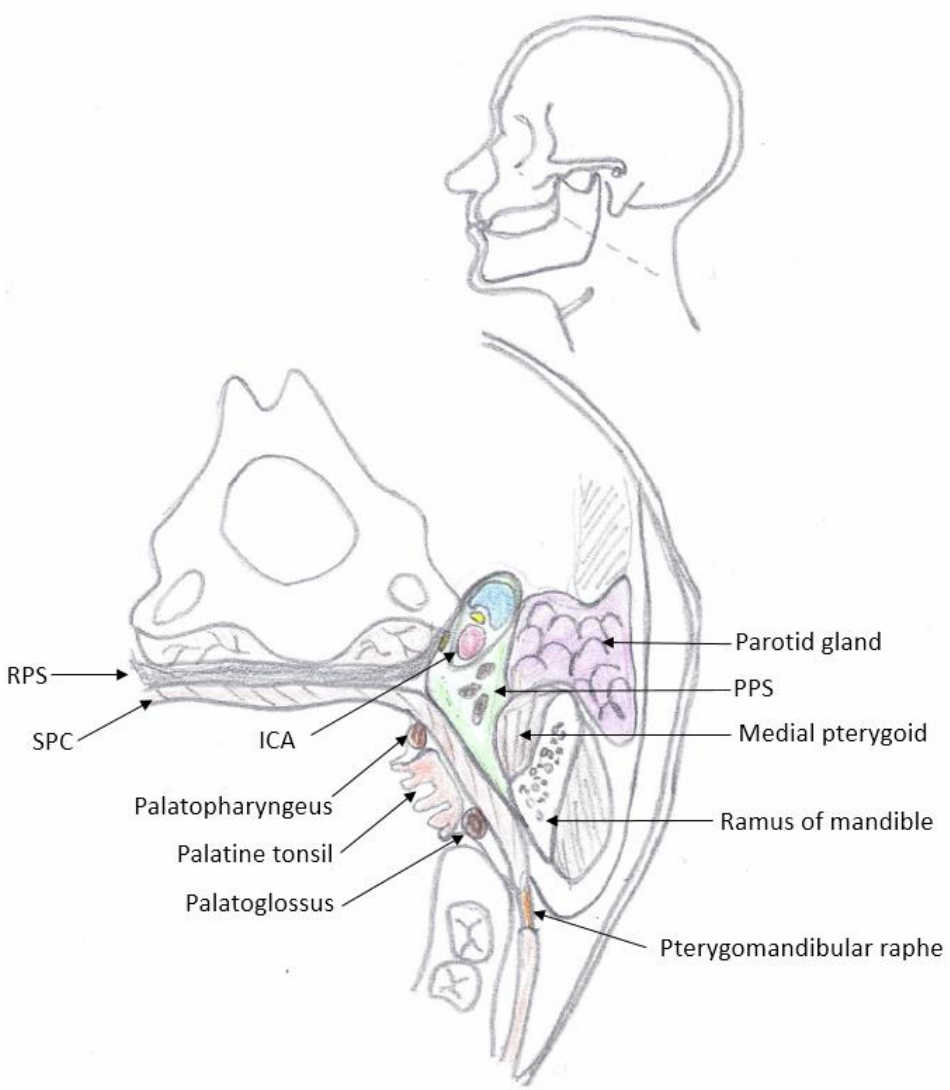

Figure 3 The oblique view through the level of the OP illustrates the position of the parapharyngeal space. Its lateral border is the parotid gland, medial pterygoid muscle and ramus of mandible. The medial border is the superior pharyngeal constrictor at this level. The space is continuous with the retropharyngeal space medially. Abbreviations: **ICA** internal carotid artery, **PPS** parapharyngeal space, **RPS** retropharyngeal space, **SPC** superior pharyngeal constrictor muscle.

The prestyloid space

The prestyloid space contains the retromandibular portion of the parotid gland, adipose tissue and the pterygoid venous plexus. Its anterolateral border is the medial pterygoid and posterolateral border is

the deep lobe of the parotid. Most lesions are found in the prestyloid space. Pleomorphic adenomas are the most common primary tumour arising from the prestyloid space [56]. These may originate from the parotid gland or the minor salivary glands. Neurogenic tumours mainly arise from branches of the trigeminal nerve at this region.

Dallan et al., produced a detailed transoral endoscopic anatomic report of the PPS where it was concluded that the SPM and SGM are key anatomical landmarks for orientation within the area [54]. Posterolateral to these two muscles are important neurovascular structures of the PPS. A future area of study that stems from this work is to relate the parapharyngeal anatomy back to the oropharyngeal mucosal anatomy. However, Dallan et al., did not provide distance measurements between PPS structures and oropharyngeal landmarks.

The poststyloid space

The poststyloid space medial border is the pharyngobasillar fascia superiorly, and the buccopharyngeal fascia of the superior and middle pharyngeal constrictor muscles, inferiorly. This space contains the following vital neurovascular structures: the ICA, ECA, IJV, the sympathetic trunk and the lower cranial nerves (CNIX, CNX, CNXI, and CNXII). Any of these structures can give rise to tumours of the PS. TORS resection of tumours of this space is of high risk. Although it is not a contraindication to using the modality. Therefore reported cases are a few [33, 57].

Neurovasculature of the parapharyngeal space

An understanding of the neurovasculature of the PPS from a medial to lateral direction is the learning curve that a TORS surgeon must undergo. Prior to TORS the medial or transoral approach to the PPS was not popular due to the limitations of poor visualisation and access. However the knowledge of the medial to lateral perspective has been growing to facilitate the use of TORS. **Table 1** summarises some of the key anatomical studies that are relevant to the TORS approaches. These studies will be discussed in the following sections.

Glossopharyngeal nerve

CNIX exits the skull base through the lateral part of jugular foramen between the ICA and IJV. It initially travels the PPS as a vertical segment then loops around the SP muscle, then continues as a horizontal segment [48]. It passes between the SPCM and IPCM. Ohtsuka et al., demonstrated through histological sectioning when there is a dehiscence between the two constrictor muscles, the CNIX became closer to the tonsillar capsule [58]. The inferior border of the SPCM corresponds to the floor of the tonsillar fossa when no dehiscence is present. The group also demonstrated from the

transoral aspect the nerve was positioned between SGM and SPM as it passed in proximity to the tonsillar fossa [58]. The study however did not measure distance from tonsillar fossa to CNIX distance.

This region is of interest to TORS radical tonsillectomy and BOT resection due to the risk of injury to CNIX. Sometimes the nerve is sacrificed to achieve adequate oncologic resection. Where possible, conservation of the nerve can have potential improvement in swallow function and avoid taste disturbance [58, 59].

The nerve has six branches. The tympanic branch leaves the inferior ganglion to enter the tympanic canaliculus of the petrous part of the temporal bone, where it passes into the middle ear innervating it, and the mastoid air cells and bony part of the auditory canal. The tympanic branch of the CNIX is also known as Jacobson's nerve. It carries preganglionic parasympathetic nerve fibres that originate at the inferior salivary nucleus. These preganglionic parasympathetic nerve fibres synapse at the otic ganglion.

The motor branch to SPM is given off when the CNIX spirals around the posterior border of SP. Conceptualising the nerve's orientation with respect to SPM is useful for TORS. Wang et al., have described the transoral anatomy of this nerve in three segments as: above, overlapping, and below the SPM. Further, they demonstrated that the nerve is crossed by the pharyngeal branch of CNX in 75% of cases [60]. An area for further study is to correlate the nerve's topography to regions of the oropharyngeal mucosa and provide proximity distance values. Lim et al., showed that CNIX can be consistently identified transorally at the junction between the posterior tonsillar fossa and the base of tongue [59]. The study however did not provide a depth from the mucosal surface to the nerve.

The carotid sinus branch passes between the ICA and ECA to innervate the carotid body's baroreceptors and chemoreceptors. Pharyngeal branches join the pharyngeal plexus on the middle constrictor innervating the mucosa of the OP for general sensation and some taste. It contains afferent nerve fibres involved in the cough and gag reflexes. It also carries parasympathetic fibres from the inferior salivary nucleus to innervate the mucous and salivary glands of the OP. The tonsillar branch supplies sensation to the mucosa of the palatine tonsil. The lingual branch innervates the posterior one third of tongue for taste and general sensation.

Vagus neve

The CNX exits the skull base through the middle compartment of the jugular foramen. The nerve is positioned posteriorly between the IJV and ICA within the carotid sheath. During transoral approach

to the PPS this nerve is not encountered due to its position being posterolateral to the ICA and IJV. During cadaveric endoscopic PPS exploration, it was found consistently at the carotid-jugular angle [54].

Within the PPS it gives off five branches. The pharyngeal plexus branch crosses the ICA separating it from the ECA. It runs inferiorly and parallel to the CNIX to join the pharyngeal plexus of the MPCM. It innervates all the muscles of the pharynx except SP, and soft palate except tensor veli palatini. The superior laryngeal nerve is medial to the ICA as it descends.

Accessory nerve

CNXI is formed by the union of the spinal and cranial roots as it exits the skull base through the middle compartment of jugular foramen lateral to CNX. All its cranial roots join CNX. Then the nerve passes posteriorly as it descends lateral to the IJV which is positioned against the lateral mass of atlas. It passes medial to the posterior belly of digastric. The nerve is crossed by the upper sternocleidomastoid branch of the occipital artery (OA) as it pierce and innervate the SCM. The nerve then passes to the posterior triangle of the neck to innervate the trapezius muscle. CNXI passes laterally quite high in the neck deep within the poststyloid space from the oropharyngeal aspect. The nerve has been visualised transorally at the level of soft palate crossing IJV [54]. The superior position and lateral path of CNXI reduces the risk of iatrogenic injury TORS of the OP.

Hypoglossal nerve

CNXII innervates all muscles of the tongue except palatoglossus which is innervated by CNX. The nerve exits the hypoglossal canal medially between the jugular foramen and the carotid canal. Thus, it is medial to the carotid sheath initially, then as it descends curling around the inferior vagal ganglion and positions itself between IJV and ICA. As it descends towards the tongue it becomes lateral to the ICA and passes anterior to it (**Figure 4**). The nerve passes medial to GCH and inferior to LA at the floor of mouth.

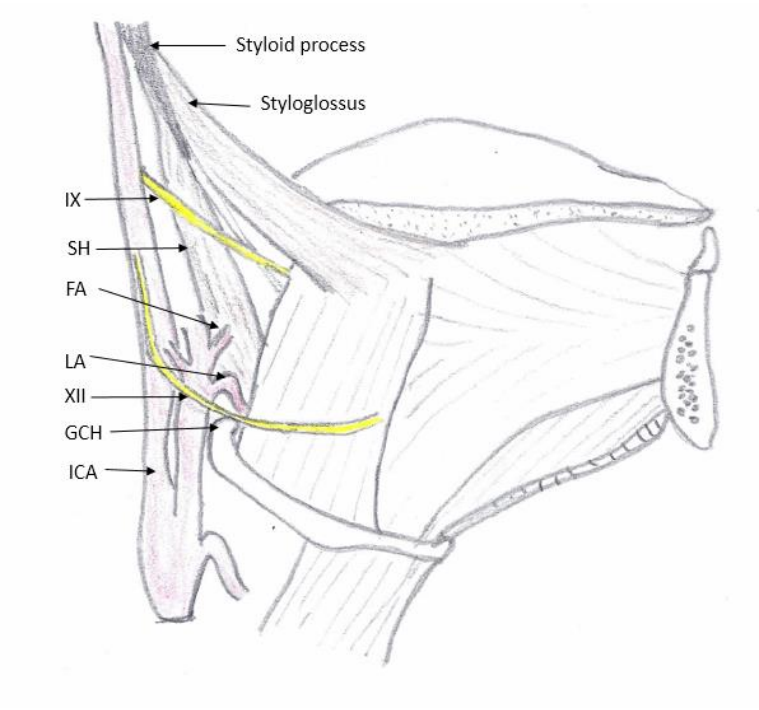

Figure 4 The styloid process and its musculature the styloglossus and stylohyoid pass towards their distal attachments at the base of tongue and hyoid bone, respectively. The distal portion hypoglossal nerve within the parapharyngeal space is intimately related to the greater cornu of hyoid and lingual artery. Abbreviations: **FA** facial artery, **GCH** greater cornu of hyoid, **ICA** internal carotid artery, **IX** glossopharyngeal nerve, **LA** lingual artery, **SH** stylohyoid

O'Malley et al., in their first clinical report of TORS BOT resections stated that the nerve is approximately 1cm deep to LA at the mouth [28]. The study however did not comment on the parapharyngeal portion of CNXII. Laurento et al., showed that the distance from CNXII-LA neurovascular bundle to the foramen caecum of tongue was 27mm inferior and 16mm lateral [41]. They also measured this neurovascular bundle to be 9mm superior to the hyoid bone. The study however only focussed the oropharyngeal portion of both CNXII and LA. The study of the inferior parapharyngeal portion of these two structures would be useful for resection of inferiorly propagating BOT tumours and proximal haemorrhage control from LA. The depth from the oropharyngeal mucosa to the PPS portion of CNXII is not well established. Dallan et al., demonstrated the transoral view of the parapharyngeal portion of CNXII which roughly corresponds to the region lateral to the BOT [54]. In this region CNXII was visualised inferior to the SGM and lateral to GCH. However, the study did not provide any depth measurements.

The nerve enters the submandibular region passing lateral to the ICA. It hooks around the OA, passing anterior to ECA, lateral to LA, medial to the anterior belly of digastric and inferior to the digastric tendon. It runs anteriorly along the lateral surface of hyoglossus muscle which separates it from LA, giving off the superior root of the ansa cervicalis before piercing mylohyoid to enter the oral cavity [52].

In a second study, Dallan et al., demonstrated the intraoral BOT anatomy from a superior to inferior view and expanded on the relationship of the LA to CNXII in this region [61]. A further step from Dallan et al.'s would be to describe the relationship between LA and CNXII within the PPS before entering the oral cavity.

These topographic relations could be supplemented with depth measurements from oropharyngeal mucosal landmarks to the PPS portion of these two structures. Further study in this region is important for TORS BOT resection. Especially for resecting inferiorly propagating tumours that have their lateral and inferior margins within the inferior PPS at this location.

Lingual nerve

LN arises from the posterior branch of the mandibular division of the trigeminal nerve inferior to the inferior border of the lateral pterygoid muscle. It passes between the medial pterygoid muscle and the mandible. The nerve is protected by the medial pterygoid muscle during TORS at this region. It may be at risk if tumour resection involves disruption of this muscle. As the nerve passes the anterior boarder of medial pterygoid, it sits lateral to the inferior portion of SGM [61]. The nerve enters the OP through the inferior border of the SPCM. Here anteriorly, the nerve is at risk during TORS radical tonsillectomy due to the proximity to the pharyngeal constrictor muscle [54].

LN provides general somatic sensation to the anterior two thirds of tongue. When passing through the PPS it is accompanied by the chorda tympani nerve 2cm from the skull base where it arises through the petrotympanic fissure [52]. The chorda tympani carries afferent taste special sensory fibres from the anterior two thirds of tongue and preganglionic secretomotor fibres to the submandibular ganglion.

Carotid sheath

The carotid sheath contains the ICA, ECA, IJV, CNX and ansa cervicalis. It is part of the deep cervical fascia extending from the margins of the carotid canal at the skull base to the root of neck where it is adhered to the medial surface of sternocleidomastoid. Inferiorly it blends in with the pretracheal fascia [52].

At the skull base the carotid sheath also contains the CNIX, CNXI and CNXII. Both CNXI and CNIX diverge from each other. Posterior to the sheath is the sympathetic trunk. Within the carotid sheath the CCA is medial to the IJV.

Internal carotid artery

The ICA bifurcates from the CCA at the inferior border of the PPS approximately at the level of the GCH. The proximal dilation of the vessel is the carotid sinus which contain baroreceptors. As the

artery branches off it travels superiorly turning posteromedial to the ECA. At its origin it is crossed by the OA, CNXII and facial vein laterally. As it ascends along the pharyngeal wall, the ascending pharyngeal artery (APA) is medial to it. Higher up in the head, the following structures separate ICA from ECA: SP, CNIX and pharyngeal branch of CNX.

The ICA travels straight to the skull base with no branches given off at the neck in the majority. However, it is not uncommon to have aberration of the parapharyngeal portion of the ICA [49, 62, 63]. Weibel and Fields classified the extracranial ICA aberrancy as tortuosity, kinking or coiling [64, 65]. Ozgur et al., showed in a cadaveric dissection study that 25% of cases had a tortuosity and 5% had kinking [49]. Through histological sectioning they demonstrated that where kinking was present, the tunica media was thin [49]. Further, at these sites dissections within tunica media and adventitia were present. These authors concluded that compromise in vessel integrity in aberrant ICA may increase likelihood of haemorrhage from direct or indirect injury. The study however did not provide distance measurements of proximity of the aberrant ICA to the lateral pharyngeal wall.

In adults, the distance from the palatine tonsil to ICA reaches 25 mm [66]. Deutch et al., showed that as body size and age increases there is positive correlation with this distance which plateaus at weight 56kg and age 12 [66]. It is a useful reference distance for peritonsillar abscess draining, tonsillectomy and more novel approaches such as TORS of the lateral pharyngeal wall.

Pfeiffer et al., published a new classification system for ICA variations and commented that an aberrant ICA in close proximity to pharyngeal wall at the level of nasopharynx and OP should be considered high risk for iatrogenic injury [66]. These areas were regarded high risk because of high chance of trauma and routine surgical procedures at the area such as tonsillectomy, peritonsillar abscess drainage and dental procedures. In that study, the grading system included the ICA proximity to the pharyngeal wall, which they measured using radiological images. The classification was recently updated to reflect the risk of ICA injury taking into account the surgical case load at each region of the pharynx [63]. The study however did not correlate ICA anatomy to a specific anatomical landmark of the pharynx such as tonsillar fossa, vallecula, and Eustachian tube. The inability to identify and measure these anatomical relationships is most likely due to the limited ability to delineate these relationships using current radiological imaging modalities. Thus, this is an area for further investigation where cadaveric dissection may be able provide important information.

External carotid artery

The ECA bifurcates from the CCA at level of the GCH (C4). It is positioned anterior to the ICA. It passes superiorly to pierce through the parotid fascia while being medial to the posterior belly of

digastric muscle and SH. Within the parotid gland it gives off the maxillary and superficial temporal arteries. At this level ECA and ICA is separated by the deep lobe of parotid, SP, CNIX and pharyngeal branch of CNX [52]. Proximally the IJV is posterior to the ECA. Distally it becomes lateral to ECA.

Lim et al., provided proximity of ECA to the lateral pharyngeal wall at level of C2/C3 intervertebral disc level which measured a mean distance of 17.6mm and 18.4mm for left and right side, respectively [59]. This level was chosen because it was easily identified in axial slice radiological images. The study does not provided correlation of these measurements to the OP mucosal anatomic sites.

The ECA is crossed by the facial vein and CNXII laterally at the region immediately above GCH. Another measurement Lim et al.'s study provided was the proximity of the ECA to GCH, which was 3.4mm and 4.4mm on the left and right side, respectively [59]. This is useful to know when resecting the inferolateral margin of a tonsil cancer or BOT cancer with TORS. Further, it would also be useful to know the proximity of the ECA at this level to the oropharyngeal mucosa and vallecula in a radiological or cadaveric study.

The ECA gives off three arteries anteriorly: superior thyroid, lingual, and facial. Two arteries branch off posteriorly along the inferior border of the posterior belly of digastric. The APA is given off medially which then ascends along the pharyngeal wall to the skull base. An uncommon variation is the APA branching off the ICA [67]. Usually the ECA is deep to the SGM and SPM muscles from the transoral perspective. Wang et al.'s dissections of the PPS showed in 8% of cases ECA can deviate medially through these two muscles. The close proximity of the ECA to the lateral oropharyngeal wall increases injury risk during TORS. It is useful to know in such cases of variation the distance from ECA to the oropharyngeal mucosa.

Ascending pharyngeal artery

The APA is given off at the proximal end of the ECA. In 75% of cases it branches from the medial aspect of the ECA [67]. It travels superiorly medial to the ICA along the pharyngeal wall in the majority. It supplies branches to the pharynx, soft palate. Its branch to the tonsil can be a source of haemorrhage during tonsillectomy and TORS radical tonsillectomy.

Dallan et al.'s endoscopic transoral PPS anatomical dissections demonstrated the artery's position as being posterior to the SP [54]. It also demonstrated its proximity to the lateral wall of the pharyngeal constrictor muscle [54]. Its terminal end supplies the skull base foramina: jugular foramen,

hypoglossal canal, and foramen lacerum. Description of its depth to the pharyngeal wall or oropharyngeal mucosal anatomic landmarks is not established.

Lingual artery

The LA arise from the ECA between the STA and the FA (**Figure 4**). It does a loop before extending further anteriorly at the level of the GCH. It is accompanied by the deep lingual vein which drains into the sublingual vein. LA passes medial to the GCH, CNXII, and SH, towards the BOT [68]. It is the chief blood supplier to the tongue and preservation of at least one of the two lingual arteries during tongue base lesion resection is important to avoid infarction of tongue [68].

Haemorrhage from the LA and its branches are possible during TORS radical tonsillectomy and TORS BOT resections [28, 32]. Proximal control of this vessel is beneficial during TORS due to the presence of numerous anastomoses distally [53]. External ligation of LA has shown a trend towards reduced severe post-operative haemorrhages in TORS cases [36]. Laurento et al., measured the lingual artery position from the foramen caecum within the OP [41]. O'Malley descried the position of LA within the OP as it would be encountered during TORS as 10mm medial to the posterolateral BOT and 15 to 20mm deep from the tongue surface [28]. The study also reported the LA is positioned lateral to IX at BOT [28]. Dallan et al., in 2013, showed the transoral superior to inferior view of the LA path within the BOT [61]. The study showed the topography of LA traverse between the genioglossus and geniohyoid muscles. The hyoglossus muscle separated the LA from XII at this level. Cohen et al., showed the LA position is different between resting and surgically positioned tongue [69]. They also showed that posterior to the horizontal line at the midway circumvallate papilla is a safe zone for BOT resection [69]. These studies do not explore the anatomy of the LA within the PPS. Gun et al., described the LA within the PS as being inferior and lateral to the SGM distal attachment at the BOT [69]. This Cohen et al.'s study however did not conduct depth measurements from the oropharyngeal mucosa to the LA at the PPS.

Facial artery

The FA branches anteriorly from ECA superior to the LA and sometimes from the linguofacial trunk. It passes superiorly along the superior constrictor, medial to the posterior belly of digastric, and SH. In the endoscopic transoral view of the PPS, the FA has been visualised anterior to ICA [54]. Gun et al's transoral dissection of PPS showed FA to be lateral to SPM and SGM approximately at level of palatine tonsil [55]. Ascending palatine artery (aPA) and tonsillar branch are given off to supply the superior constrictor, tonsil and soft palate. The aPA's close proximity to the pharyngeal constrictor, posterior to the SP was demonstrated transorally by Dallan et al. [54]. Variations of the aPA branching

origin was reported by Wang et al. In that study the aPA crossed the SGM 12.6 mm from the muscle's BOT insertion [67].

The tonsillar branch and aPA of FA are in close proximity to the tonsillar fossa. Gun et al.'s transoral dissections of the lateral pharyngeal wall revealed that the tonsillar fossa corresponded to the inferomedial portion of the PPS [55]. These studies did not measure its proximity to the lateral pharyngeal wall or the oropharyngeal mucosal sites. The proximity of the FA to SPM and SGM is also useful to know when exploring the PPS transorally which is currently not established.

The tonsillar branch of FA pierces the superior constrictor to enter lateral surface of tonsil [70]. This is the main arterial stream of the tonsil [53]. The FA travels deep to the submandibular gland indenting its medial surface. Here it makes an S-shaped turn and hooks over the superior border of the submandibular gland and then over the mandible. The external palatine vein drains the tonsil area into the facial vein.

Occipital artery

The OA is given off approximately at the same level as the FA and travels posteriorly deep to the posterior belly of digastric. It is crossed by the CNXII medially. The inferior branch to sternocleidomastoid of the OA holds the nerve down at this position. The upper sternocleidomastoid branch is a guide to the CNXI anteriorly at the superior border of sternocleidomastoid [52].

The OA continues posteriorly deep to the digastric notch indenting the base of skull at the occipitomastoid suture to supply the posterior scalp region. Due to its posterior course, the vessel is not encountered commonly in TORS of the OP and prestyloid space.

Maxillary artery and superficial temporal artery

The maxillary artery and the superficial temporal arteries are the terminal branches of the ECA given off within the parotid tissue. The superficial temporal artery travels superiorly supplying temporalis muscle and lateral scalp. The maxillary artery traverses medially within the infratemporal fossa lateral to the medial pterygoid.

Internal jugular vein

The IJV commences at the jugular bulb at the posterior compartment of the jugular foramen. The inferior petrosal sinus is its first tributary. At this level it is crossed by the CNXI laterally. The CNX lies between the medial border of the IJV and the ICA within the carotid sheath. It passes lateral to ICA as it descends. Due to its lateral position in the PPS, it is not frequently encountered during TORS. Dallan et al., demonstrated its endoscopic transoral topography lateral to ICA and posterior to SP at level above the soft palate and at level of the palatine tonsil [54].

Posterior to the IJV outside the carotid sheath is the cervical plexus arising through levator scapulae, phrenic nerve lying on anterior scalene and middle scalene. As it descends inferiorly it receives the following tributaries within the PPS: the pharyngeal plexus, facial, lingual and superior thyroid vein.

Lymphatics of the head and neck

The lymphatic drainage of the head and neck is such that there are numerous outlying nodes which are subcutaneous. All these nodes eventually drain to the deep cervical nodes. These nodes are scattered along the carotid sheath anteriorly and posteriorly. They are medial to the SCM. These are roughly divided into an upper group and a lower group. The upper group is found medial to the posterior belly of digastric. Thus the superior jugular chain lymph nodes are within the PPS. It also includes the jugulo-digastric nodes. This group receives lymphatics from the ear, posterior tongue, nose, sinuses, pharynx and the upper larynx. These lymph nodes often received metastases from the tonsillar fossa [70].

The lower group are at the level of the tendon of omohyoid thus they are outside the PPS. They are the jugulo-omohyoid group. The upper and lower groups are connected by lymphatic channels. They drain the anterior face, anterior tongue, lower larynx, thyroid and mediastinum. The left side lower deep cervical nodes drain to the thoracic duct. The right side lower deep cervical nodes drain to the lymphatic duct or right brachiocephalic vein. The retropharyngeal lymph nodes lie in the adipose tissue anterior to the prevertebral muscles and posterolateral to the lateral wall of the pharynx. It is divided to two groups – the medial group at the midline and the lateral group (nodes of Rouviere) medial to the ICA. They receive drainage from the OP [52].

The Level system to describe the lymph node positions of the neck is commonly used in clinical practice to describe the position of lymph nodes of interest. This system divides the neck to six levels. Level I is divided into two subgroups which are the Level IA - submental group and Level IB - submandibular group. The anterior belly of the digastric muscle and the hyoid bone form the triangular border of the submental group. The lymph nodes here are most likely to harbour metastatic disease originating from the floor of mouth, anterior tongue, anterior alveolar ridge and lower lip. The submandibular group is bordered by the anterior and posterior belly of digastric muscle, the mandibular body, and the stylohyoid muscle. The submandibular gland is sometimes removed when node clearance is undertaken in this zone [16]. Cancers that originate from the oral cavity, anterior nasal cavity, midface soft tissue and submandibular gland are likely to metastasize to Level IB.

Level II is the group of lymph nodes known as the upper jugular group. It is also subdivided into two groups. The vertical plane created by the CNXI is considered to be the division between subgroups

with Level IIB being in the superior position [16]. The group of lymph nodes from the skull base to the level of the inferior border of the hyoid bone, and around the upper third of the IJV are included in the Level II group. The anterior boundary is the lateral border is the stylohyoid muscle and the posterior boundary is the posterior edge of the SCM. Metastases received to this group of lymph nodes are from the nasal cavity, pharynx, oral cavity, larynx and the parotid gland.

Level III is known as the middle jugular group. It contains the lymph nodes around the middle third of the IJV from the inferior border of the hyoid bone superiorly to the inferior border of the cricoid cartilage inferiorly. The lateral edge of the sternohyoid muscle forms the anterior boundary. The posterior boundary is the posterior edge of the SCM. Cancers originating from the oral cavity, pharynx and larynx can metastasise to this group [16].

Level IV is the lower jugular group around the inferior third of the IJV. This zone extends from the inferior border of the cricoid superiorly to the clavicle inferiorly. The lateral border of the sternohyoid muscle is the anterior boundary of Level IV. The posterior boundary is the posterior edge of the SCM. These lymph nodes in this level can harbour metastases from cancers originating at the hypopharynx, larynx and cervical oesophagus.

Level V is known as the posterior triangle which is further subdivided to level VA and level VB. The lymph nodes along the distal half of CNXI, along the transverse cervical artery and the supraclavicular nodes are contained in Level V. The superior boundary is the point of convergence of the proximal attachment of the SCM and the trapezius muscle. The inferior boundary is the clavicle. The horizontal plane at the level of the inferior border of the cricoid cartilage arch divides this level further to level VA superiorly and level VB inferiorly [16]. Level VA contains the lymph nodes associated with CNXI. Level VB contains the lymph nodes associated with the transverse cervical artery and the supraclavicular nodes. Level VA is likely to receive metastases from the nasopharynx and OP. Metastases from the thyroid gland are likely to be found at level VB lymph nodes.

Level VI is known as the anterior or central compartment lymph nodes. This group contains the pretracheal nodes, paratracheal nodes, the precricoid node, and the lymph nodes along the recurrent laryngeal nerve. The inferior border of the hyoid bone is superior boundary and the suprasternal notch is the inferior boundary. The CCA forms the lateral boundary. The nodes here can harbour metastases from the thyroid gland, larynx, pyriform sinus and cervical oesophagus [16].

Summary

The transoral surgical approaches are gaining popularity with utility of TORS for resection of benign and malignant neoplasms of the palatine tonsil, BOT and PPS. The approach challenges the surgeon to conceptualise the anatomy of the PPS in a medial to lateral perspective. This has sparked an interest in reviewing the PPS anatomy from a transoral perspective. The key studies that contribute to our understanding of the transoral anatomy for TORS are summarised in **Table 1**. The development of novel technologies have opened a knowledge gap and an enthusiasm to revisit the parapharyngeal space anatomy which promoted the current study.

The pre-styloid space of the PPS is immediately lateral to the pharynx and is a relatively safe zone. The post-styloid space posterolateral to the styloid diaphragm contain the vital neurovascular structures of the PPS: ICA, ECA and the lower cranial nerves. The SPM and SGM are key anatomical landmarks for orientation within the PPS during TORS.

Post-operative haemorrhage is the most common complication of TORS [35]. LN, CNIX are at risk of injury during TORS radical tonsillectomy while achieving an adequate lateral margin of tumour. The CNXII and LN are at risk during tumour inferior margin resection during TORS radical tonsillectomy and BOT resections. Knowing the ICA relationship to the pharyngeal wall is vital to avoid catastrophic haemorrhage during TORS.

The relationship of these structures to specific oropharyngeal mucosal landmarks with depth measurements is a potential area for further study. Knowing the normal medial to lateral depth to these structures from the OP is useful to avoid injury and to appreciate tumour related structural displacements. TORS outcomes have the potential to improve if there is greater appreciation of the likelihood of known complications that can be avoided through the application of new detailed anatomical information.

Aims of the study

1. Describe the topography and measure the distance to key neurovascular structures of the PPS relative to SPM and SGM.

2. Describe the PPS neurovascular relationships relative to the tonsillar fossa region with key depth proximity measurements from the lateral pharyngeal wall, oropharyngeal mucosa and tonsillar fossa apex.

3. Describe the inferior PPS neurovascular relationship to the lateral pharyngeal wall, oropharyngeal mucosa, vallecula, and foramen caecum at the BOT region.

Table 1*: Summary table of publications relevant to anatomy for transoral robotic surgery of the oropharynx and parapharyngeal space. Abbreviations:* ***n****, the number of study materials used. Where different types of material are used in a single study, the number is stated in the respective order.* ***APA****, ascending pharyngeal artery,* ***aPA*** *ascending palatine artery,* ***CNIX*** *glossopharyngeal nerve,* ***CNX*** *vagus nerve,* ***CNXI*** *accessory nerve,* ***CNXII*** *hypoglossal nerve,* ***ICA*** *internal carotid artery,* ***IJV*** *internal jugular vein,* ***LA*** *lingual artery,* ***SPM*** *stylopharyngeus,* ***SGM*** *styloglossus,* ***TORS*** *transoral robotic surgery,* ***BOT*** *base of tongue,* ***OP*** *oropharynx*

Paper	**Study material (n)**	**Transoral anatomy contribution for TORS**	**Areas for further study**
Laurento et al., 1997 [41]	Cadavers (10)	From foramen caecum, LA and CNXII neurovascular bundle is 2.7cm inferior and l.6cm lateral. This neurovascular bundle is 0.9cm superior to the hyoid bone.	LA root/ LA at PPS measurements.
Ohtsuka et al., 2002 [58]	Cadavers & histology (55, 37)	Tonsil fossa muscular dehiscence brings glossopharyngeal nerve close to the tonsillar capsule in 21.5% of cases. CNIX is between SGM and SPM as it descends towards tongue base.	Distance from tonsillar fossa to IX. Proximity to SPM & SGM distance.
O'Malley et al., 2006 [28]	Cadavers, live canine, clinical trial (3,2, 3)	LA 1 cm medial to posterolateral BOT and 1.5-2 cm deep into tongue muscle, CNXII 1 cm deep to LA, CNIX medial to LA at BOT.	Parapharyngeal portion of LA.
Weinstein et al., 2007 [32]	Clinical trial (27)	TORS radical tonsillectomy technique description, intraoperative LA haemorrhage warning at general BOT level resection.	LA haemorrhage danger zone.
Ozgur et al., 2007 [49]	Cadavers & histology (50, 50)	ICA medially tortuous in 25%, 5% had kinking of dissected specimens. Kin -ked ICAs had thin tunica media and dissections in tunica media and adventitia.	Pharyngeal aspect correspondence to position of aberrant ICA. Distance

			measurements from ICA to OP.
Pfeiffer et al., 2008 [62]	Radiology (21)	Aberrant ICA closest distance to pharyngeal wall was 7mm (range 0.8 to 17.9mm). New classification taking into account ICA relation to pharyngeal wall and pharyngeal region.	Correlation with cadaveric material and to specific oropharyngeal mucosal landmarks.
Dallan et al., 2011 [54]	Cadavers (6)	Descriptive transoral endoscopic anatomy of the parapharyngeal space. SPM and SGM transoral view of orientation described and established as key landmarks. Endoscopic transoral orientation of ICA, ECA, FA, APA, aPA, IJV, CNIX, CNX, CNXI, and CNXII.	Relate PS structures to oral mucosa landmarks.
Moore et al., 2012 [70]	Descriptive review	Descriptive anatomy of lateral OP, palatine tonsil and tongue base with emphasis on TORS approach. Transoral robotic techniques for lateral oropharyngectomy and BOT cancer resection.	Topographical relations from transoral view.
Dallan et al., 2013 [61]	Cadavers & radiology (7, 10)	Superior to inferior transoral anatomy of tongue base. Medial to lateral dissection of BOT through tongue intrinsic musculature is safe. LA on lateral surface of genioglossus, CNXII on lateral surface of hyoglossus.	LA and CNXII topography at the inferior PPS region. Distance from OP to PPS LA and CN XII.
Lim et al., 2013 [59]	Cadavers & radiology (6, 2)	CNIX at junction of posterior tonsillar pillar and BOT. Lateral pharyngeal wall to ECA at C2/C3 intervertebral disc level on left and right, 17.6mm and 18.4mm, respectively. Greater cornu of hyoid to ECA at C6 vertebrae level on left and right, 3.4 and 4.3mm, respectively.	Tonsillar fossa to CNIX distance. Measurements from medial pharyngeal wall. Relation to LA and ICA to medial pharyngeal wall and tonsillar fossa.

Wang et al., 2014 [67]	Cadavers (6)	Ascending palatine artery originated from FA in 67% of cases. Ascending palatine artery is crossed by SGM 12.6mm from tongue base insertion. In 8% of cases ECA bulged medially towards pharynx between SGM and SPM.	The arterial vessels' distances to OP mucosa.
Cohen et al., 2016 [69]	Cadavers (5)	LA position differed between resting and surgically positioned tongue. Posterior to the horizontal line at the midway circumvallate papilla is a safe zone for BOT resection.	Distance to parapharyngeal LA portion from OP.
Gun et al., 2016 [55]	Cadavers (5)	Descriptive transoral anatomy - SGM, SPM, LA, FA, CNIX. Stylohyoid ligament as a key landmark is situated between SGM and SPM. At SGM insertion to tongue base, LA is lateral and inferior to SGM. Lateral aspect of tonsillar fossa corresponds to inferomedial PPS.	Distances from medial oropharyngeal mucosa l to LA, FA, LN, ICA. Vallecula to LA, FA, and GCH distances.
Pfeiffer et al., 2015 [63]	Radiology (125)	Grading system for the risk of injury to aberrant ICA accounting for case load at each pharyngeal region.	Link to medial pharyngeal wall specific landmarks and provide depth measurements.
Wang et al., 2016 [60]	Cadavers (8)	CNIX described in three segments with respect to its relationship to SP. 75% of the time CNIX is crossed by the pharyngeal branch of CNX, and 25% of the time parallel.	CNIX distance to oropharyngeal mucosal landmarks.

Methods

Human cadaveric material

Ethics approval was granted for the study through the Bond University Human Research Ethics Approval Committee (RO1546). Formaldehyde-fixed cadaveric head and neck specimens were sourced from the Bond University Medical Program gross anatomy dissection series between 2015 and 2016. Cadavers with a history of neck procedures or primary or metastatic malignancy involving the pharynx at time of death were excluded from the study. Age range of dissected subjects were 66 to 94 years. Two cadaveric heads sectioned mid-sagitally were dissected from the pharyngeal aspect to familiarise the medial to lateral PPS anatomy. This was followed by dissection of thirteen coronally sectioned cadaveric head and neck specimens.

Cadaver preparation

Each intact cadaver's CCA and IJV were injected on both sides with coloured latex dye. A 3cm incision was made along the anterior border sternocleidomastoid muscle at the root of neck. The tissue was dissected down to the SCM muscle and its distal one third was well defined. The muscle was retracted laterally here and the carotid sheath was identified. Within the carotid sheath CCA and IJV were identified. A metal cannula was introduced to each vessel with a small incision. Normal saline was injected to flush the vessels to inflate the vessels and clear the lumen. Next 5-10mL of red coloured latex was injected to the CCA. Adequate perfusion was confirmed when colour injection was observed on the contralateral or ipsilateral oral mucosa. IJV was injected with 15mL of blue latex and adequate perfusion was confirmed the same way. Post injection the cadavers were left in the freezer for 24 hours before sectioning to ensure setting of the latex. The cadaver preparation process described by Wang et al. was used in our study [67].

The injected cadavers were decapitated at the root of neck with a powered saw. Mid-sagittal sections were made with a thin hacksaw blade. The coronal sections were made superior to inferior along a plane anterior to the prevertebral musculature. The cervical vertebrae and its lateral processes were used as a guide, confirmed through palpation. Furthermore, on the decapitated specimen, inferiorly the prevertebral muscles were easily identified to achieve the correct plane.

Dissection steps

Dissections were performed with the aid of a surgical microscope on the left side and right side on all cadaveric specimens. Measurements were made to ipsilateral landmarks within the PPS and oropharynx utilising a digital Vernier calliper.

Mid-sagittal sectioned cadavers

The following key pharyngeal mucosal landmarks were identified: palatine tonsil, palatoglossal arch, palatopharyngeal arch, BOT, foramen caecum, and vallecula. The dissection was performed in four main steps. The first step was to remove the pharyngeal mucosa using a combination of shape scalpel scissor dissection. Palatoglossus, palatopharyngeus, salpingopharyngeus, superior and middle pharyngeal constrictor muscles were identified. The second step involved removal of the superior and middle pharyngeal constrictor. Care was taken to identify and leave the buccopharyngeal fascia with only muscle removed during this step. Next the buccopharyngeal fascia was divided to enter the PPS. GCH was identified inferiorly. The adipose tissue that was encountered were carefully removed to identify the next anatomical structure. SPM distal attachment was identified when the pharyngeal wall was reflecting off. The SGM distal attachment at the BOT was identified by dissecting superior and lateral to the GCH.

The third step was to expose the poststyloid space. The prestyloid space adipose tissue was removed completely. SPM and SGM were further dissected superiorly towards their proximal attachment at the styloid process.

The final step was to dissect the PPS neurovasculature from the inferior PPS towards the skull base. The path of the following vascular structures were identified: CCA, IJV, ICA, ECA, LA, FA, APA, and aPA. The carotid sheath was identified at the level of the hyoid bone. Then the sheath was dissected inferior to the GCH to identify the CCA and IJV. The CCA was dissected superiorly to identify the bifurcation to ICA and ECA. From this point the branches of ECA were dissected as they were encountered as the dissection progressed superiorly.

Following lower cranial nerves were identified at the level of the OP: CNIX, CNX, and CNXII. The CNIX was identified at the point it pierces the pharyngeal constrictor muscle. The proximal portion of the nerve was dissected superiorly from this point. The CNX was first found between the CCA and IJV within the carotid sheath. Next the nerve was dissected superiorly.

Photographs were taken at the beginning and end of each step to keep record of the observed topographical relationships and anatomical variations.

Coronal sectioned cadavers

The prevertebral fascia was removed to expose the pharynx on the midline and the PPS lateral to the pharynx. The buccopharyngeal fascia was identified and dissected off. The posterior aspect of the pharyngeal constrictor muscle was incised at the midline to ender the pharynx. Within the pharynx

the following key anatomical landmarks were identified with pin: vallecula, left and right tonsillar fossa apex (TFA), and foramen caecum.

The GCH was identified with palpation. The CCA was dissected inferior to the GCH till the bifurcation to ICA and ECA was discovered. Lateral to this the IJV was identified. ICA and IJV path was dissected superiorly, towards the skull base. The variations of the ICA path as it ascended to the skull base was noted. The extracranial proximal portion of the lower cranial nerves CNIX, CNX, CNXI and CNXII were identified as the superior portion of the IJV was dissected. From that point these nerves were dissected inferiorly along their path.

Near the skull base the superior laryngeal nerve (SLN) branching off the CNX was identified. Next this nerve was dissected to identify its branches the internal laryngeal nerve (ILN) and external laryngeal nerve (ELN). The ILN and ELN were dissected medially towards the larynx and cricothyroid muscle, respectively.

Next attention was directed towards the proximal portion of the ECA. STA and LA were identified. LA path was dissected from the ECA toward the point where the vessel pass anterior to the posterior border of the hyoglossus muscle. The inferior portion of CNXII at proximity to the GCH was identified. The nerve was dissected anteriorly to the point it enters the submandibular space. The FA's pathway was dissected from the ECA towards the mandible and stopped where it exited the PPS. The aPA branch off pattern from the FA was observed and this artery was dissected to its distal end. The frequency of the presence of the linguofacial trunk was recorded. The APA branch off point at the ECA was identified and dissected superiorly.

Distal attachment of the SPM at the pharyngeal constrictor muscle was identified and dissected towards its proximal attachment at the styloid process. The prestyloid adipose tissue anterior to the SPM was removed. From the styloid process SHM and SGM muscles were identified and dissected towards their distal attachment sites. The length of SGM and SPM were measured and their midpoints were marked with a pin. The position of the midpoint of SGM and SPM were correlated to the subregions of the pharynx on the axial plane.

Photographs were taken of the neurovascular and muscular structural relationships at the inferior PPS adjacent the BOT, the PPS adjacent the tonsillar fossa and PPS region encompassing the styloid apparatus.

Measurements

Following the completion of the dissection distances to key neurovascular and muscular structures were measured from nine key landmarks:

1. Oropharyngeal mucosal surface
2. Lateral wall of the pharyngeal constrictor
3. Midline BOT at the foramen caecum
4. Vallecula
5. GCH
6. Superior pole of tonsillar fossa
7. Styloid process tip
8. Midpoint of SPM
9. Midpoint of SGM

The distances from the following structures to the oropharyngeal mucosa were measured on the axial plane (**Figure 5**):

1. SPM midpoint
2. SGM midpoint
3. LA at PPS closest distance
4. LA branch off point at ECA
5. FA at PPS closest distance
6. FA branch off point at ECA
7. CNIX at level of SP midpoint
8. CNXII at GCH level
9. LN at its most inferior margin

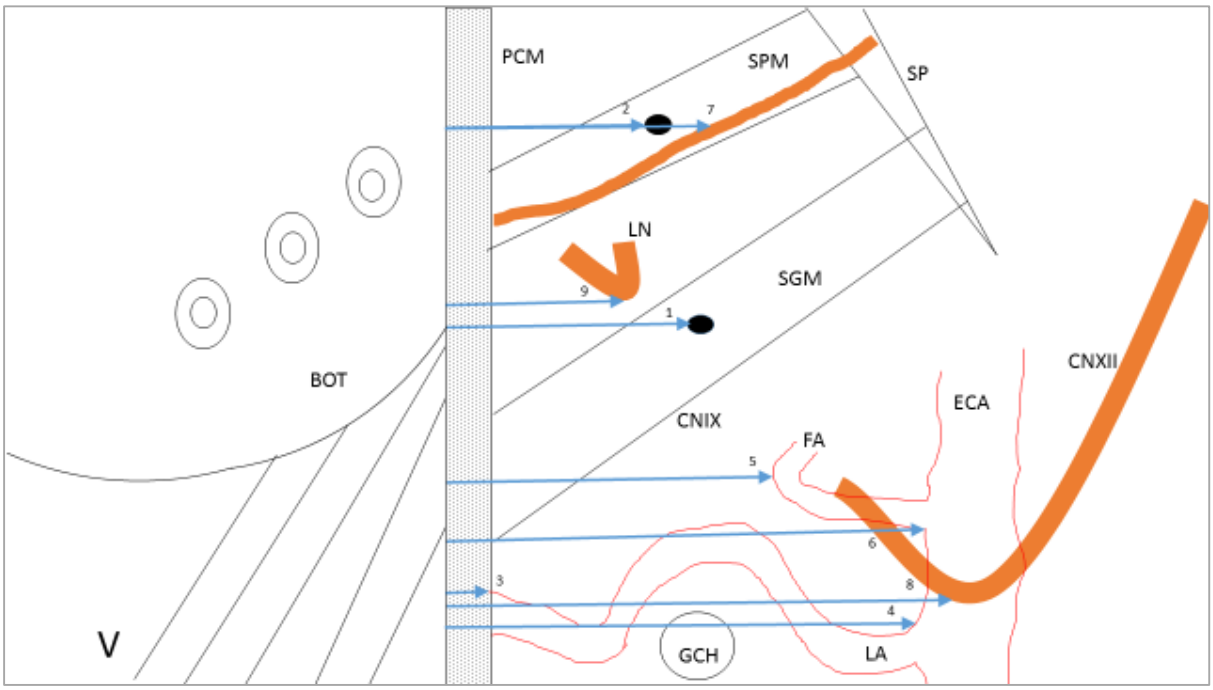

Figure 5: A schematic drawing of a right sided parapharyngeal space and portion of the ipsilateral oropharynx. The blue arrows represent distances measured from the oropharyngeal mucosal surface to structures of the ipsilateral parapharyngeal space. The corresponding numbers represent the structure to which the measurement is made to. 1. Stylopharyngeus muscle midpoint, 2. Styloglossus midpoint, 3. Lingual artery at parapharyngeal space closest distance, 4. Lingual artery branch off point at external carotid artery, 5. Facial artery at parapharyngeal space closest distance, 6. Facial artery branch off point at external carotid artery, 7. Glossopharyngeal nerve at level of stylopharyngeus midpoint, 8. Hypoglossal nerve at greater cornu of hyoid level, 9. Lingual nerve at its most inferior margin. The **black dot** represents the midpoints of the stylopharyngeus and styloglossus muscles. **Abbreviations**: **BOT** base of tongue, **CNIX** glossopharyngeal nerve, **CNXII** hypoglossal nerve, **ECA** external carotid artery, **FA** facial artery, **GCH** greater cornu of hyoid bone's posterior end. **LN** lingual nerve, **PCM** pharyngeal constrictor muscle, **SGM** styloglossus muscle, **SP** styloid process, **SPM** stylopharyngeus muscle, **V** vallecula midpoint.

The measurements were repeated from each of the above structures to the lateral wall of the pharyngeal constrictor muscle on the axial plane (**Figure 6**).

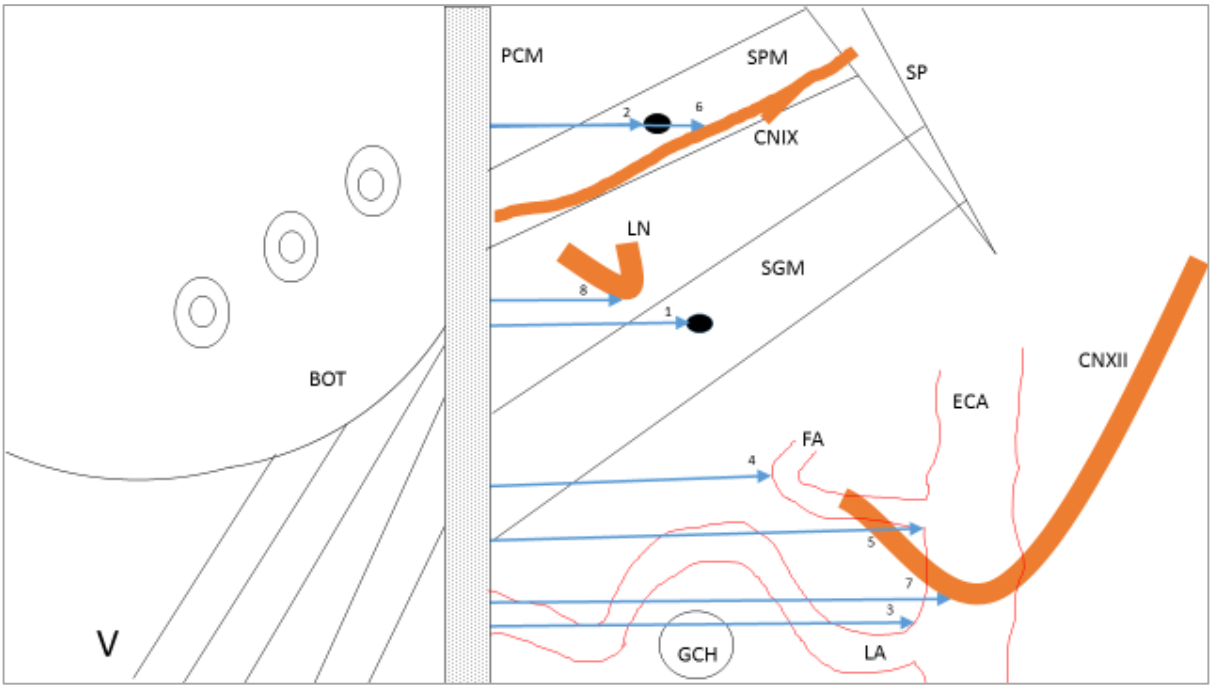

Figure 6: A schematic drawing of a right sided parapharyngeal space and portion of the ipsilateral oropharynx. The blue arrows represent distances measured from the lateral surface of the pharyngeal constrictor muscle to structures of the ipsilateral parapharyngeal space. The corresponding numbers represent the structure to which the measurements are made to. 1. Stylopharyngeus muscle midpoint, 2. Styloglossus midpoint, 3. Lingual artery branch off point at external carotid artery, 4. Facial artery at parapharyngeal space closest distance, 5. Facial artery branch off point at external carotid artery, 6. Glossopharyngeal nerve at level of stylopharyngeus midpoint, 7. Hypoglossal nerve at greater cornu of hyoid level, 8. Lingual nerve at its most inferior margin. The **black dot** represents the midpoints of the stylopharyngeus and styloglossus muscles. **Abbreviations**: **BOT** base of tongue, **CNIX** glossopharyngeal nerve, **CNXII** hypoglossal nerve, **ECA** external carotid artery, **FA** facial artery, **GCH** greater cornu of hyoid bone's posterior end. **LN** lingual nerve, **PCM** pharyngeal constrictor muscle, **SGM** styloglossus muscle, **SP** styloid process, **SPM** stylopharyngeus muscle, **V** vallecula midpoint.

The linear distance from midline BOT at the foramen caecum to the following structures were measured (**Figure 7**):

1. LA at PPS closest distance
2. LA branching off point at ECA
3. CNXII at PPS closest distance
4. FA branch off point at ECA
5. FA at PPS closest distance
6. CNIX at PPS closest distance

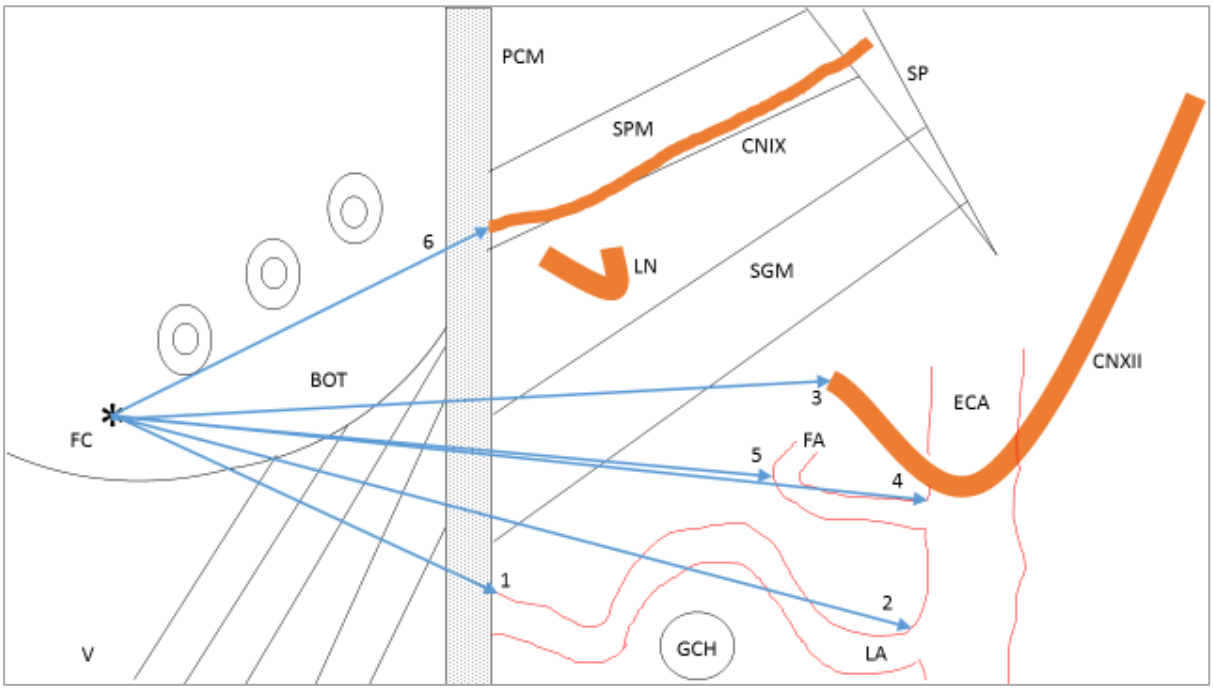

***Figure 7**: A schematic drawing of a right sided parapharyngeal space and portion of the ipsilateral oropharynx. The foramen cecum of tongue base is marked with an asterisk. The blue arrows represent distances measured from the foramen cecum to structures of the ipsilateral parapharyngeal space. The corresponding numbers represent reference points to which the measurements are made to. 1. Lingual artery at parapharyngeal space closest distance, 2. Lingual artery branch off point at external carotid artery, 3. hypoglossal nerve at parapharyngeal space closest distance, 4. Facial artery branch off point at external carotid artery, 5. Facial artery at parapharyngeal space closest distance, 6. Glossopharyngeal nerve at parapharyngeal space closest distance. **Abbreviations**: **BOT** base of tongue, **CNIX** glossopharyngeal nerve, **CNXII** hypoglossal nerve, **ECA** external carotid artery, **FA** facial artery, **FC** foramen cecum, **GCH** greater cornu of hyoid bone's posterior end. **LN** lingual nerve, **PCM** pharyngeal constrictor muscle, **SGM** styloglossus muscle, **SP** styloid process, **SPM** stylopharyngeus muscle, **V** vallecula midpoint*

The linear distance from the vallecula to the following structures were measured (**Figure 8**):

1. LA at PPS closest distance
2. LA branch off at ECA
3. CNXII at PPS closest distance
4. FA at PPS closest distance
5. FA branch off point at ECA

These distances are measured from the midline position of the vallecula. In the sagittal plane this position would closely fall in line with the position of the foramen caecum of BOT.

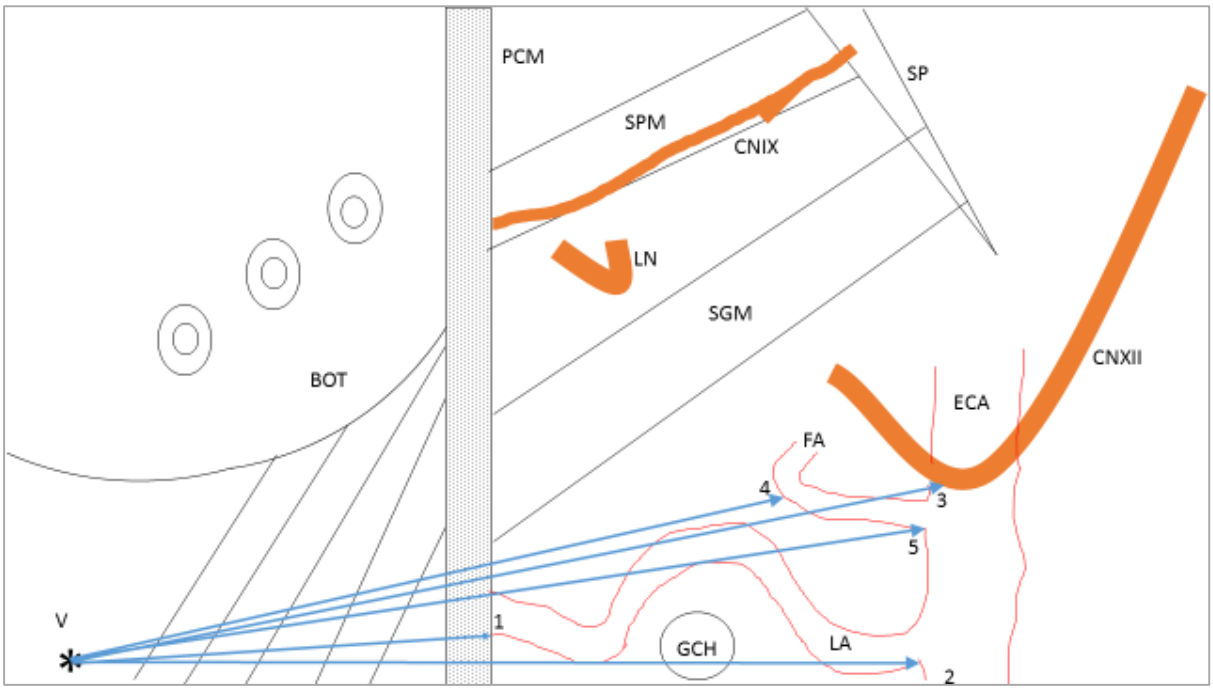

Figure 8: A schmetatic drawing of a right sided parapharyngeal space and portion of the ipsilateral oropharynx. The blue arrows represent distances measured from the midpoint of vallecula, which is marked with an asterisk, to structures of the ipsilateral parapharyngeal space. The corresponding numbers represent reference points to which the measurements are made to. 1. Lingual artery at parapharyngeal space closest distance, 2. Lingual artery branch off at external carotid artery, 3. Hypoglossal nerve at parapharyngeal space closest distance. 4. Facial artery at PPS closest distance, 5. Facial artery branch off point at external carotid artery. **Abbreviations**: **BOT** base of tongue, **CNIX** glossopharyngeal nerve, **CNXII** hypoglossal nerve, **ECA** external carotid artery, **FA** facial artery, **GCH** greater cornu of hyoid bone's posterior end. **LN** lingual nerve, **PCM** pharyngeal constrictor muscle, **SGM** styloglossus muscle, **SP** styloid process, **SPM** stylopharyngeus muscle, **V** vallecula midpoint

The linear distance from the following structures to GCH were measured (**Figure 9**):

1. Vertical distance to LA
2. LA branching off point at ECA
3. CNXII at PPS closest distance
4. LN at PPS closest distance
5. FA at PPS closest distance
6. FA at branch off point from ECA

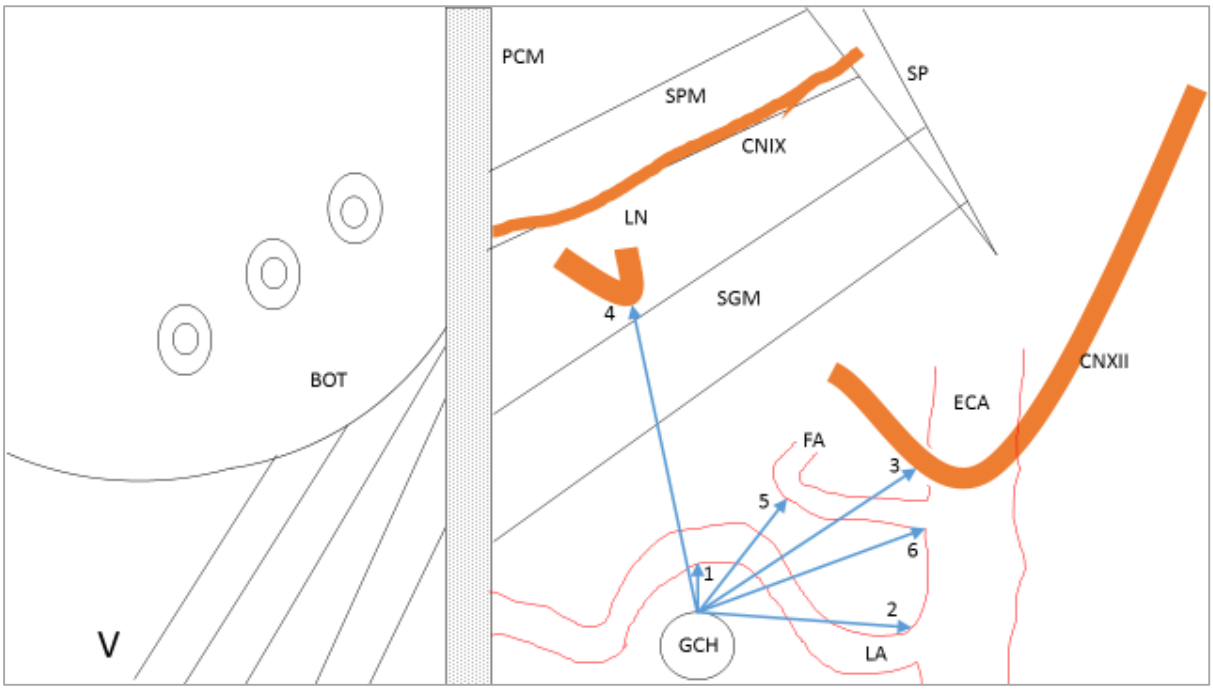

Figure 9: A schematic drawing of a right sided parapharyngeal space and portion of the ipsilateral oropharynx. The blue arrows represent distances measured from the posterior end of greater cornu of hyoid bone. The corresponding numbers represent reference points of the ipsilateral parapharyngeal space to which the measurements are made to. **Abbreviations**: **BOT** base of tongue, **CNIX** glossopharyngeal nerve, **CNXII** hypoglossal nerve, **ECA** external carotid artery, **FA** facial artery, **GCH** greater cornu of hyoid bone's posterior end. **LN** lingual nerve, **PCM** pharyngeal constrictor muscle, **SGM** styloglossus muscle, **SP** styloid process, **SPM** stylopharyngeus muscle, **V** vallecula midpoint

The distance from the following structures to the ipsilateral superior pole of tonsillar fossa was measured on the axial plane (**Figure 10**):

1. ICA
2. ECA
3. APA
4. aPA
5. Styloid process tip
6. SPM midpoint
7. SGM midpoint

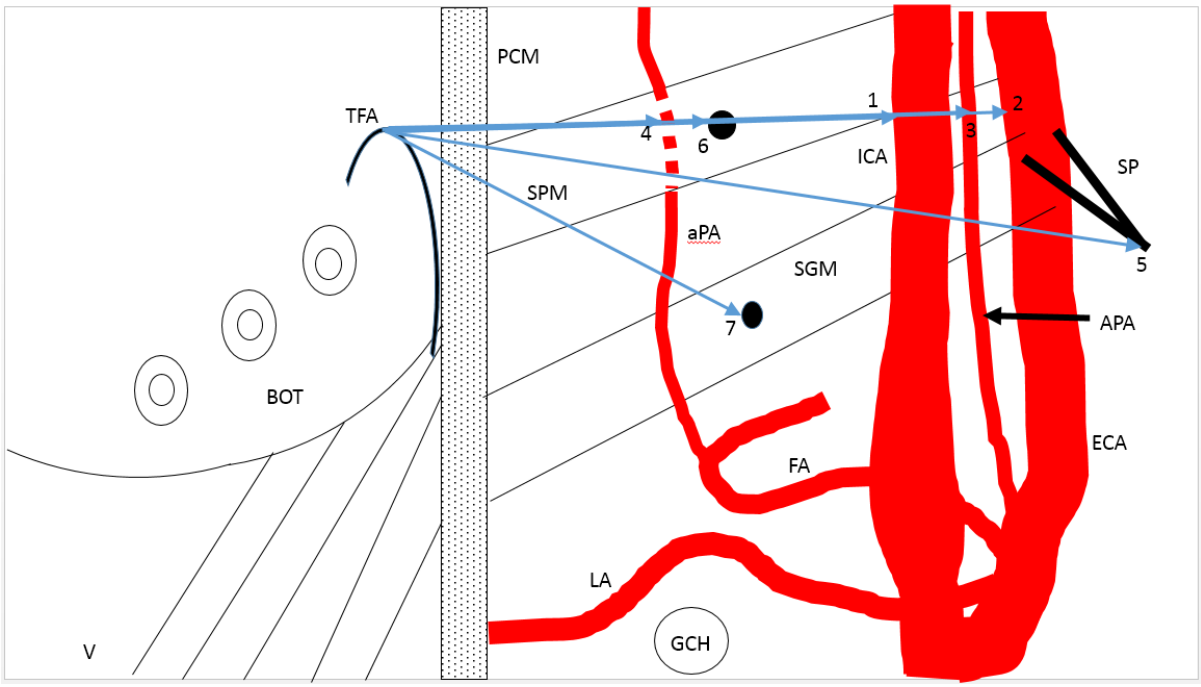

Figure 10: A schematic drawing of a right sided parapharyngeal space and portion of the ipsilateral oropharynx. The **black dot** represents the midpoints of the stylopharyngeus and styloglossus muscles. The blue arrows represent distances measured from the tonsillar fossa apex. The corresponding numbers represent reference points of the ipsilateral parapharyngeal space to which the measurements are made to. **Abbreviations**: **APA** ascending pharyngeal artery, **aPA** ascending palatine artery, **BOT** base of tongue, **ECA** external carotid artery, **FA** facial artery, **GCH** greater cornu of hyoid bone's posterior end, **ICA** internal carotid artery, **PCM** pharyngeal constrictor muscle, **SGM** styloglossus muscle, **SP** styloid process, **SPM** stylopharyngeus muscle, **V** vallecula midpoint

The distance from the following structures to the styloid process distal tip was measured on the axial plane (**Figure 11**):

1. CNIX
2. ECA
3. ICA
4. The pharyngeal mucosa
5. The lateral wall of the pharyngeal constrictor muscle

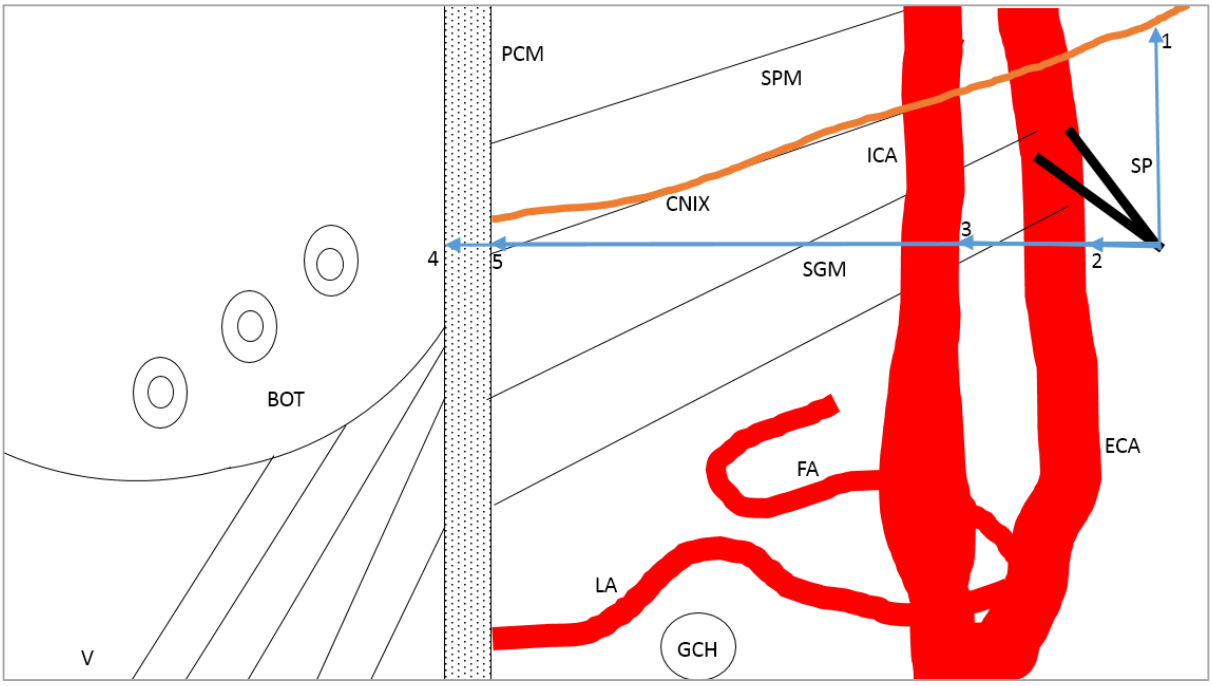

Figure 11: A schematic drawing of a right sided parapharyngeal space and portion of the ipsilateral oropharynx. The blue arrows represent distances measured from distal end of the styloid process. The corresponding numbers represent reference points of the ipsilateral parapharyngeal space to which the measurements are made to. **Abbreviations**: **BOT** base of tongue, **ECA** external carotid artery, **FA** facial artery, **GCH** greater cornu of hyoid bone's posterior end, **ICA** internal carotid artery, **PCM** pharyngeal constrictor muscle, **SGM** styloglossus muscle, **SP** styloid process, **SPM** stylopharyngeus muscle, **V** vallecula midpoint

The linear distance from following structures to the midpoint of SPM was measured (**Figure 12**):

1. Horizontal distance to ECA
2. Horizontal distance to ICA
3. Vertical distance to LA
4. LA branch off at ECA
5. Vertical distance to FA
6. Facial artery branch off point at ECA
7. OA branch off point at ECA
8. CNIX
9. Styloid process tip

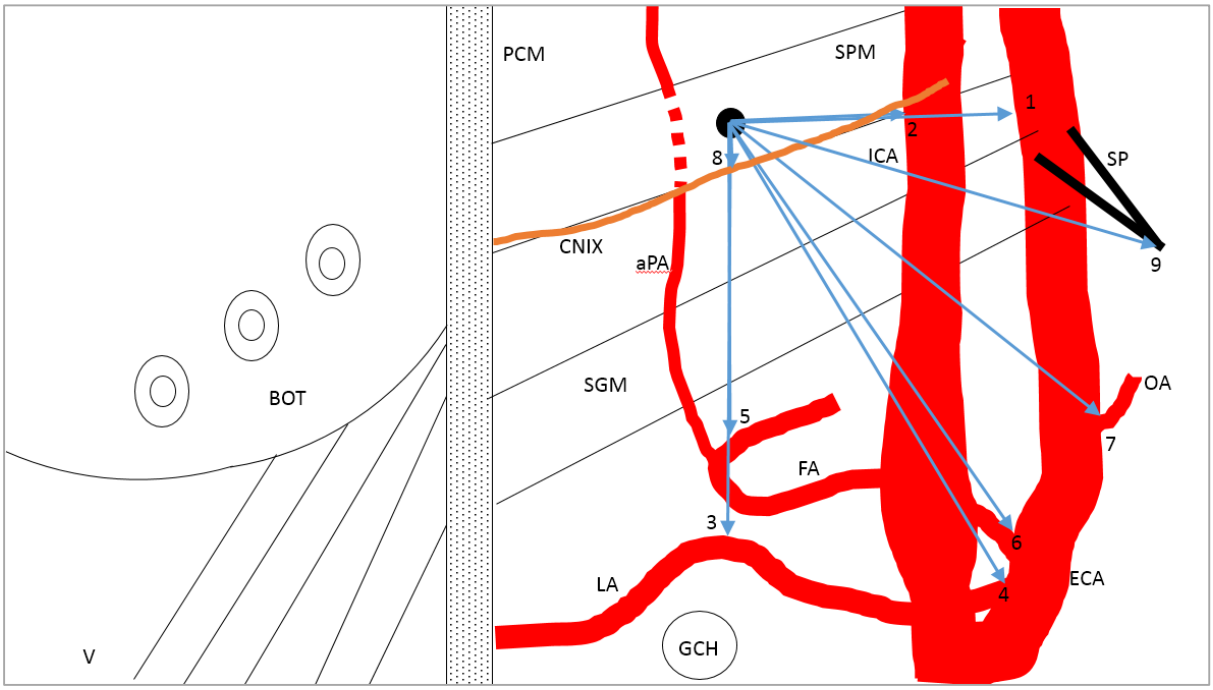

Figure 12: A schematic drawing of a right sided parapharyngeal space and portion of the ipsilateral oropharynx. The **black dot** represents the midpoint of the stylopharyngeus muscle. The blue arrows represent distances measured from the stylopharyngeus muscle midpoint. The corresponding numbers represent reference points of the ipsilateral parapharyngeal space to which the measurements are made to. **Abbreviations**: **aPA** ascending palatine artery, **BOT** base of tongue, **ECA** external carotid artery, **FA** facial artery, **GCH** greater cornu of hyoid bone's posterior end, **ICA** internal carotid artery, **PCM** pharyngeal *constrictor muscle*, ***SGM*** *styloglossus muscle*, ***SP*** *styloid process*, ***SPM*** *stylopharyngeus muscle*, ***V*** *vallecula midpoint*

The measurements were repeated from each of the above structures to the midpoint of SGM (**Figure 13**).

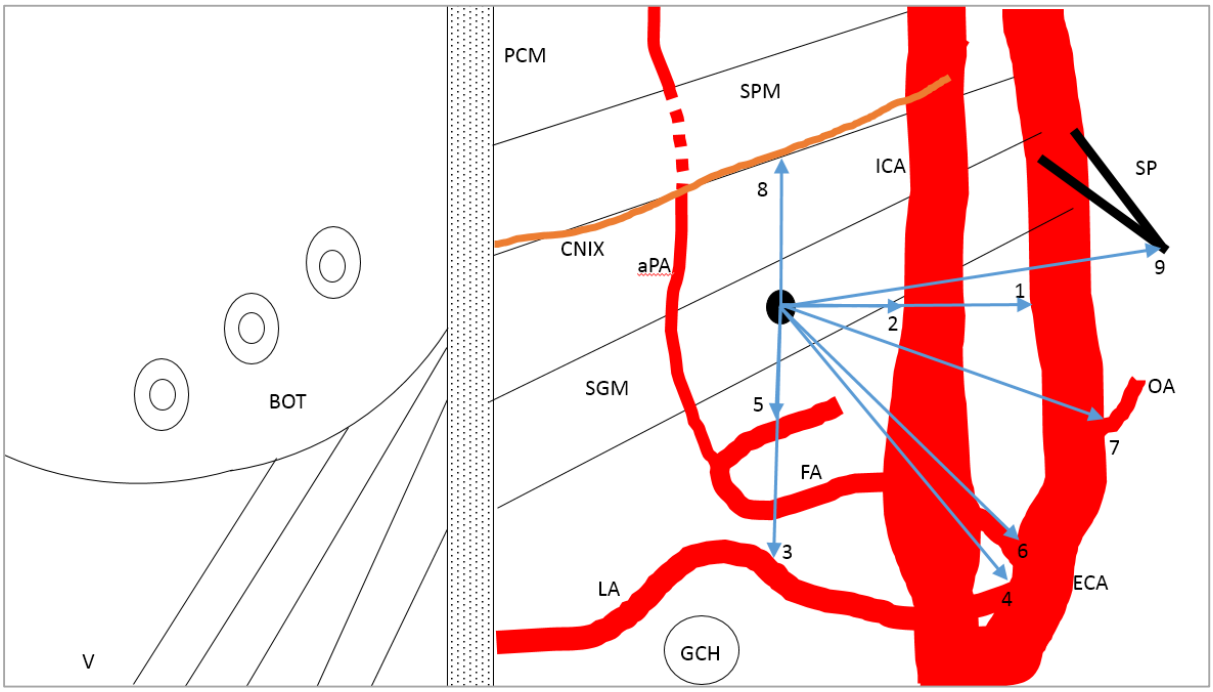

***Figure 13**: A schematic drawing of a right sided parapharyngeal space and portion of the ipsilateral oropharynx. The **black dot** represents the midpoint of the styloglossus muscle. The blue arrows represent distances measured from the styloglossus muscle midpoint. The corresponding numbers represent reference points of the ipsilateral parapharyngeal space to which the measurements are made to. **Abbreviations**: **aPA** ascending palatine artery, **BOT** base of tongue, **ECA** external carotid artery, **FA** facial artery, **GCH** greater cornu of hyoid bone's posterior end, **ICA** internal carotid artery, **OA** occipital artery, **PCM** pharyngeal constrictor muscle, **SGM** styloglossus muscle, **SP** styloid process, **SPM** stylopharyngeus muscle, **V** vallecula midpoint*

Data Analysis

Statistical analysis was performed on SPSS (IBM SPSS Statistics, version 24, Armonk, NY, USA).

For each measurement from left side and right side was summarised with a mean, standard deviation and range. Paired t-test was performed to check for significant difference between left and right side for each measurement.

Results

Sagittal sectioned cadaver dissection

The exploration of the PPS began with the dissection of the hemisected head and neck specimens. The medial to lateral dissections from the oropharyngeal mucosa to the PPS were conducted in four hemisected specimens. The midsagittal hemisected specimen revealed the relative positions of the vallecula of epiglottis, foramen cecum and tonsillar fossa on the oropharyngeal mucosa. The removal of the oropharyngeal mucosal layer exposed the medial aspect of the three pharyngeal constrictor muscles to view. The separation between the superior and middle constrictor muscle was deduced based on the direction of the muscle fibres. A variable degree of dehiscence between these two layers were observed in each specimen. The SPM and CNIX were observed passing through this dehiscence (**Figure 14C**).

The path of SPM and CNIX were able to be traced superiorly once the pharyngeal constrictors was removed. Once this layer of thin muscles was dissected off, a network of arteries, veins and nerves was found traversing through the buccopharyngeal fascia to supply the muscle. Dissection lateral to this fascia revealed the SGM and SPM muscles on its entire length from distal to proximal attachment sites. There was always an intimate relationship between the SPM and CNIX. Where the nerve would be consistently found at the inferior border of the proximal part of the SPM near its attachment to the styloid process (**Figure 14D and F**). At this level of dissection superiorly, the prestyloid space was composed of with adipose tissue (**Figure 14E**).

Once this adipose tissue was removed the medial aspect of the parotid was encountered. The parotid tissue covered the medial side of the medial pterygoid muscle. Lateral to the adipose tissue of the prestyloid space, the medial pterygoid muscle was encountered (**Figure 14F**). Posterior to the medial pterygoid muscle, the ECA and ICA was found at close proximity to the SPM and SGM muscles' proximal attachment sites (**Figure 14F**). The SPM muscle and CNIX passes between the ICA and ECA. The proximal end of the muscle was often in contact with the ICA and ECA.

At the level of the vallecula, when the middle pharyngeal constrictor and the buccopharyngeal fascia was removed, the GCH, CNXII, and LA were encountered. The LA was often encountered making a loop above the posterior tip of the GCH before travelling to the tongue base. CNXII was found lateral to the level of the GCH. CNXII came into view from posterior aspect of ICA. Superior to the LA, the FA was found looping over the superior border of SHM and disappearing out of view laterally (**Figure 14F**).

The mid-sagittal specimen dissection limited the study from viewing the poststyloid space in its entirety. The space was well confined by the bulk of the tongue base anteriorly and the cervical vertebrae posteriorly. Further, in this dissection approach the destruction of medially positioned oropharyngeal landmarks made distance correlations between the oropharyngeal mucosa and PPS structures impossible. Thus, it was decided to expand the study with coronally sectioned cadavers for improved access.

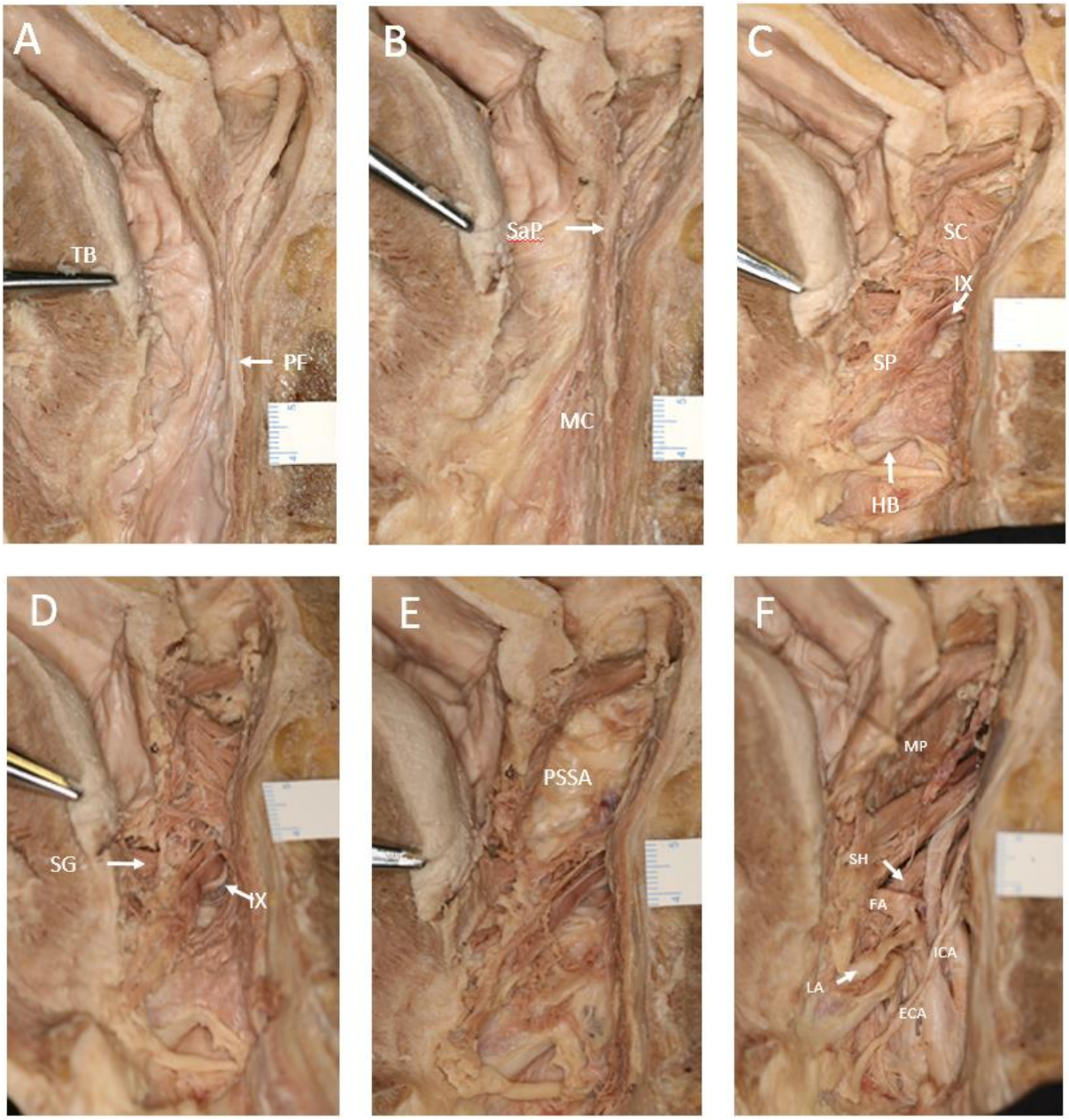

Figure 14 Mid-sagittal section of head and neck specimen. A. pharyngeal mucosa before dissection. **B.** Medial aspect of the pharyngeal constrictor muscles. **C**. stylopharyngeus passing through superior and middle constrictor, hyoid bone inferiorly. **D.** Stylopharyngeus and distal styloglossus attachment. **E.** Superior constrictor and middle constrictor removed. Prestyloid space adipose tissue present superiorly. **F.** Poststyloid space dissection with external carotid artery and internal carotid artery in view. Superiorly stylopharyngeus muscle, styloglossus muscle and, inferiorly the distal portion of stylohyoid present. **Abbreviations**: **TB** tongue base, **PF** prevertebral fascia, **MC** middle constrictor, **SaP** salpingopharyngeus, **SP** stylopharyngeus muscle, **HB** hyoid bone, **SC** superior constrictor, **IX** glossopharyngeal nerve, **SGM** styloglossus muscle, **PSSA** prestyloid space adipose tissue, **LA** lingual artery, **FA** facial artery, **ECA** external carotid artery, **ICA** internal carotid artery, **SH** stylohyoid, **MP** medial pterygoid muscle.

Coronal section dissections

Thirteen coronally sectioned cadavers which equated to twenty-six sides were dissected to obtain further correlation between the oropharyngeal mucosal landmarks and the PPS neurovascular structures. These specimens revealed the poststyloid space better than the mid-sagitally sectioned specimens. They also allowed depth measurements from the oropharynx to the neurovasculature of the PPS (**Figure 15**). The focus was on observing anatomical relations from the PPS structures to oropharynx, anatomical variations and distance measurements between key anatomical landmarks.

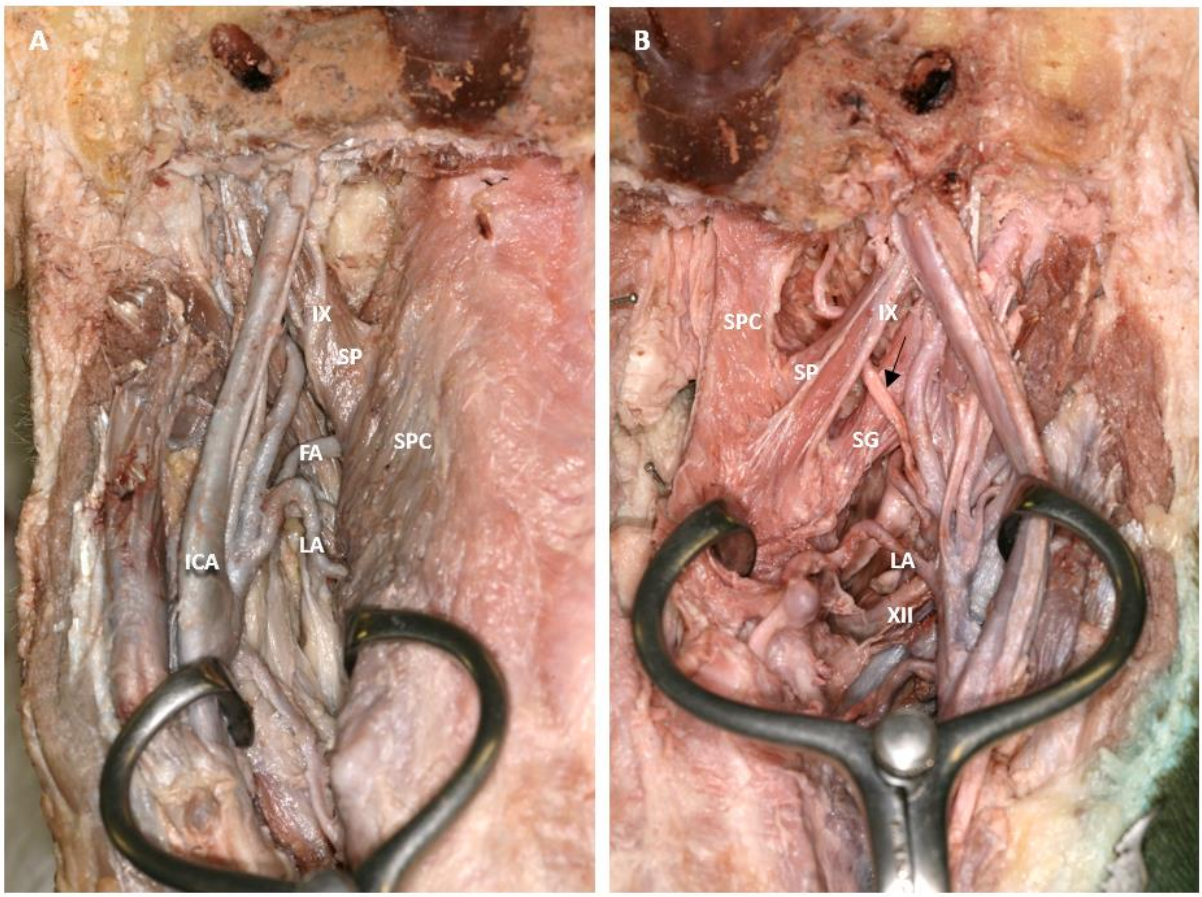

Figure 15 A. *Posterior view of the left parapharyngeal space. The prestyloid space adipose tissue is anterior to the stylopharyngeus muscle. Glossopharyngeal nerve descends towards the superior pharyngeal constrictor along the posterior aspect of stylopharyngeus muscle. The internal carotid artery is retracted laterally to demonstrate the path of the lingual artery and facial artery. The facial artery travels close to the superior pharyngeal constrictor muscle. The lingual artery makes a loop before piercing the superior pharyngeal constrictor.* ***B.*** *The posterior view of the right parapharyngeal space. The internal carotid artery is retracted laterally to demonstrate the topography of the stylopharyngeus muscle, styloglossus muscle, and the ascending palatine artery (black arrow). The prestyloid space adipose tissue is removed to show the path of ascending palatine artery.* ***Abbreviations****:* ***FA*** *facial artery,* ***ICA*** *internal carotid artery,* ***IX*** *glossopharyngeal nerve,* ***LA*** *lingual artery,* ***PA*** *prestyloid space adiposity,* ***SG*** *styloglossus muscle,* ***SP*** *stylopharyngeus muscle,* ***SPC*** *superior pharyngeal constrictor muscle,* ***XII*** *hypoglossal nerve.*

Foramen caecum of tongue base to PPS structures

Table 2 summarises the key distances measured from the foramen caecum of tongue base. In the majority of specimens, the LA bifurcation from ECA is approximately at a level above the greater cornu of hyoid bone. It had a tortuous path with often making a loop superiorly above the distal end of the GCH before moving anteriorly pass the posterior border of hyoglossus muscle to exit the PPS. This often occurred at the level of the vallecula. The distance from the foramen cecum to the LA at the PPS piercing the constrictor was 21mm. There was no statistically significant difference between this distance between the left and right sides (P-value 0.07). However, the mean distance from the foramen cecum to the proximal LA branch off point at the ECA had a statistically significant difference between both sides (P-value 0.012), where right side was 34.3mm and left was 27.4mm.

The PPS portion of the CNXII that exit to the mouth at the anterior edge of PPS was a mean distance of 24.9mm from the foramen cecum. There was no statistically significant difference between the left and right side (P-value 0.067). Parallel to the foramen cecum region, the CNIX pierced the junction

	Mean on right [mm] (SD)	Mean on left [mm] (SD)	P-value*	Overall mean [mm] (SD)	Overall range [mm] max- min
LA at PPS closest distance	22.5 (2.3)	19.4 (4.5)	0.07	21 (3.8)	27.3 - 12.7
LA branch off point at ECA	34.3 (5.2)	27.4 (5.5)	0.012	30.9 (6.3)	43.3 - 19.2
CNXII at PPS closest distance	26.6 (3.1)	23.2 (4.8)	0.067	24.9 (4.3)	32.6 - 14.7
FA branch off point at ECA	35.4 (4.6)	28.8 (5.7)	0.029	32.1 (6.1)	41.7 - 19.2
FA at PPS closest distance	29.9 (5.2)	24.9 (5.2)	0.068	27.4 (5.7)	38.3 - 16.6
CNIX at PPS closest distance	24.4 (3.4)	20.9 (3.6)	0.063	22.7 (3.8)	30.7 - 16.8

Table 2: Distance from the foramen caecum of tongue base to key landmarks. Abbreviations: **ECA** external carotid artery, **FA** facial artery, **LA** lingual artery, **PPS** parapharyngeal space, **CNIX** glossopharyngeal nerve, **CNXII** hypoglossal nerve, **SD** standard deviation, *****Two-tailed Paired T-test

between the SPC and MPC. This position was a mean distance of 22.7mm from the foramen cecum with no statistical significance between both sides (P-value 0.63).

The FA branch off point at the ECA to the foramen cecum showed a statistically significant difference (P-value 0.029) between right side and left side, 35.4mm and 28.8mm, respectively. In all the specimens dissected, the FA travelled about 5mm medially towards the pharynx before making a U-turn around the anterior border of the SHM (**Figure 15**). The mean closest distance from the foramen cecum to the PPS portion of FA at this point was 27.4mm with no statistically significant difference between sides (P-value 0.068). The FA then traversed laterally and inferiorly on the medial aspect of the submandibular gland before hooking over the body of the mandible.

Facial artery variation: The linguofacial trunk

Out of 26 sides of the coronally sectioned specimens the linguofacial trunk was present in five specimens (19%) (**Graph 1**). This trunk branched off the ECA above the GCH (**Figure 16**). It overall had a greater size compared to the FA and LA of other specimens. The trunk was approximately 5-10mm in length and bifurcated within the PPS to give the LA inferiorly and the FA superiorly.

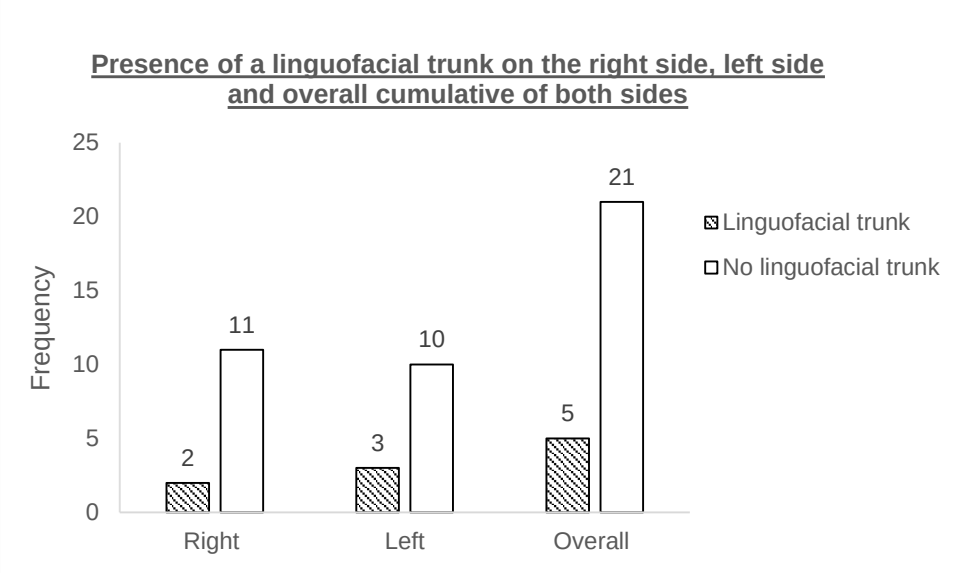

Graph 1 The graph illustrates the frequencies of the presence of the linguofacial trunk on the right side, left side and cumulative of both sides.

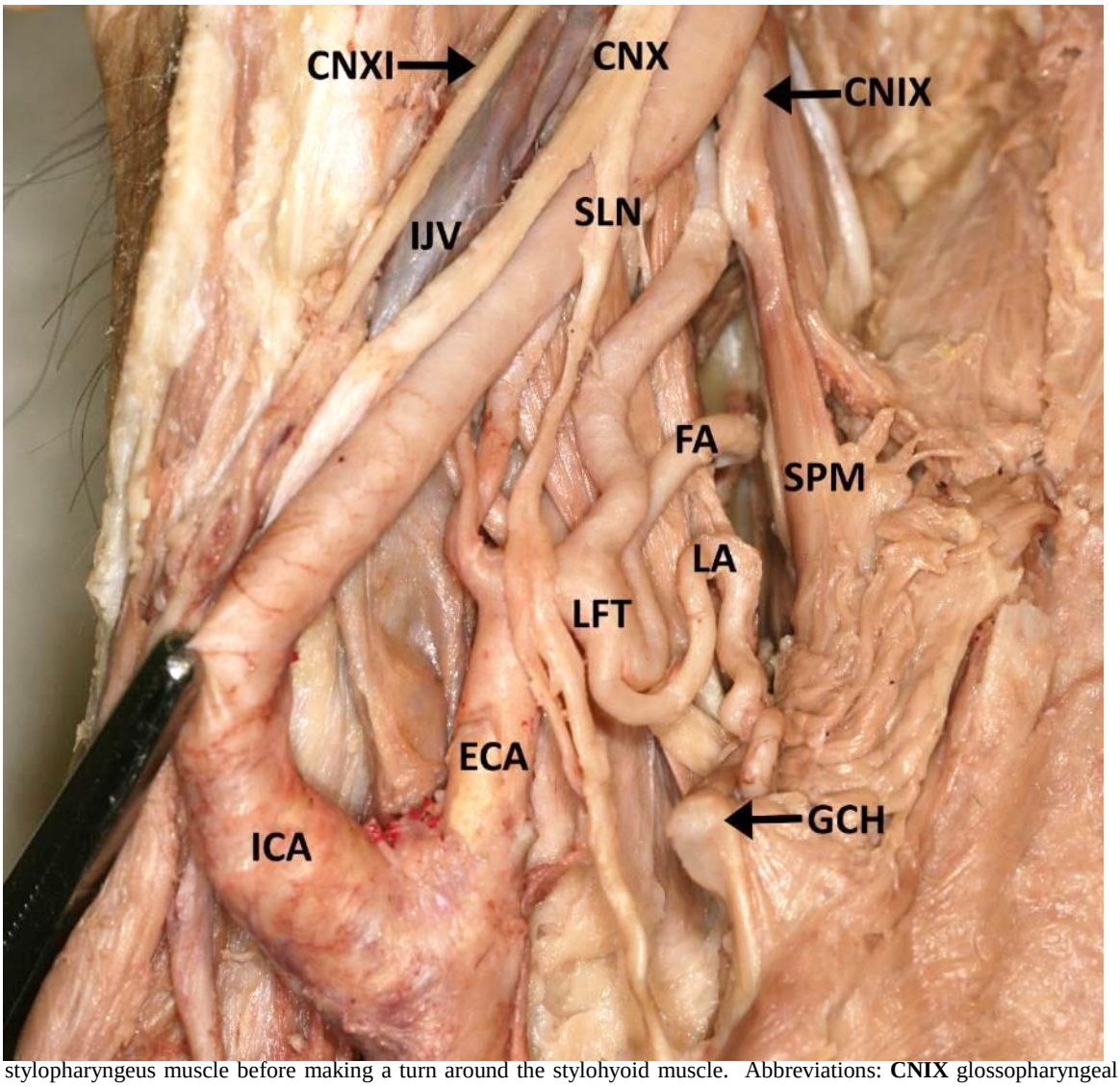

Figure 16 The Lingual artery and facial artery has a common origin from the external carotid artery as the linguofacial trunk. The internal carotid artery is retracted laterally to reveal the branches of the external carotid artery. The facial artery's proximal portion projects medially towards the stylopharyngeus muscle before making a turn around the stylohyoid muscle. Abbreviations: **CNIX** glossopharyngeal nerve, **CNX** vagus nerve, **CNXI** accessory nerve, **ECA** external carotid artery, **FA** facial artery, **GCH** greater cornu of hyoid bone, **ICA** internal carotid artery, **IJV** internal jugular vein, **LFT** linguofacial trunk, **SLN** superior laryngeal nerve, **SPM** stylopharyngeus muscle.

Vallecula to PPS structures

The LA, FA and the CNXII relation to the vallecula was further assessed with distance measurements. The measurements from the vallecula to other structures is summarised in **Table 3**. For all these measurements there was no statistically significant difference between the sides. The parapharyngeal part of the LA was a mean distance of 23.6mm from the vallecula. It branched off the ECA, a mean distance of 36.8mm from the vallecula. The point where the LA exit the PPS to enter the mouth corresponded on the axial plane to the mid pharyngoepiglotic fold level. The CNXII within the PPS was 26.3mm from the vallecula. The FA branched from the ECA a mean distance of 39mm from the

vallecula. The PPS portion of FA's closest distance was 35.4mm from the vallecula. This position was where the FA made a turn around the SHM muscle (**Figure 16**).

	Mean on right [mm] (SD)	Mean on left [mm] (SD)	P-value*	Overall mean [mm] (SD)	Overall range [mm]
LA at PPS closest distance	24.2 (2.9)	22.9 (4.1)	0.37	23.6 (3.5)	28.8 - 17.3
LA branch off point at ECA	37.3 (6.2)	36.3 (6.4)	0.67	36.8 (6.2)	52.2 - 27.9
CNXII closest distance	26.9 (3.6)	25.8 (5.5)	0.536	26.3 (4.6)	37.4 - 19.5
FA at PPS closest distance	37.0 (4.8)	33.8 (7.9)	0.252	35.4 (6.6)	52.1 - 22.9
FA branch off point at ECA	39.9 (4.4)	38.0 (6.3)	0.318	39.0 (5.4)	52.1 - 31.2

Table 3: Distance from midline vallecula to key landmarks. Abbreviations: **ECA** external carotid artery, **FA** facial artery, **LA** lingual artery, **PPS** parapharyngeal space, **CNXII** hypoglossal nerve, **SD** standard deviation, *****Two-tailed Paired T-test

Correlations between the ipsilateral tonsillar fossa apex level and the PPS

The distance measurements from the ipsilateral tonsillar fossa apex to four key arteries and the styloid apparatus at the PPS are summarised in **Table 4**. The ICA proximity to the ipsilateral tonsillar fossa apex was observed and the distance was measured. Overall this distance had a wide range from 24.1mm to 6.8mm. There was a statistically significant difference between sides for the ICA proximity to the tonsillar fossa apex (P-value 0.014). It was a mean distance of 17.8mm from the right tonsillar fossa apex and 14.4mm from the left. The frequency of the tortuosity of the ICA in the 26 dissected sides are summarised graphically in **Graph 2.** There were 10 sides (38%) of the total sides where a tortuous ICA was present. There was an equal number of ICAs tortuous on either side **(Graph 2**). Three specimens had tortuous ICAs on both sides.

	Mean on right [mm] (SD)	Mean on left [mm] (SD)	P-value*	Overall mean [mm] (SD)	Overall range [mm]
Internal carotid artery	17.8 (4.4)	14.4 (3.6)	0.014	16.1 (4.3)	24.1 - 6.8
External carotid artery	20.6 (5.7)	20.0 (4.4)	0.771	20.3 (5.0)	27.8 - 10.2
Ascending pharyngeal artery	16.6 (6.4)	16.0 (8.7)	0.834	16.3 (7.4)	32.5 - 7.4
Ascending palatine artery	11.2 (2.1)	8.4 (2.4)	0.003	10.1 (2.6)	15.0 - 4.9
Styloid process, tip	21.7 (6.9)	18.9 (4.4)	0.155	21.1 (5.8)	32.2 - 6.5
Stylopharyngeus, midpoint	18.0 (3.3)	17.2 (4.3)	0.731	17.6 (3.8)	24.8 - 10.3
Styloglossus, midpoint	17.9 (4.9)	17.0 (4.2)	0.353	17.5 (4.5)	27.0 - 10.9

Table 4: Distance from the ipsilateral tonsillar fossa apex to key landmarks on the axial plane. Abbreviations: **SD** standard deviation, *****Two-tailed Paired T-test

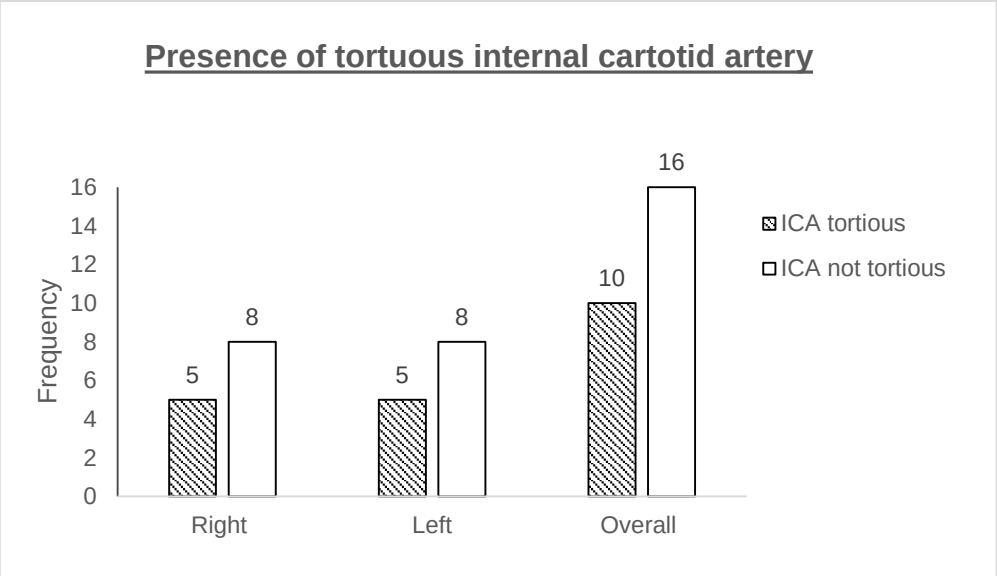

Graph 2: The graph represents the frequency of the presence of a tortuous parapharyngeal portion of the internal carotid artery on the right side, left side and overall sum of both sides. Abbreviations: **ICA** internal carotid artery

The ECA was more lateral and anterior to the ICA from the tonsillar fossa apex. Thus it was a mean distance of 20.3mm from the tonsillar fossa apex with no statistically significant difference between both sides. The APA often branched off from the posterior aspect of the ECA in most specimens. It was in close proximity to the superior pharyngeal constrictor muscle as it ascended in its vertical path to the skull base. It provided multiple small branches to the pharyngeal constrictor muscles at various levels. This also included branches to the tonsillar fossa. The APA was a mean distance of 16.3mm from the tonsillar fossa apex on the axial plane. There was no statistically significant difference between sides. In some instances, the proximity was affected by the tortuosity of the ICA (**Figure 17 and 18**). Where an ICA kink would push the APA more medially (**Figure 17B**). APA branch off point was often found in the region of posterior aspect of the ECA. Sometimes the branch off point is medial. Often ascends medial to ICA supplying multiple unnamed small branches at various levels towards the pharyngeal constrictor muscle.

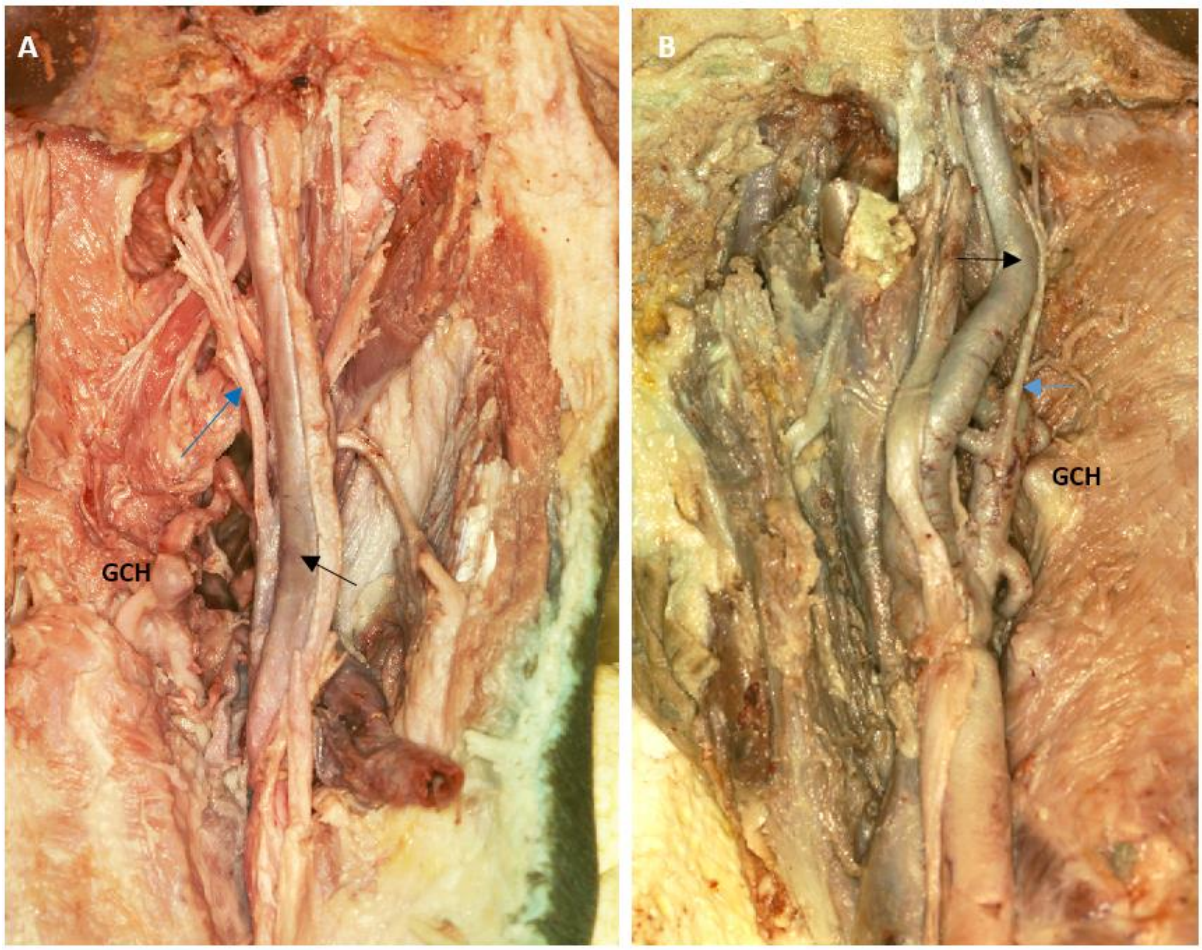

Figure 17 A. The relatively straight path of the internal carotid artery (black arrow) within the right parapharyngeal space. The ascending pharyngeal artery (blue arrow) is medial to the internal carotid artery. **B.** An aberrant internal carotid artery which classifies as tortuosity (black arrow) within the left parapharyngeal space. Note the close proximity of the internal carotid artery and the ascending pharyngeal artery medially (blue arrow). The lingual artery branch off point is immediately above the posterior edge of greater cornu of hyoid bone. Abbreviation: **GCH** greater cornu of hyoid

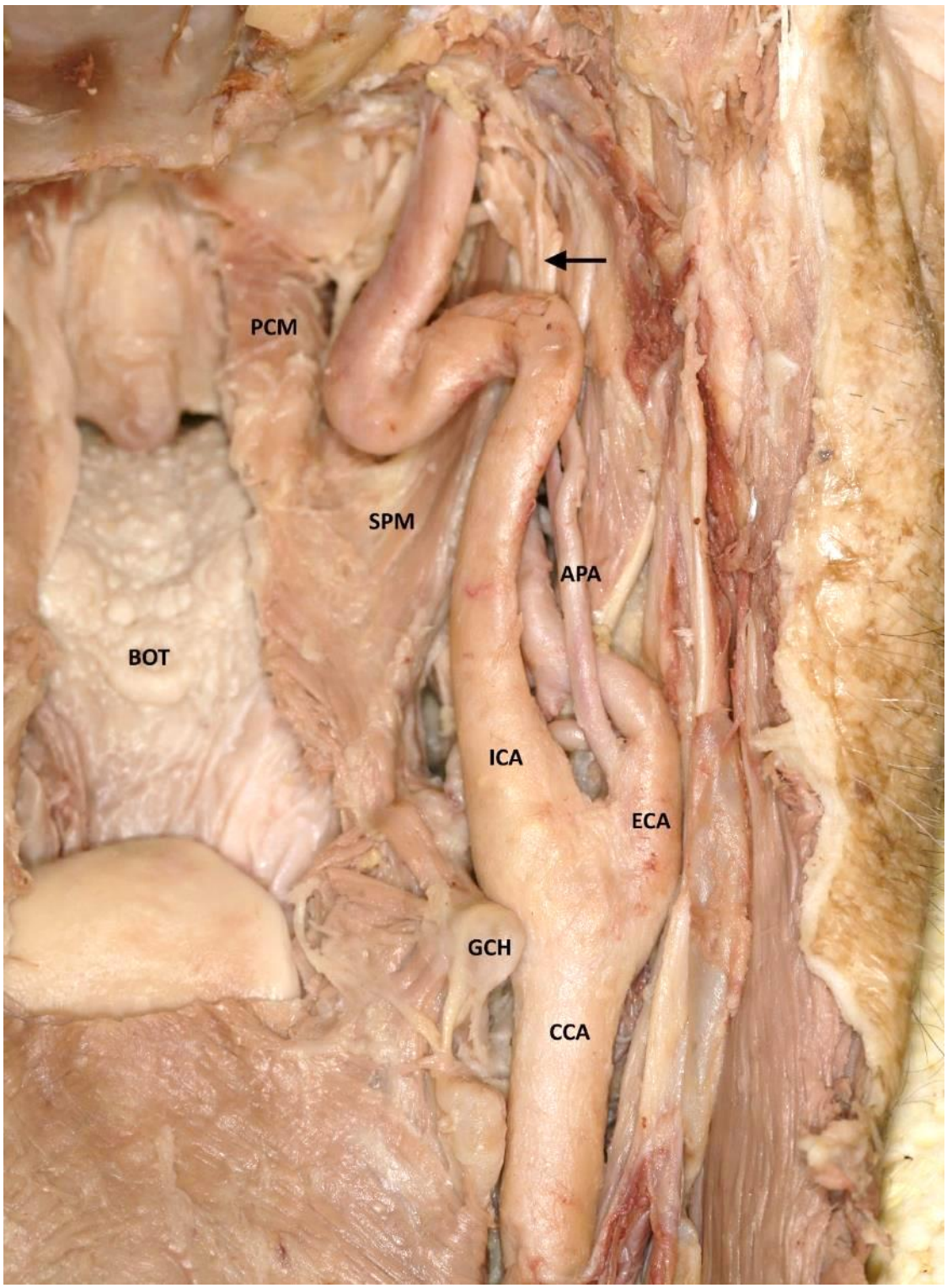

Figure 18 A right parapharyngeal space with the pharyngeal constrictor muscle partially removed posteriorly at the level of the oropharynx to reveal the base of tongue and tonsil region. The internal jugular vein was removed for clarity of the carotid system. The right internal carotid artery is tortuous approximately at the level of the tonsillar fossa. Note the close proximity of the internal carotid artery to the pharyngeal constrictor muscle at this level. The ascending pharyngeal artery's branches supply the superior aspect of the stylopharyngeus muscle (arrow). Abbreviations: **APA** ascending pharyngeal artery, **BOT** base of tongue, **CCA** common carotid artery, **GCH** greater cornu of hyoid bone, **ICA** internal carotid artery, **PCM** pharyngeal constrictor muscle, and **SPM** stylopharyngeus muscle.

ECA superior to the FA branch off point, ascended in the space anterior to the SHM and posterolateral to SGM. From this space the artery deviated further laterally. It gave off the occipital branch of SCM directly rather than as a branch of OA in some specimens. There were small branches from ECA that supply the SPC inferior portion. These arteries were given off inferior to the LA branch off point on the ECA (**Figure 19**).

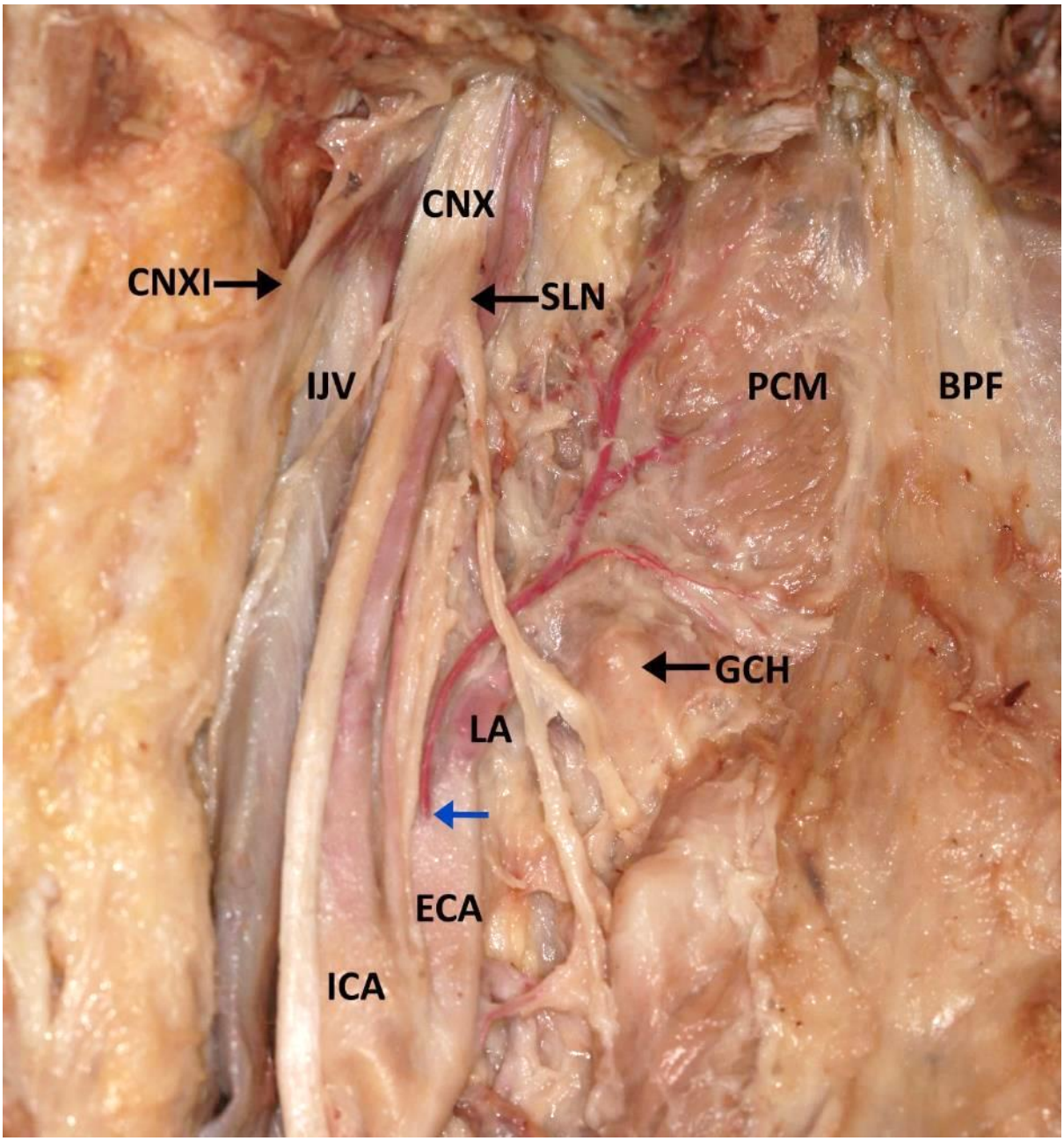

Figure 19 *A small unnamed arterial branch is given off the external carotid artery before the lingual artery branch off point (blue arrow). This vessel passes anterior to the inferior portion of the superior laryngeal nerve, then passes medially to supply multiple branches to the posterior aspect of the pharyngeal constrictor muscle. Abbreviations:* ***BPF*** *buccopharyngeal fascia,* ***CNX*** *vagus nerve.* ***CNXI*** *accessory nerve,* ***ECA*** *external carotid artery,* ***GCH*** *greater cornu of hyoid bone, ICA internal carotid artery, IJV internal jugular vein,* ***PCM*** *pharyngeal constrictor muscle,* ***SLN*** *superior laryngeal nerve*

The aPA branched off the FA in most cases (81%) before it passed laterally towards the SHM muscle. It branched directly from the ECA in 19% of cases (**Figure 7B**). Where it branched off directly from ECA, the branch off point was immediately superior to the FA branch off point. Overall there was no notable side preference for this variation with three occasions branching from the right ECA and two occasions from the left ECA (**Graph 3**). It ascended medially towards pharyngeal musculature while passing between the SPM and SGM. It supplied branches to the tonsillar fossa and to the superior pharyngeal constrictor muscle at multiple levels. The aPA was a mean distance of 11.2mm from the right tonsillar fossa apex and 8.4mm from the left tonsillar fossa apex. This difference was statistically significant (P-value 0.003). The aPA as it passed between SGM and SPM gave off muscular branches that pierce the SGM. It also supplies small branches to the distal end of the SPM. In one specimen there was an additional accessory APA that was given off from the medial aspect of ICA.

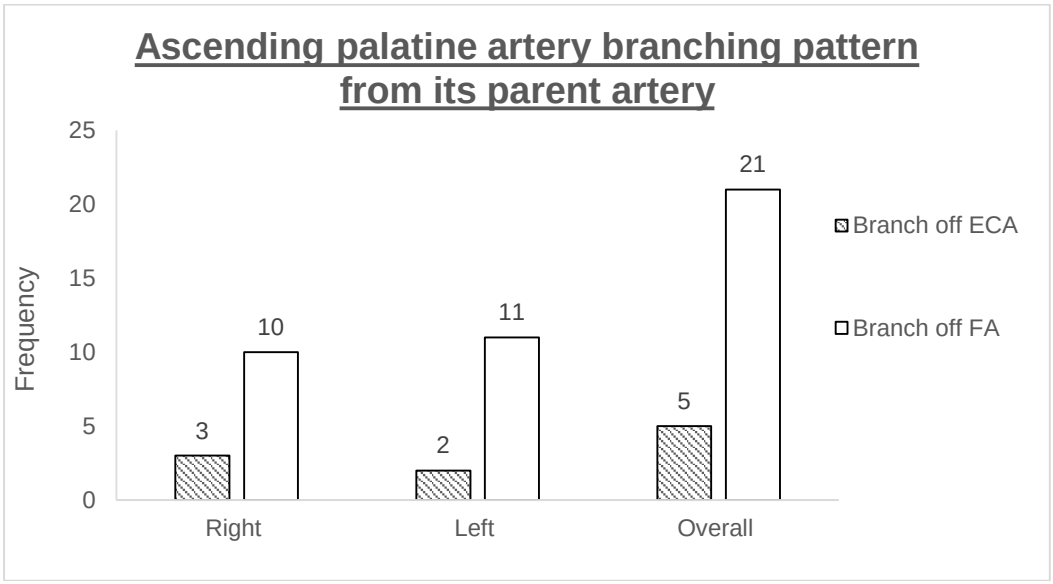

***Graph 3**: Graph represents the frequency of the ascending palatine artery origin from facial artery or directly from the external carotid artery on the right side, left side and overall sum of both sides. Abbreviations: **ECA** external carotid artery, **FA** facial artery.*

The styloid process was discovered by following the SPM proximally from its distal attachment at the pharynx. This attachment point corresponded to the tonsillar fossa medially. By following the dissection superiorly along the muscle, the styloid process was discovered. The tip of the styloid process was on average 21.1mm from the tonsillar fossa apex. There was no statistical significance between sides for this distance (P-value 0.155). Overall there was a wide range for this distance measurement from 6.5 mm to 32.2 mm (**Table 4**). The SGM muscle was discovered at its distal attachment. This position corresponded to the tongue base region medially at the oropharynx.

Relative to the SPM attachment at the pharynx, the SGM distal attachment was more inferior and anterior (**Figure 15B**).

The space between the SPM and SGM was occupied by adipose tissue. Within this the main artery discovered was the aPA. The midpoints of SPM and SGM correlated to the tonsillar fossa region medially. The mean distance from the midpoint of SPM to the tonsillar fossa apex was 17.6 mm. There was no statistical significance between sides for this measurement (P value 0.731). The mean distance from the midpoint of SGM to the tonsillar fossa apex was similar at 17.5mm with no statistical significance between sides (P-value 0.353).

The styloid process' distal end relations at the PPS and correlation to oropharynx

The styloid process tip was often covered out of view by the muscles originating from the styloid process in the majority of specimens. Posteriorly it related to the SHM, medially to SPM and anteriorly to SGM. The styloid process passed obliquely towards the midline of the pharynx. It was not in contact with the pharyngeal constrictors in any of the specimens. The tip of the styloid process was positioned in the space between the ICA and ECA in most cases, with the ICA being posteromedial and ECA anterolateral. Thus, these two arteries were very closely related to the styloid process tip. A summary of the distances measured from the tip of the styloid process are displayed in **Table 5**.

	Mean on right [mm] (SD)	**Mean on left [mm] (SD)**	**P-value***	**Overall mean [mm] (SD)**	**Overall range [mm]**
Glossopharyngeal nerve	4.7 (1.9)	5.2 (2.7)	0.838	5 (2.9)	13.1 - 2.2
External carotid artery	5.2 (3.0)	7.4 (4.4)	0.181	6.3 (3.8)	15.5 - 1.2
Internal carotid artery	5.9 (2.6)	6.5 (4.7)	0.481	6.2 (3.7)	20.7 - 1.8
Medial pharyngeal constrictor	21 (6.9)	19.5 (7.3)	0.475	20.2 (6.7)	34.6 - 6.8
Lateral pharyngeal constrictor	16.9 (7.2)	13.8 (6.7)	0.175	15.3 (7.0)	28.5 - 2.3

Table 5: *Distance from the ipsilateral distal end of styloid process to key landmarks on the axial plane. Abbreviations:* ***SD*** *standard deviation,* *******Two-tailed Paired T-test*

The ICA was a mean distance of 6.2mm from the styloid process tip with no statistical significance between the sides (P-value 0.481). There was a wide range for this distance from 1.8mm to 20.7mm (**Table 5**). Similarly, the ECA was a mean distance of 6.3mm lateral from the styloid tip. There was no statistical significance between sides for this measurement (P-value 0.181). This measurement also had a wide range from 1.2mm to 15.5mm. From the oropharyngeal mucosal surface, the tip of the styloid process was a mean distance of 20.2mm on the axial plane. At this plane it was 15.3mm

from the lateral surface of the pharyngeal constrictor muscle. The CNIX was a mean distance of 5mm anterior from the distal end of the styloid process.

CNX was identified between the ICA and IJV. Superiorly, the inferior cervical ganglion was prominent. Inferior to this the superior laryngeal nerve was given off. This nerve is given off at approximately at a level above the tonsillar fossa, on the axial plane. It branched off to internal laryngeal nerve superiorly and external laryngeal nerve inferiorly. This division often occurred superior to the greater cornu of hyoid. The superior laryngeal nerve and its branch off point was close to the proximal LA medial aspect. (**Figure 16 and 19**). It can also be closely associated with the middle and inferior pharyngeal constrictor muscles. This neve is posterior to a small arterial vessel that supply the SPC in one specimen (**Figure 19**).

Posterior end of greater cornu of hyoid bone relations

In the coronally sectioned specimens the posterior end of GCH was visible lateral to the middle pharyngeal constrictor (**Figure 17**). It was then further confirmed with palpation. The distances measured from the GCH to the LA, FA, ECA, LN and CNXII are summarised in **Table 6**. The LA was consistently found superior to the GCH. It was measured to be a mean distance of 3.5mm superior to the posterior end of the GCH. There was no statistical significance between the sides (P-value 0.937). The artery often had a hairpin loop above this landmark. The LA only had a short course from this point before exiting the PPS to enter the mouth by passing medial to the hyoglossus muscle.

At this region the CNXII is found lateral to the LA and lateral to the hyoglossus muscle as it passed anteriorly to enter the mouth. **Figure 15B** illustrates the medial position of the LA with respect to the CNXII relationship. By following the LA laterally to its proximal end, the ECA in the carotid sheath was revealed. The distance from the GCH to the ECA where LA originated, was a mean distance of 11.4 mm with no statistical significance between sides (P-value 0.272). The proximal LA also gave small branches to the superior aspect of thyrohyoid muscle.

There was often a vein tributary between the pharyngeal wall and the CNXII. The LA and GCH was posterior to this vein. Where the nerve made a turn from its vertical path to pass anteriorly towards the mouth, this angle of the nerve was held down by a superior thyroid artery branch which hooked over the neve (**Figure 20**). This artery is usually given off the OA as the inferior branch to sternocleidomastoid muscle in the majority of specimens. In another specimen, this branch was directly given off by the ECA.

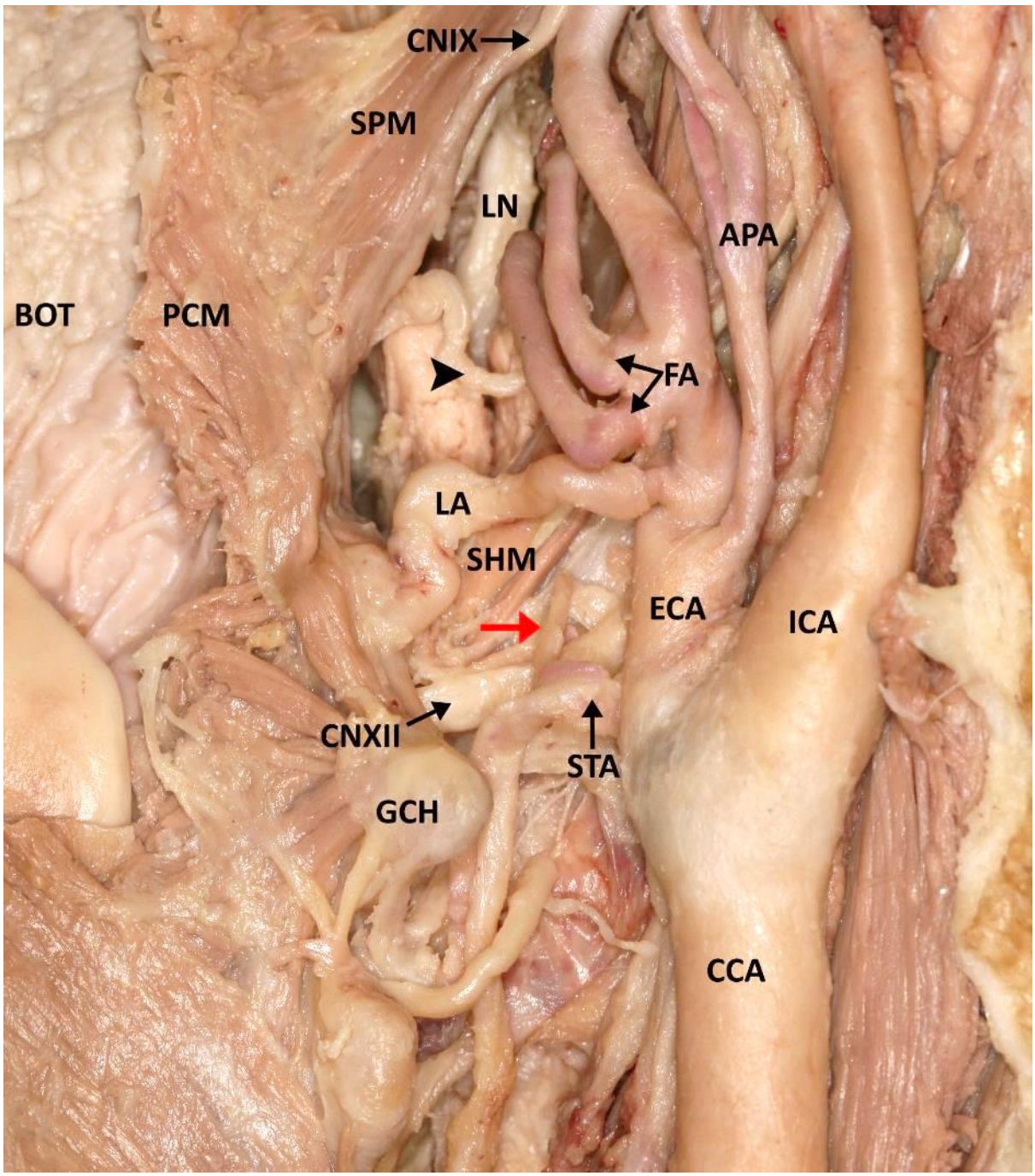

Figure 20: A right parapharyngeal space dissection. The internal carotid artery is retracted laterally to reveal the branches of the external carotid artery. A portion of the pharyngeal constrictor muscle is removed to reveal the base of tongue. An arterial branch from the proximal portion of superior thyroid artery (red arrow) passes over the medial aspect of the hypoglossal nerve. There is a duplication of the facial artery. The inferiorly positioned facial artery gives rise to a branch (arrow head) that supplies the inferior edge of the distal attachment of the stylopharyngeus muscle. Abbreviations: **APA** ascending pharyngeal artery, **BOT** base of tongue, **CCA** common carotid artery, **CNIX** glossopharyngeal nerve, **CNXII** hypoglossal nerve, **ECA** external carotid artery, **FA** facial artery, **GCH** greater cornu of hyoid bone, **LN** lingual nerve, **PCM** pharyngeal constrictor muscle, **SHM** stylohyoid muscle, **SPM** stylopharyngeus muscle, **STA** superior thyroid artery

The FA was found superior to the GCH distal end and LA. Its closest distance to the GCH was 15.1mm with no statistical significance between both sides (P-value 0.44). This point on the FA corresponded to its closest proximity to the pharynx. This section of the artery was also the portion that made a turn around the SHM (**Figure 15A**). The FA branch off point from the ECA was 16mm lateral to the GCH distal end with no statistical significance between sides (P-value 0.773).

	Mean on right [mm] (SD)	**Mean on left [mm] (SD)**	**P-value***	**Overall mean [mm] (SD)**	**Overall range [mm]**
Vertical distance to LA	3.5 (1.5)	3.6 (1.7)	0.937	3.5 (1.6)	7.0 - 1.2
LA branch off point at ECA	10.4 (4.8)	12.3 (4.1)	0.272	11.3 (4.5)	17.7 - 2.2
CNXII at PPS closest distance	11.0 (2.9)	11.8 (3.9)	0.377	11.4 (3.4)	18.2 - 5.7
LN at PPS closest distance	28.4 (5.2)	28.5 (3.9)	0.656	28.4 (4.5)	37.8 - 18.2
FA at PPA closest distance	14.6 (5.6)	15.6 (4.5)	0.44	15.1 (5.0)	27.5 - 5.2
FA at branch off point at ECA	15.8 (6.4)	16.2 (4.1)	0.773	16.0 (5.2)	33.1 - 7.6

Table 6**: Distance from posterior end of ipsilateral greater cornu of hyoid bone to key landmarks. Abbreviations: **FA** facial artery, **LA** lingual artery, **LN** lingual nerve, **PPS** parapharyngeal space, **CNXII** hypoglossal nerve, **SD** standard deviation, ** Two-tailed Paired T-test*

The LN was a mean distance of 28.4mm anterior to the GCH distal end. The closest distance to the GCH corresponded the 'L' shaped turn the nerve took at the inferior margin of the medial pterygoid muscle (**Figure 21**). This region was anterior to the point where LA entered the mouth. The LN enters the mouth and exited the PPS at the inferior edge of superior pharyngeal constrictor where the muscle inter-digitates with the buccinator muscle at the pterygomandibular raphe. The LN's 'L' shaped turning point was inferior to the inferior border of the SGM and anterior to this muscle. The nerve was found dissecting in the space between the pharynx and the medial pterygoid muscle.

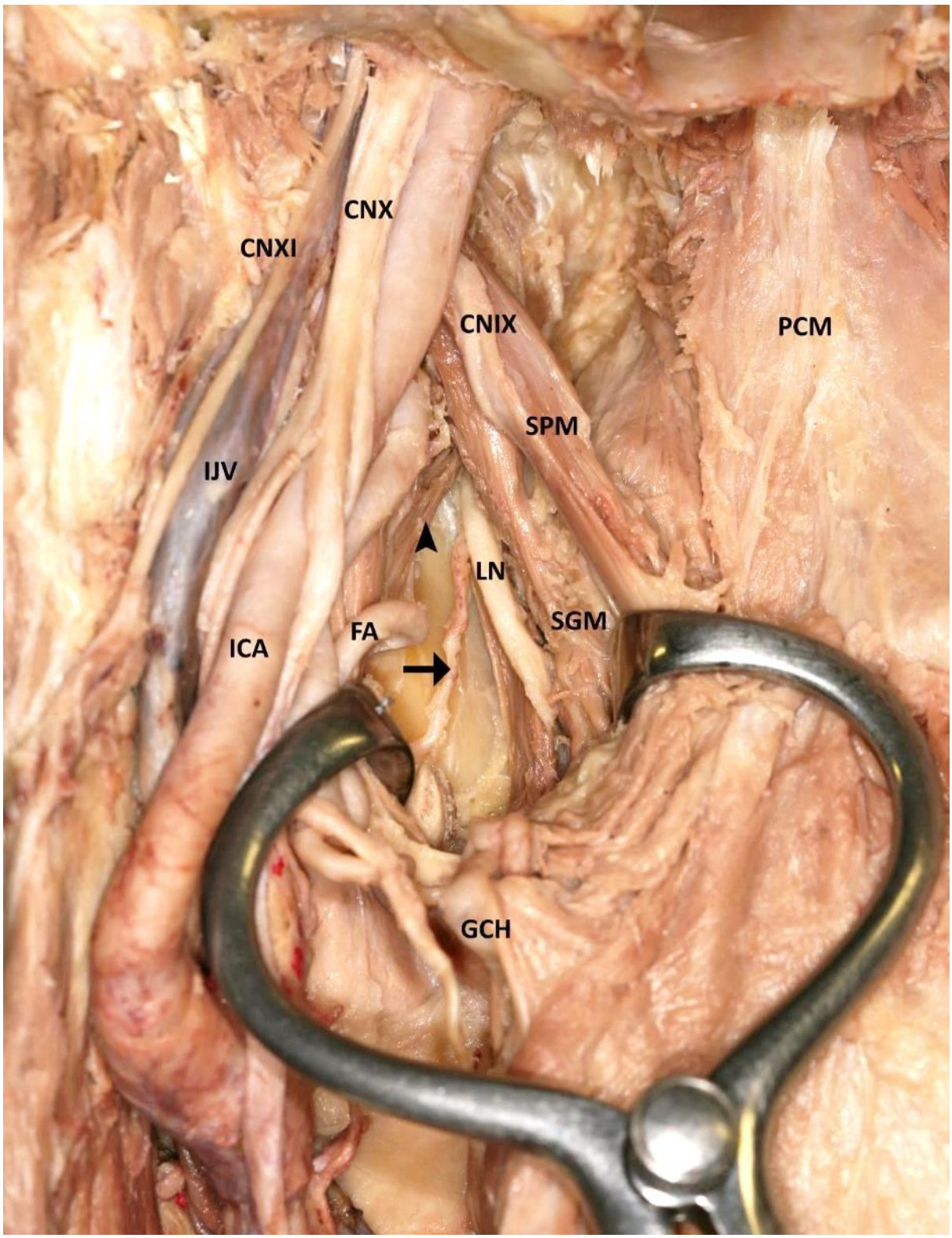

Figure 21 A left side parapharyngeal space dissection with the internal carotid artery and external carotid artery retracted laterally. The medial pterygoid muscle (arrow head) is partially dissected to show the lingual nerve and a pterygoid branch of the maxillary artery (black arrow). The lingual nerve makes an L-shaped turn towards the mouth approximately at the level of the distal attachment of the styloglossus muscle. Abbreviations: **CNIX** glossopharyngeal nerve, **CNX** vagus nerve, **CNXI** accessory nerve, **ECA** external carotid artery, **FA** facial artery, **GCH** greater cornu of hyoid bone, **ICA** internal carotid artery, **IJV** internal jugular vein, **PCM** pharyngeal constrictor muscle, SGM styloglossus muscle, **SPM** stylopharyngeus muscle

The stylopharyngeus muscle's midpoint and its relations

The SPM's distal attachment onto the pharynx was discovered superior to the FA's closest position to the pharynx musculature (**Figure 15A**). The attachment site across all specimens corresponded to the junction between superior and middle pharyngeal constrictors muscles. The CNIX was often discovered to pierce the pharyngeal constrictor at this level. Its descent towards the pharynx was along the inferior border of the SPM (**Figure 15A** and **19**). In one specimen, the left SPM had a thin accessory muscle accompanying the main muscle belly. The CNIX was closely associated with the larger main muscle belly on this specimen. The contralateral side of this specimen did not have the same variation.

In another specimen the SPM had a thin segment that extended inferiorly to attach to the pharyngeal constrictor at the level of the GCH. There are branches from the APA that supply the superior portion of the SPM (**Figure 15A**). In one specimen the SPM distal attachment had small arterial branch directly supplied from the ECA (**Figure 22**). In all specimens the midpoint of the SPM corresponded to the tonsillar fossa, medially. The proximity of the midpoint of the SPM to adjacent anatomical structures measured across the 26 specimen sides are summarised in **Table 7**. There was no statistically significant difference between sides for these measurements.

	Mean on right [mm] (SD)	**Mean on left [mm] (SD)**	**P-value***	**Overall mean [mm] (SD)**	**Overall range [mm]**
External carotid artery	8.9 (3.2)	8.9 (4.7)	0.972	8.9 (3.9)	17.1 - 2.8
Internal carotid artery	2.0 (1.4)	2.1 (1.9)	0.968	2.1 (1.6)	4.7 - 0
Vertical distance to LA	27.6 (4.9)	26.5 (5.5)	0.201	27.0 (5.1)	36.9 - 14.3
LA branch off point at ECA	33.2 (5.2)	32.3 (6.4)	0.806	32.7 (5.7)	43.3 - 21.4
Vertical distance to FA	19.2 (3.1)	19.7 (3.4)	0.658	19.5 (3.2)	24.9 - 13.6
FA branch off at ECA	27.0 (4.0)	27.5 (7.3)	0.562	27.3 (5.8)	37.9 - 15.7
OA branch off at ECA	25.4 (7.4)	21.1 (8.4)	0.368	23.8 (7.8)	36.2 - 11.4
Glossopharyngeal nerve	2.4 (1.5)	1.5 (1.6)	0.117	1.9 (1.6)	4.6 - 0
Styloid process tip	8.5 (2.9)	8.1 (5.1)	0.278	8.3 (4.1)	19.3 - 3.9

Table 7**: Distance from midpoint of stylopharyngeus muscle to key landmarks. Abbreviations: **FA** facial artery, **LA** lingual artery, **OA** occipital artery, **PPS** parapharyngeal space, **SD** standard deviation, ***Two-tailed Paired T-test

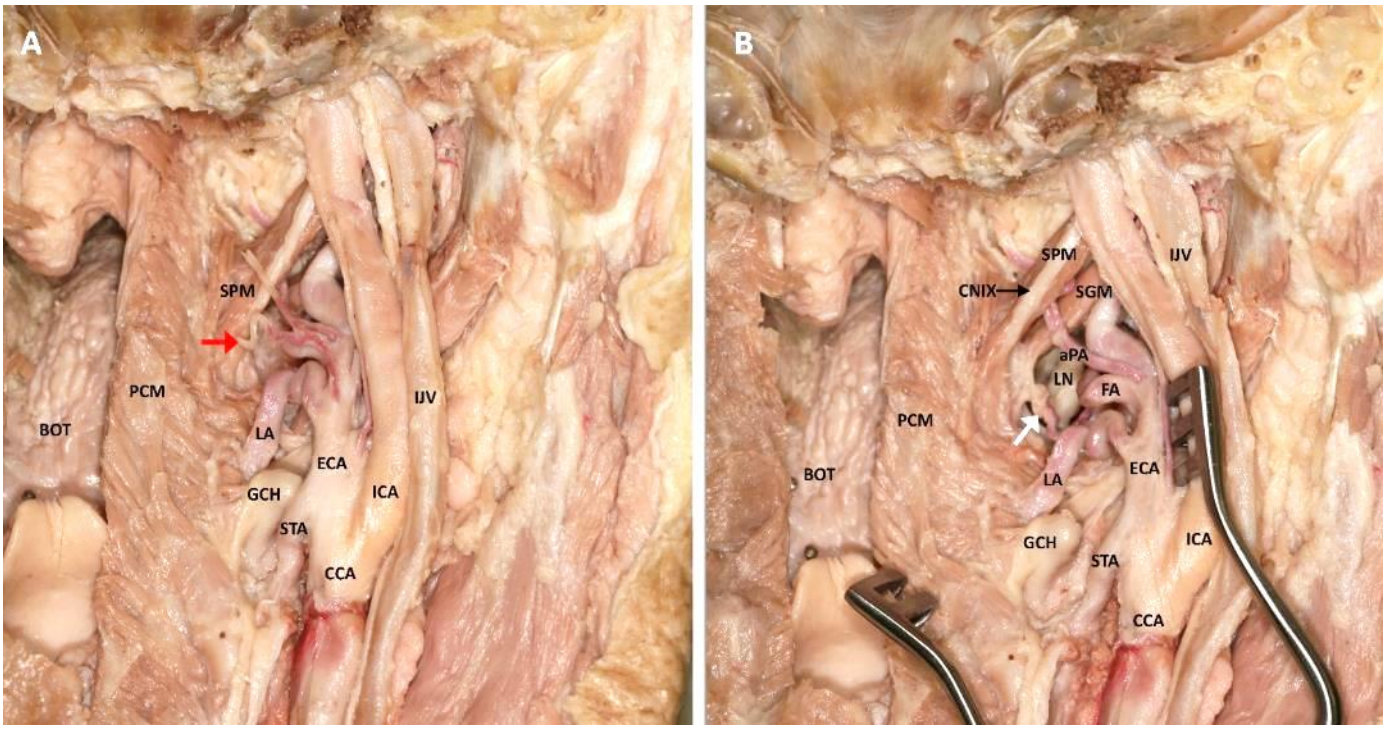

Figure 22 A. Right parapharyngeal space dissection with the posterior aspect of the pharyngeal constrictor muscle partially removed to reveal the oropharynx. There is a small branch directly given off from the posterior aspect of the external carotid artery supplies the distal portion of the stylopharyngeus muscle (red arrow). **B.** The same right parapharyngeal space dissection with the internal carotid artery reflected laterally. The styloglossus muscle distal attachment is supplied by a branch from the facial artery (white arrow). The lingual nerve was found in the space anterior to the styloglossus muscle. The ascending palatine artery if given off directly from the external carotid artery just superior to the facial artery origin in this specimen. As the ascending palatine artery passes between the stylopharyngeus and styloglossus muscle, it becomes closer to the lateral wall of the pharyngeal constrictor muscle. Abbreviations: **aPA** ascending palatine artery, **BOT** base of tongue, **CCA** common carotid artery, **CNIX** glossopharyngeal nerve, **ECA** external carotid artery, **FA** facial artery, **FA** facial artery, **GCH** greater cornu of hyoid, **IJV** internal jugular vein, **PCM** pharyngeal constrictor muscle, **SGM** styloglossus muscle, **SPM** stylopharyngeus muscle, **STA** superior thyroid artery.

The ICA was very closely associated with the SPM midpoint. It was 2.1mm posterior from the SPM midpoint. In 26% of specimen sides (n= 7) the ICA was in contact with the midpoint of SPM. The ECA was a mean distance of 8.9mm lateral to the SPM midpoint. There was variability of this distance from 2.8mm to 17.1mm. There was ECA tortuosity at this level as the vessel passed anterior to SHM and posterolateral to SGM muscle. The OA branch off point from the ECA was a mean distance of 23.8mm inferior to the SPM midpoint. The FA and LA branch off points from ECA was a mean distance of 27.3mm and 32.7mm, respectively. The closest mean vertical distance to the PPS portion of the FA and LA from the SPM midpoint was 19.5mm and 27.0mm, respectively.

FA has a branch to the distal SPM where it attaches to the pharynx, this branch is given off at the inferior aspect of the artery before aPA is given off. The aPA was often given off from the superior aspect of the FA. The proximal small branches of FA are given off in a space bound by three muscles

(**Figure 22** and **23**). This forms a triangular boundary, with the medial pterygoid muscle laterally, the SPM and SGM superiorly, and the GCH bone inferiorly (**Figure 22**). In this space the FA also supplies a small branch to SHM. The FA segment distal to its aPA branch, gave off branches to the distal ends of SPM, SGM and SHM as it turned around SHM. Posterior belly of digastric is lateral to the SHM and its distal portion was supplied by small branches of LA.

Figure 23 A right parapharyngeal space dissection with retraction of the internal carotid artery medially and external carotid artery laterally to reveal conceptual triangle. The borders of the triangle are composed of the greater cornu of hyoid bone inferiorly, stylopharyngeus and styloglossus muscles superiorly, and the medial pterygoid muscle laterally. The facial artery enters this space as it curves around the medial aspect of the stylohyoid muscle. This space contains a branch from the facial artery that supplies the distal attachment of the styloglossus muscle (red arrow head) and the ascending palatine artery that passes superiorly between the stylopharyngeus muscle and styloglossus muscle. Abbreviations: **aPA** ascending palatine artery, **CCA** common carotid artery, **CNIX** glossopharyngeal nerve, **ECA** external carotid artery, **FA** facial artery, **ICA** internal carotid artery, **LN** lingual nerve, **MPM** medial pterygoid muscle, **PCM** pharyngeal constrictor muscle, **SHM** stylohyoid muscle.

The CNIX travels along the posterior aspect and inferior border of the muscle belly of the SPM towards the pharynx (**Figure 15**). In one specimen there was a variation, where the nerve began its

descent on the posterior aspect of the proximal SPM then passed to the anterior aspect of the SPM muscle as it approached the distal end. The neve was a mean distance of 1.9mm lateral from the midpoint of SP muscle. The nerve was in contact with the midpoint of SP in 26% of cases (n = 7). The styloid process distal end was a mean distance of 8.3mm superior and lateral to the SPM midpoint. There was a wide range of this measurement from 3.9mm to 19.3mm.

Styloglossus muscle midpoint and its relations

The same anatomical relations as to SPM midpoint were also measured to the SGM midpoint in the 26 dissected specimen sides. The distance measurements are summarised in **Table 8**. Most of these anatomical structures were posterior and lateral to the SGM. The only statistically significant difference between sides, was the mean distance from LA to SGM midpoint vertical distance (P-value 0.016). Where the distance from the right side was 25.1mm and from the left 22.2mm. The FA mean vertical distance to SGM midpoint was 14.6mm.

	Mean on right [mm] (SD)	**Mean on left [mm] (SD)**	**P-value***	**Overall mean [mm] (SD)**	**Overall range [mm]**
External carotid artery	5.3 (3.1)	5.6 (3.8)	0.753	5.5 (3.4)	16.1 - 1.4
Internal carotid artery	6.8 (1.8)	6.8 (1.8)	0.987	6.8 (1.8)	9.5 - 3.0
Vertical distance to LA	25.1 (6.5)	22.2 (6.6)	0.016	23.6 (6.6)	39.6 - 14.2
LA branch off point at ECA	31.0 (6.2)	28.7 (7.4)	0.196	29.8 (6.8)	42.5 - 18.7
Vertical distance to FA	14.2 (3.7)	15.1 (4.2)	0.442	14.6 (3.9)	27.4 - 7.3
FA branch off at ECA	21.7 (5.5)	23.1 (8.5)	0.495	22.4 (7.1)	42.4 - 10.9
OA branch off at ECA	24.3 (6.1)	23.2 (10.9)	0.078	23.8 (8.5)	44.1 - 5.4
Glossopharyngeal nerve	4.4 (2.0)	5.1 (2.0)	0.305	4.8 (2.0)	8.7 - 1.9
Styloid process, tip	9.5 (5.4)	9.2 (6.0)	0.64	9.3 (5.6)	22.1 - 1.5

Table 8: Distance from midpoint of styloglossus muscle to key landmarks. Abbreviations: **FA** facial artery, **LA** lingual artery, **OA** occipital artery, **PPS** parapharyngeal space, **SD** standard deviation, ***Two-tailed Paired T-test

The ICA was a mean distance of 6.8mm from the SGM midpoint in a posterior and slightly lateral direction. The ECA was more posterior and more lateral compared to ICA with a mean distance of 5.5mm from the SGM midpoint. The OA branch off point from the ECA was a mean distance of 23.8mm from the midpoint. FA and LA branch off points from the ECA was 22.4mm and 29.8mm, respectively. The CNIX was a mean distance of 4.8mm posterior to the SGM midpoint. The styloid process distal end was situated superior to the SGM midpoint in most cases. In one specimen, this structure was situated inferior to the SGM midpoint on both sides. The mean distance between the SGM midpoint and styloid process distal end was 9.3mm.

Oropharyngeal mucosal surface to PPS landmark relations on the axial plane

Measurements from OP mucosal surface to two key muscles (SGM and SPM), two branches of the ECA (LA and FA) and three nerves (LN, CNIX and CNXII) were measured on the axial plane across 26 sides. All the measurement obtained are summarised in **Table 9**. There was no statistically significant difference of measurements between sides.

	Mean on right [mm] (SD)	**Mean on left [mm] (SD)**	**P-value**	**Overall mean [mm] (SD)**	**Overall range [mm]**
Stylopharyngeus, *midpoint*	17.3 (5.2)	16.1 (5.4)	0.549	16.6 (5.2)	28.3 - 8.6
Styloglossus, *midpoint*	18.2 (5.4)	16.4 (3.6)	0.303	17.3 (4.60	26.9 - 9.0
LA at PPS closest distance	5.5 (1.0)	6.0 (2.4)	0.44	5.7 (1.8)	12.3 - 2.7
LA at ECA branch off	15.4 (4.2)	13.3 (3.7)	0.248	14.4 (4.0)	23.8 - 7.1
FA at PPS closest distance	10.3 (3.9)	8.7 (2.9)	0.269	9.5 (3.4)	18.7 - 4.4
FA at ECA branch off	15.4 (4.2)	12.7 (3.6)	0.187	14.0 (4.1)	21.4 - 6.6
Glossopharyngeal nerve	4.6 (1.0)	4.8 (1.0)	0.696	4.7 (1.0)	6.6 - 2.8
Hypoglossal nerve	9.6 (2.8)	8.7 (1.7)	0.252	9.1 (2.3)	13.1 - 4.3
Lingual nerve	10.2 (3.5)	10.2 (2.70)	0.857	10.2 (3.1)	16.1 - 6.3

Table 9: Distance from the oropharyngeal mucosal surface to key landmarks on the axial plane. Distance between the closest parts of the structures measured. **ECA** external carotid artery, **FA** facial artery, **LA** lingual artery, **PPS** parapharyngeal space, **SD** standard deviation, *****Two-tailed paired T-test

The SPM and SGM midpoint to OP mucosa mean distance was similar, 16.1mm and 16.4mm, respectively. The LA was a mean distance of 5.7mm from the OP mucosa at the point it passes anterior to the hyoglossus muscle's posterior border to exit the PPS. The LA branch off point from the ECA was a mean distance of 14.4mm from the OP mucosa. The FA closest distance to the OP mucosal surface on the axial plane was a mean distance of 9.5mm. The FA's origin at the ECA was 14.0mm from the OP mucosal surface.

The CNIX exited the PPS between the superior and middle pharyngeal constrictor muscles. The nerve at this point was a mean distance of 4.7mm from the OP mucosal surface. The CNXII, at the position where it made a turn anteriorly to enter the oral cavity from the PPS, was measured to be a mean distance of 9.1mm from the OP mucosal surface. This region was at close proximity to the GCH (**Figure 20**).

During the dissection, the LN appeared to view anterior to the SGM between the inferior portion of the medial pterygoid muscle and ramus of mandible (**Figure 20** and **Figure 22**). The nerve was found within the adipose tissue anterior to SGM. The LN travels anteriorly towards the mouth at the level of the distal end of the SGM. With respect to the submandibular gland the LN is medial, anterior and superior. At this point, superior to the superior border of the submandibular gland the LN makes a

turn anteriorly. The distance from OP mucosa to this point of the nerve was measured to be a mean distance of 10.2mm.

Lateral surface of the pharyngeal constrictor muscle to PPS landmark relations on the axial plane

On the axial plane, measurements were made across 26 specimens from the lateral surface of the pharyngeal constrictor muscle (**Table 10**). SPM and SGM midpoints were 13.0 mm and 14.1 mm from lateral surface of the pharyngeal constrictor muscle, respectively. The LA branch off point at ECA was 13.5mm on the right and 9.8mm on the left from LSPCM. This difference was statistically significant between sides (P-value 0.046). The FA was a mean distance of 6.7mm from the lateral surface of the pharyngeal constrictor muscle. The FA origin at the ECA was a mean distance of 12.5mm. In most specimens the point of the FA that was closest to the pharyngeal constrictor corresponded to the mid-tonsillar fossa region on the axial plane. In one specimen, on left sided, the FA branched off more superiorly, thus the branch off point from ECA corresponded to the superior tonsillar fossa region.

	Mean on right [mm] (SD)	**Mean on left [mm] (SD)**	**P-value**	**Overall mean [mm] (SD)**	**Overall range [mm]**
Stylopharyngeus midpoint	13.4 (4.3)	12.7 (4.5)	0.747	13.0 (4.3)	21.7 - 5.9
Styloglossus midpoint	14.5 (5.5)	13.6 (3.0)	0.602	14.1 (4.4)	23.9 - 4.1
LA at ECA branch off	13.5 (4.1)	9.8 (2.8)	0.046	11.6 (3.9)	21.3 - 5.6
FA at PPS closest distance	7.9 (4.4)	5.4 (3.5)	0.11	6.7 (4.1)	16.3 - 1.5
FA at ECA branch off	14.8 (5.7)	10.4 (3.7)	0.092	12.5 (5.2)	26.3 - 3.5
Hypoglossal nerve	3.2 (1.6)	3.5 (1.3)	0.492	3.3 (1.5)	6.5 - 1.4
Lingual nerve	3.0 (1.1)	3.0 (0.8)	0.953	3.0 (1.0)	6.0 - 1.6

Table 10: Distance from lateral surface of the pharyngeal constrictor muscle to key landmarks on the axial plane. **ECA** external carotid artery, **FA** facial artery, **LA** lingual artery, **PPS** parapharyngeal space, **SD** standard deviation, *****Two-tailed paired T-test

The distances to the nerves LN and CNXII were also measured from the lateral surface of the pharyngeal constrictor muscle. The LN measurement was made at the point the nerve emerged between the medial pterygoid muscle and ramus of mandible to turn anteriorly towards the mouth (**Figure 20**). The CNXII was closely associated with the lateral surface of the pharyngeal constrictor muscle at the inferior PPS. It was a mean distance of 3.3mm from the lateral surface of the pharyngeal constrictor muscle. The point corresponded to a position where the nerve turned anteriorly near the GCH to advance anteriorly towards the mouth. This turning point corresponded to the level of the linguoepiglottic fold on the axial plane at the OP. The STA had small branches to inferior pharyngeal constrictor muscle at the inferior PPS region.

Discussion

The transoral surgical anatomy of PPS represents a paradigm shift that had gained interest in the contemporarily field of otolaryngology-head and neck surgery. The approach is gaining popularity due to improvements in surgical technology allowing for favourable factors for safe transoral surgery. Transoral laser microsurgery, endoscopic approaches and TORS for benign and malignant tumours of the PPS has been described [8, 33, 71, 72, 73]. TORS is the most recent of these advents. It has been widely used for oncologic surgery of the tonsil, tongue base and PPS [8, 32, 33].

The parapharyngeal space adjacent the base of tongue

In our study we chose the foramen cecum of BOT as a landmark for measurement of distances to PPS structures because it was an easily identifiable landmark for TORS. The closest mean distance to the PPS portion of the LA from the foramen cecum was 21mm (SD 3.8mm) (**Table 2**). To the best of our knowledge, this distance has not been measured before. Laurento et al., have shown the position of the LA and CNXII at the mouth as 2.7cm inferior and 1.6cm lateral to the foramen caecum [41]. O'Malley et al., have stated that the LA was encountered 1cm medial to the posterolateral BOT and 1.5-2cm deep to the tongue [28]. The focus of our study was the LA at the PPS just before it entered mouth at the posterior border of the hyoglossus muscle. This position corresponded to the linguoepiglottic fold on the oropharyngeal aspect. Thus this oropharyngeal landmark with combination of the measured distance maybe further helpful for surgeons to avoid injury to the PPS portion of the LA during TORS.

Prophylactic transcervical arterial ligation has shown a trend towards decrease major haemorrhage events post TORS in a retrospective review of 224 cases [36]. Similar results were demonstrated in a larger retrospective observational study by Polleli et al. [74]. They recommended transcervical ligation for the higher T-stage tumours as they were associated with higher rates of haemorrhage. It is these higher stage tumours that require incisions extending towards the PPS thus the high risk of vascular injury. We hope the utility of our study findings by surgeons may contribute to reduce the risk of such adverse events.

The LA branch off point from the ECA was a 30.9mm (SD 6.3mm) from the foramen cecum (**Table 2**). This measurement serves as an aid to know the proximity of the ECA at the lower PPS. This

measurement showed a statistically significant difference between sides. A similar anatomical study of looking at the LA distance from the foramen cecum did not show such a significance between sides [42]. It is possible that this result was due to chance considering the small sample size. One cadaver had considerable divergence of the right ECA laterally which gave a distance of 43.3mm which may have pushed the mean distance of the right side higher to 34.3mm compared to 27.4mm on the right side (**Table 2**).

The FA at the PPS is 27.4mm from the foramen cecum (**Table 2**). Haemorrhage from the FA injury is possible during TORS radical tonsillectomy and BOT resections. In Mandelet al.'s study for haemorrhage control with staged transcervical ligation, the FA was one of the three main vessels they had ligated [36]. The FA branch off point at the ECA was 32.1mm (SD 6.1mm) from the foramen cecum with a difference between sides (P-value 0.029). This difference may be due to chance. Similar to the earlier LA branch off point from the ECA measurement this measurement too had possibly been affected by the outlier specimen with a right-sided laterally deviating ECA. This may explain why mean distance of the FA origin was further away from the foramen cecum on the right side (**Table 2**).

The PPS portion of the CNIX was a mean distance of 22.7mm lateral from the foramen cecum of tongue base. This position of the nerve corresponded to the level of the foramen cecum. Thus this measurement on the horizontal plan may serve as a practical vantage point for surgeons to estimate position during TORS of the OP to avoid injury. Ohtsuka et al., have shown in cadaveric dissections and histological sectioning that the CNIX's lingual branch was adhered to the tonsillar capsule in 21.5% of cases when the muscular dehiscence between the superior and middle pharyngeal constrictor was prominent [58]. Lim et al., have shown in their anatomical study of cadavers that the CNIX was found lateral to the superior pharyngeal constrictor at the junction between the BOT and the posterior tonsillar pillar and the BOT [59]. Injury to this nerve can cause a taste disturbance. In large oncologic resections the conservation of CNIX may not be possible. In emerging robotic obstructive sleep surgery and lingual tonsillectomy [75, 76] our measurements could be utilised to avoid damaging the CNIX at the PPS during these relatively novel procedures.

The PPS portion of the LA was a mean distance of 23.6mm (SD 3.5mm) from the vallecula (**Table 3**). The root of LA at the ECA was a mean distance of 36.8mm (SD 6.2mm) from the vallecula. Similarly, the FA at the PPS and at its root at the ECA was 26.3mm (SD4.6) and 35.4mm (SD 6.6).

The LA artery is closer than the FA at this point overall. LA has been involved in massive haemorrhage in Polleli et al., series that looked at TORS complications [74]. Thus, careful dissection at this level is warranted.

The parapharyngeal space adjacent the vallecula

Measurements from the vallecula were made for better understanding the proximity of neurovasculature of the PPS at to this region for TORS oncologic resections. As part of TORS of the BOT resection, the first step is often making the inferior cut at the vallecula [28]. The LA at the PPS was a mean distance of 23.6mm (SD 3.5) from the vallecula. Dallan et al.'s cadaveric study showed the LA position at the BOT region in the mouth [61]. The robotic cadaveric dissections showed the LA entering the mouth on a plane between the genioglossus muscle medially and the hyoglossus muscle laterally. Our measurement represents the distance to the LA lateral to this entrance point at the PPS. We also supplemented this distance by providing the distance from vallecula to the LA origin at the ECA, which was 36.8mm (SD 6.2). This measurement maybe useful for the surgeon to gain a sense of proximity to the ECA at the level of the vallecula.

The FA closest point at the PPS was superior and lateral to the vallecula. This closest distance represented the proximal portion of the FA that traverse in a hook-link fashion around SHM before heading inferiorly towards the submandibular gland. The vallecula to FA at PPS closest mean distance was 35.4mm (SD 6.6mm). Furthermore, lateral from this position was the origin of the FA at the ECA which was a mean distance of 39mm (SD 5.4mm). Usually during TORS BOT resections, the next step after the vallecula resection is to divert the attention to making the lateral and superior resections at the oropharyngeal mucosa [28]. These two distances of the FA maybe beneficial to note when the TORS surgeons performed the lateral cuts.

In our study the closest mean distance from the vallecula to the PPS portion of the CNXII was 26.3mm (SD 2.6mm). Anatomical dissections by Dallan et al. demonstrated that the CNXII was in contact with the lateral surface of the hyoglossus muscle at the BOT region [61]. Our focus was on the BOT and attention to the PPS lateral to this region was not addressed and distance measurements from landmarks were not conducted in Dallan et al.'s study. We hope our measurements add further information on the findings of Dallan et al.'s study. The distance provided can be used to estimate the position of the CNXII when entering the PPS to achieve adequate tumour margins during TORS.

The parapharyngeal space adjacent the tonsillar fossa

The apex of the tonsillar fossa was a mean distance of 16.1mm to the ICA. There was a statistically significant difference between sides (P-value 0.014). Deutch et al., showed through study of MRI scans that as adulthood is reached the tonsillar fossa to ICA distance reaches an asymptote at 25mm with no discrepancy between sides [66]. One possible reason for the difference maybe the difference in the population of patients. Our study population composed of cadaveric subjects over 65 years. Age related changes in the cervical spine and ICA morphology possibly could have brought the ICA closer to the tonsillar fossa in our study. Furthermore, the measurement modality was different. Deutch et al., used MRI images to measure distances which could affect measurement accuracy. They also used a surrogate marker for the tonsillar fossa. The measurements were taken from the torus tubarius, which was used as an estimate for the tonsillar fossa position. In our study the difference in sides perhaps due to the prevalence of tortuosity of the ICA bringing the ICA closer to the tonsillar fossa or simply statistical coincidence due to the small sample size of 26 sides.

In our study the ICA was tortuous in 38% of cases. This may account for the moderate range in our measurement from 6.8mm to 24.1mm. Ozgur et al., showed by cadaveric dissection that 25% of cases had medially deviating ICA tortuosity which had brought the ICA closer to the pharyngeal constrictor muscle [49]. They also showed through histological examination of that kinked ICAs had vessel wall changes that may predispose them to iatrogenic injury. The arterial wall's tunica media was thin with less muscle fibres. The tunica adventitia had more vasa vasorum. Both the tunica media and tunica adventitial had dissections in the kinked segments of the ICA. This emphasises the importance of reviewing the ICA morphology in preoperative MRI and CT scans prior to TORS procedures to avoid injury to ICA.

Pfeiffer et al., have analysed radiologic images of aberrant parapharyngeal segments of ICAs' proximity to the pharyngeal wall to produce a clinical grading system [62]. The closet distance to pharyngeal wall on their study was 0.8mm on a 4 year old child. In that patient the position corresponded to the nasopharyngeal level. In that study, measurements were taken from the closest distance dimension at multiple levels of the pharynx including nasopharynx, OP, and hypopharynx regions. The overall average distance they concluded on their series of 35 cases was a distance of 7mm from the pharyngeal wall. This is a close match to our closest measurement of 6.8mm at the tonsillar fossa level (**Table 4**). The furthest distance in their study of the ICA from the pharyngeal wall was 17.9 which illustrates that overall an aberrant ICA is closer to the pharyngeal wall. Unlike

our study, Pfeiffer et al. had subjects form a wider age range, from children to adults. Our measurement maybe more representative of the patients who are undergoing oncologic surgery at the tonsillar fossa region.

In 2016, Pfeiffer et al., modified their grading system to reflect the clinical significance of the position of aberrancy taking into account the procedure case load at each region of the pharynx [63]. Grade I was regarded as low risk and included the ICA that was 10mm or more from the pharyngeal wall. Grade VII denoted the highest risk group where the ICA was 2mm or less from the pharyngeal wall. The ICA position parallel to the nasopharynx or oropharynx location was overall regarding as higher risk of injury due to frequent surgical procedures on this region compared to the hypopharynx. Our measured distance from the tonsillar fossa is valuable as it be considered a high risk of injury location according to this classification. Furthermore, we have given the measurement from a position more localisable area rather than to a broad area such as the OP.

In our study the ECA was found to be a mean distance of 20.3mm from the tonsillar fossa apex. Given the ECA is more laterally positioned to the ICA, this not so much at risk of injury compared to the ICA at the tonsillar fossa region. Wang et., have however shown anatomical variations of the ECA that can increase the risk of injury of the artery [67]. In their cadaveric study a medially deviating ECA through the SPM and SGM was present in 8% of cases. Wang et al., did not make any anatomical measurements from PPS structures to the oropharynx. In our study we did not observe such a characteristic variation although deviation of ECA was present in some specimens. The closest distance of the ECA to the tonsillar fossa apex in our study was 10.2mm.

The APA was found to be a mean distance of 16.3mm from the tonsillar fossa apex. It is one of the arteries that provided blood supply to the tonsil thus a source of bleeding during TORS radial tonsillectomy. Wang et al, study of arterial variations encountered through the transoral approached showed at APA originated from the medial surface of the ECA in 75% of cases [67]. The same study also demonstrated that the APA crosses the SGM muscle 12.6mm from its BOT attachment. We hope our study further supplements these findings to accurately identify and control bleeding from the APA during TORS radical tonsillectomy.

The aPA is another artery that has potential to cause haemorrhage when completing the lateral extent of tumour resection in TORS radical tonsillectomy procedure. The mean distance from the tonsillar

fossa apex to the aPA had a statistically significant difference between sides (P-value 0.003) with 11.2mm on the right and 8.4mm on the left side (**Table 4**). The reason for this side difference is possibly a statistical coincidence due to small sample size. The aPA in our study was quite intimately related to the SGM and SPM muscles. This artery passed between the two muscles in most cases. In the TORS radical tonsillectomy step where the SPM and SGM is skeletonised, the aPA would likely be encountered. The knowledge of the topography of the artery may serve in easy identification and haemorrhage control from the vessel during TORS.

We found the average distance to the styloid tip from the tonsillar fossa apex to be 21.1mm. In a study of endoscopic transoral dissections, the styloid process was often hidden behind the SPM and was reported to be easily identified with palpation [54]. Gudis et al., have reported successful TORS styloidectomy for a patient with Eagle Syndrome [77]. The patient presented with unilateral throat pain that had been caused by an elongated styloid process. Subsequently this patient was surgically treated with a successful TORS tonsillectomy, styloidectomy and pharyngoplasty. This is another relatively novel utility of TORS in skull base surgery. We hope that our measurement from the styloid tip would assist the surgeon to estimate depth and safely perform the TORS styloidectomy (**Table 5**).

We have provided mean distance from the SPM and SGM midpoint to the tonsillar fossa apex which are 17.6mm and 17.5mm, respectively. Dissection observations confirmed that the midpoints of these muscles corresponded to the tonsillar fossa region. Dallan et al., through their endoscopic transoral dissections concluded that the SPM and SGM were key anatomical landmarks for orientation at the PPS when operating via the transoral approach [54]. During TORS radical tonsillectomy the SPM and SGM must be dissected and divided when achieving a lateral tumour margin [29]. The distance measurements provided may benefit surgical navigation during the TORS radial tonsillectomy. The measurement could be used to estimate and anticipate the depth to these muscles.

The styloid process as a potentially useful landmark for TORS

The styloid process length has been known to be of variable length and an elongated styloid process has been implemented in the symptomatology of Eagle Syndrome [78]. Often patients with this syndrome present with unilateral symptoms of throat pain, neck pain, odynophagia and dysphagia. The symptoms are attributed to the irritation caused by the elongated styloid process. The variability in length of the styloid process was also present in our study. All the measurements from the styloid process tip showed a wide range (**Table 5**).

The CNIX was a mean distance of 5mm (SD 2.9mm) from the styloid process tip. The nerve was posterior to the styloid process tip in most cases. However, there was great variation of the position of the tip. Knowing the position of the styloid tip relative to the CNIX is useful for TORS led styloidectomy to accurately localising the styloid process. Gudis et al., 2011 described the treatment via TORS of a patient who presented with Eagle Syndrome [77]. They described performing a robot assisted tonsillectomy, pharyngoplasty and styloidectomy. The patient did not experience any complications and resolution of symptoms were reported. The CNIX could possibly be encountered due to its close relationship to the readily identifiable key landmark muscle – the SPM. From there both nerve and muscle could be tracked superiorly towards the styloid process.

Furthermore, Guidis et al., concluded that the excellent stereoscopic visualisation with TORS would serve well for future skull base procedures near this area [77]. We hope the measurements we have provided serve well for navigating this area. With regard to avoiding large vessel haemorrhage, we have reported the mean distance from the styloid tip to the ICA and ECA, which were 6.2mm and 6.3mm, respectively (**Table 4**). Both these distances had a wide range due to high variability of the position of the styloid tip. In some instances, the styloid tip was very close to these two arteries.

The axial plane distance measurements from the medial surface and lateral surface of the pharyngeal constrictor muscle to the styloid tip maybe useful for anticipating the structure at the start of the TORS procedure. From the medial surface of the pharyngeal constrictor to the styloid tip was a mean distance of 20.2mm (SD 6.7mm) on the horizontal place. However, in practise the dissection may not always begin directly adjacent the styloid tip level on the horizontal plane. Reviewing the preoperative imaging to estimate the corresponding mucosal level adjacent the styloid tip and using our study measurement as a guide would be the possible way to help the surgeon plan the procedure and navigate during the procedure towards the styloid tip. A similar principle could be utilised in using the lateral surface of pharyngeal constrictor muscle to the styloid tip mean distance measurement which was 15.3mm (SD 7.0mm) to the styloid tip. Guidis et al., performed a pharyngoplasty along with the styloidectomy procedure [77]. If this method is utilised then knowing the distance from the lateral surface of this pharyngoplasty flap to styloid process tip could be useful.

Parapharyngeal space topographical anatomy adjacent the greater cornu of hyoid bone

The GCH marks the inferior border of the inverted pyramid shaped PPS. Knowing the topographic anatomy near this area is particularly useful for TORS of the BOT lesions. This is especially true if dissections needed to be extended laterally to achieve adequate tumour margins. The LA was often closely associated with the posterior end of the GCH. It was consistently found to be superior the GCH posterior end. We have provided the mean vertical distance from GCH posterior end to the LA which was 3.5mm (SD 1.6mm).

Dallan et al., have shown the topography of the LA within the base of tongue region through robotic-aided dissection of cadaver specimens [61]. The study demonstrated that the plane lateral to the genioglossus muscle is the area where the LA injury is risk would be high. The study however did not extend the dissection furthermore lateral to the hyoglossus muscle to show the proximal extent of the LA. Our dissections which focussed more on the PPS portion of the LA adding further information to the topography of the LA that can be used in TORS.

To gain an appreciation for the proximity of the ECA near this area, we have also provided the mean distance from GCH to the LA branch off point at ECA which was 11.3mm (SD 4.5mm). Lim et al., have measured the distance from GCH to ECA at the level of C6 vertebrae level on CT scans [59]. In our study the ECA was 4.3mm on the right and 3.4mm on the left side from the ipsilateral GCH. These distances were measured on the axial plane. Our measurements to the ECA rather focussed on the origin of the LA on ECA so the measurements were not always exactly on the axial plane measured horizontally to the ECA. This would explain this difference of about 6 to 7mm in our study. Gun et al., 2016 also demonstrated the LA position at the junction between the SGM and BOT in transoral cadaveric dissections [55]. At this point the proximal portion of the LA was found between the GCH and SGM. Then the more distal portion of the LA was demonstrated to pass deep and lateral to the SGM giving off dorsal lingual branches.

CNXII is closely related to the LA and GCH at the inferior PPS. We measured the mean distance from the GCH posterior end to the CNXII to be 11.4mm (SD 3.4mm) (**Table 6**). The LA is crossed by the CNXII laterally at the point where the LA makes a loop superiorly [55]. In our dissections the loop of the LA was often found just superior to the posterior end of GCH. Dallan et al.'s endoscopic dissections showed the position of CNXII more proximal and inferior to the SGM muscle distal attachment [54]. It was found at this location to be small compared to its size viewed from the lateral

aspect. The LA branches and lingual vein branches were medial to the CNXII. This location corresponds to the anterior edge of the PPS. In our study we have assessed the CNXII from a position slightly more lateral from the GCH. This supplements the knowledge already gained through the previous studies that focussed more closely to the transoral anatomy of the nerve mainly as it appeared in the mouth [54, 61].

The LN was a mean distance of 28.4mm anterior to the GCH. The nerve is at risk of injury during TORS radical tonsillectomy, where the nerve was found in the space lateral to the pharyngeal constrictor muscle and anteromedial to the medial pterygoid muscle [55]. In our study we made the measurement from GCH to gain an overall understanding of the wider field available for the TORS of the PPS.

The position of the FA was also assessed relative to the position of the GCH. The FA was a mean distance of 15.1mm (SD 5.0mm) from the GCH (**Table 6**). Generally the position of this artery was more superior to the LA. Injury to the artery is a source of haemorrhage with TORS procedures [74]. Some groups have suggested external ligation in select cases prior to the TORS procedure [34, 36, 74]. The knowledge of the artery's position relative to the GCH is still important because the topographic variation may result in close proximity to the GCH. The measurement range illustrates that the closest distance from the FA to the GCH was 15.1mm (SD 5.0mm) (**Table 5**). The measurement to the FA origin at the ECA from the GCH was also a similar value 16.0mm (SD 5.2mm). This value also had a wide range (7.6mm to 33.1mm). This demonstrated that the position of the FA relative to GCH is more variable than the position of the LA relative to the GCH.

It is possible that the presence of the linguofacial trunk may have contributed to the above measurement variations. In our study the linguofacial trunk was present in 5 specimen sides (19%) (**Graph 2**). This could be considered quite a common occurrence. In one cadaver based study conducted in South Korea, the presence of a common origin of the superior thyroid artery and lingual artery was also described as another possible branching pattern variation of the ECA branches [79]. In the aforementioned study the presence of a thyrolingual trunk or a linguofacial trunk was observed at a frequency of 16.6% (five dissections). The study however did not report the individual occurrence of the linguofacial trunk separate to the frequency of the thyrolingual trunk. Thus it was not possible to conclude how many of those five cadavers contained a linguofacial trunk. In our study we did not observe the occurrence of the thyrolingual trunk in any cadaver. Another cadaveric study conducted

in Brazil reported the frequency of linguofacial trunk in 19.4% of case (Seven hemisected sides) [79]. In the aforementioned study the linguofacial trunk was the most common anatomical variation of the branching pattern of the thyroid artery, LA and FA. The next most common variation was the presence of the thyrolingual trunk in 2.8% of cases [79].

In our study when the linguofacial trunk was present the measurement of the FA origin was made to the origin of this trunk at the ECA. This trunk was a relatively higher calibre vessel than either of the two other arteries. Thus, a high degree of caution should be exercised in the inferior PPS dissections to avoid injury to this structure. The surgeon should pay close attention to the possibility of the FA position being near the GCH. Perioperative imaging would be useful for early recognition of the presence of the linguofacial trunk to plan the TORS procedure accordingly.

The stylopharyngeus muscle and styloglossus muscle midpoints as useful landmarks for transoral surgical approaches

The SPM midpoint was readily identified in all specimens of the study. The coronal sectioning of the cadaver allowed visualisation of the entire length of this muscle. Because the dissection was approached from the posterior aspect of the specimen, the SPM was the first of the muscles originating from the styloid process that was visualised. The SGM was found anterior to this muscle. In the TORS approach where incisions are made at the anterior and medial boundaries of the PPS, the SGM would be encountered first. However, because of the relative close proximity of these muscles superiorly as they converge to a common origin at the styloid process, it is possible to encounter the SGM and SPM almost simultaneously if not soon after the first one is identified. The post-styloid space which is posterior-lateral to these two muscles contain the carotid arteries and the lower cranial nerves.

The midpoint of SPM to the ECA on the axial plane was mean distance of 8.9mm (SD 3.9mm) (**Table 7**). The mean distance from the SGM to the ECA was 5.5mm (SD 3.4mm) (**Table 8**). Usually this measurement would be made to the vessel positioned posterior to these muscles. Wang et al., described a variation where the ECA bludged medially between the SPM and SGM in 8% of cases in their cadaveric study [67]. This variation would bring the ECA close to the pharyngeal wall and increase risk of injury to the vessel during TORS. Wang et al.,'s study however did no distance measurements from the SPM and SGM to the ECA [67]. Our study provided a mean distance measurement that is useful to know for the surgeon to navigate the PPS near the SPM and SGM.

The mean distance from the midpoint of the SPM to the ICA was 2.1mm (SD 1.6mm). In some instances, the midpoint of this muscle was in direct contact with the ICA. This relationship was very similar to Dallan et al.'s endoscopic transoral anatomy study where the ICA was reported to be closely associated with the ICA [61]. In the present study, we have provided a mean measurement of this proximity to add to the growing knowledge base. The measurement is useful during TORS radical tonsillectomy procedure where the SPM and SGM would need to be divided to achieve a lateral margin of tumour excision. To achieve this step safely the SGM an SPM muscles need to be dissected to clearly define them. The carotid pulsation needs close attention as these muscles are divided. We can confirm with a mean distance measurement that the ICA is very close to the artery so careful dissection and transection is warranted. Especially in cases where the SPM would be in contact with the ICA.

The mean distance from the SGM midpoint to the ICA was 6.8mm (SD 1.8mm) (**Tables 7 and 8**). The transection of this muscle along with the SPM is a key step in TORS radical tonsillectomy [32]. Wang et al.[67], had measured the length of the SGM muscle as a part of their anatomical study however they did not measure the proximity to vessels from the muscle. We hope our distance measurements further strengthens the PPS anatomical knowledge for TORS. The SGM is more anterior to the ICA than the SPM. Thus, there were no cases where the ICA was in direct contact with SGM unlike the SPM. Surgeons may transect the SGM with more confidence with regard to avoiding injury to the ICA.

The LA vertical distance from the SPM and SGM midpoints were 27.0 (SD 5.1mm) and 23.6mm (SD 6.6mm), respectively. Similarly, the LA branch off point form the ECA was measured from the SPM and SGM midpoints which were 32.7mm (SD 5.7mm) and 29.8mm (SD 6.8mm), respectively. The LA was always inferiorly positioned with respect to the midpoints of SGM and SPM. The SGM midpoint was slightly inferior to the SPM midpoint. Thus, the LA was closer to the SGM midpoint. Overall, the risk of injury to the main trunk of the artery during transection of these muscles maybe low. However, during TORS radical tonsillectomy the risk of injuring the artery is high during the resection of the BOT margin [32]. This step is usually performed after the SPM and SGM is transected. It is possible that the measurements from the midpoint will aid the surgeon to avoid injury to the LA when attention is switched to the inferior portion of the dissection.

Similar mean distance measurements were made from the SPM and SGM midpoints to the FA (**Tables 7 and 8**). The FA was closer to the SGM midpoint than the SPM midpoint (14.6mm vs 19.5mm, respectively). Dallan et al.'s endoscopic transoral anatomical study concluded that the SGM and SPM should be considered as key anatomical landmarks for orientation within the PPS [54]. Gun et al., have recently furthered this knowledge through transoral endoscopic dissection of cadavers, where they concluded that the stylohyoid ligament was also an important landmark for orientation [55]. This ligament is often found between the SPM and SGM. From the transoral approach it was more readily appreciated after the entering the PPS via incision through pharyngobasillar fascia. The palatopharyngeal muscle direction would somewhat be parallel to the stylohyoid ligament. The study also presented how the FA appeared relative to the SGM in the transoral endoscopic view. However, that study did not measure distances between structures. Our study's contribution of measurements may further supplement the knowledge contributed by these cadaveric studies that focussed on topographic anatomy.

We have attempted to define a relatively high vascular area around the distal end of the SPM and SGM (**Figure 22**). Wang et al., described the path of the aPA which is a branch of the FA relative to the SGM, where the aPA crossed the SGM 6.6mm from the artery's point of origin [67]. The distal attachment of the SPM at the pharyngeal constrictor muscle and the SGM distal attachment at the BOT were supplied by small unnamed arterial branches of the LA and FA (**Figure 19, 21, and 22**). The advantage of our study design was vessels that supply the posterior aspect of the SPM and SGM were easily identifiable. Most other studies had the dissection performed from the anterior aspect of the PPS thus would not have found these vessels unless they divided the muscles to explore the post-styloid space. In some cases, there were small arteries directly branching off the ECA that supplied the SPM's distal attachment area posteriorly (**Figure 21**). Anterior to this area we have described a relatively high vascular area where the branches from the LA and FA supply the distal segments of the SPM and SGM (**Figure 22**). In this area the aPA can be found branching off the FA. This could be conceptually perceived as a triangular zone: The SPM and SGM superiorly, the pharyngeal constrictor medially, the medial pterygoid muscle laterally, and the GCH bone inferiorly. It is worth exploring and viewing this area through endoscopic transoral dissection to confirm if this zone of caution could still be perceived with the same muscular borders. Whether defining this zone would aid TORS of this area could be tested via robotic dissection of cadavers at this zone.

The CNIX was a mean distance of 1.9mm (SD 1.6mm) from the SPM midpoint on the axial plane (**Table 7**). There is a very close relationship between the SPM and the CNIX. It was often in contact with the muscle's posterior surface and descended towards the BOT along the muscle's inferior edge (**Figure 15 and 21**). Wang et al., showed two main topographic patterns of the CNIX at the BOT [60]. In 75% of cases CNIX is crossed by the pharyngeal branch of CNX laterally. In 25% of cases both of these nerves would run parallel towards the BOT region. The study also described the extracranial portion of the CNIX in three main segments taking into consideration its relationship to SPM [60]. We have measured the mean distance of this nerve from the SPM midpoint which we hope supplements the topographic knowledge for TORS of the PPS.

The mean measurement of the SGM midpoint to the CNIX was 4.8mm (SD 2.0mm) (**Table 8**). From the transoral dissections of the PPS this nerve was visualised positioned between the SGM and SPM [55, 59]. The nerve is not as closely related to the SGM as it is with the SPM. The measurement is useful for localisation of the nerve in TORS, considering the SGM is one of the readily identifiable landmarks for the transoral PPS approaches [54]. Overall in our study the midpoints of these muscles corresponded to the oropharynx, in particular the zone parallel to the tonsillar fossa. Thus, these measurements made from the SPM and SGM midpoints would be useful for the TORS radical tonsillectomy procedure to estimate distances from important cranial nerves and blood vessels.

The styloid tip to the SPM and SGM mean measurement was 8.3mm (SD 4.1mm) and 9.3mm (SD 5.6mm) (**Table 7 and Table 8**). Both measurements had a wide range. It is possible that this is due to the great variability of the styloid process length. Successful TORS for styloidectomy in a patient who presented with Eagle Syndrome has been reported by Guidis et al. [77]. Kamil et al., reported the use of TORS to treat a patient who presented with similar symptoms [81]. However, in this report the patient had an elongated calcified stylopharyngeus muscle and tendon that was responsible for the symptoms of odynophagia and neck pain. The calcification composed the full length of the SPM from its origin at the styloid process to its insertion at the pharynx. The patient was successfully treated with TORS to remove the calcified segment and confirmed full symptom resolution at week three follow up. The mean measurements from the SPM midpoint and SGM midpoint to the styloid process tip presented in our study may facilitate similar procedures in the future.

The parapharyngeal neurovasculature topographical and morphometric relationships to the oropharyngeal mucosa and lateral surface of the pharyngeal constrictor muscle

One of the strengths in the coronally dissected specimens in the present study was the ability to deduce the relationship of the PPS structures to the OP mucosa and pharyngeal constrictor muscle wall. In our initial dissections of the mid-sagitally dissected cadavers the OP mucosa and the constrictor muscle wall was removed step by step to enter the PPS. Thus, it was not possible to relate the oropharyngeal mucosal landmarks to the laterally positioned PPS accurately. Furthermore, it was not possible to measure the distances from the oropharyngeal mucosa nor the pharyngeal constrictor muscle to the PPS structures on the axial plane. The coronally sectioned specimens allowed these measurements to be taken because the PPS could be dissected without the destruction of the pharyngeal constrictor muscle. Simultaneously it was possible to gain access to the posterior pharynx through a midline incision longitudinally on the posterior aspect of the pharyngeal constrictor muscle. This allowed axial plane measurements from the oropharyngeal mucosa and lateral wall of the pharyngeal constrictor muscle. It also allowed to correlate the PPS anatomy to oropharyngeal mucosal landmarks.

Another advantage of the coronally sectioned cadaver dissection over transoral dissections was that the cadaver did not need dissection from the transcervical perspective to confirm the discovered structures. This was because a given structure could be dissected on its entirety within the PPS on the coronally sectioned cadaver to make confirmation. We hypothesize this is a better method because with transcervical dissection it is possible to disrupt the topography of anatomical structures.

We measured the distance from the SPM and SGM midpoints to the oropharyngeal mucosa (**Table 9**). Considering these are two key landmarks for TORS of the PPS, we hope these measurements maybe be useful for accurate and efficient dissection towards these structures. Similarly mean distance to these muscles were also measured from the lateral aspect of the pharyngeal constrictor muscle. We hope these measurements would also serve useful in instances where the mucosa would be disrupted by tumour to accurately estimate distance by placing more reliance on the lateral surface of the pharyngeal constrictor muscle.

The PPS portion of the LA was a mean distance of 5.7mm (SD 1.8mm) from the mucosal surface of the oropharynx on the axial plan (**Table 8**). The LA course of within the mouth and the topography of the vessel within oral cavity has been studied in some detail [38, 51, 58, 66], 42]. This is because the haemorrhage from this artery and its branches are quite common during excision of tongue base

lesions [36, 69]. TORS for lingual tonsillectomy has also been described [75]. Son et al., have shown through cadaveric dissections and histologic sections that there is a relatively avascular plane between the lingual tonsil and the intrinsic tongue muscles [75]. We hope to add more information to the course of the LA by providing the distance to PPS portion of the LA. This position corresponds to the LA before it passes to the mouth at the hyoglossus posterior edge. To the best of the author's knowledge this distance has not been reported in the literature before.

The LA branch off point from the ECA was a mean distance of 14.0mm (SD 4.1mm) from the OP mucosa and 11.6mm (SD 3.9mm) from the lateral surface of pharyngeal constrictor muscle (**Table 9 and 10**). These measurements offer an estimate to the proximity of the ECA at the BOT level because the LA branch off point corresponded to the BOT region of the OP. Lim et al., measured the ECA proximity to the GCH on CT scans however did not comment on the proximity of the ECA from the oropharynx or the pharyngeal constrictor [59].

The mean closest distance from the FA at the PPS to OP mucosal surface was 9.5mm (SD 3.4mm). The mean measurement was also taken from the lateral surface of the pharyngeal constrictor muscle which was 6.7mm (SD 4.1mm) (**Table 10**) This portion of the FA was positioned in the highly vascular area bound by the SHM, SPM and medial pterygoid muscle as described earlier (**Figure 22**). This area corresponded to the BOT and inferior tonsillar fossa region. Care should be taken when performing transoral dissecting at this zone to avoid injury to the FA here. Inferior to this zone the FA approached the submandibular gland and indented the superior medial portion of the gland. Poille et al.'s large institutional retrospective chart review revealed some of the patients that had sever haemorrhage complication had bleeding from the LA or FA [74]. Some of these patients required interventional radiologic embolisation of the culprit artery while others required transcervical vessel control in theatre.

In a similar way, mean measurements were taken from the FA branch off point at the ECA to the OP mucosa and lateral surface of the pharyngeal constrictor muscle. From the OP mucosa the FA origin at the ECA was 14.0mm (SD 4.1mm) (**Table 9**). From the lateral surface of the pharyngeal constrictor muscle the FA origin at ECA was 12.5mm (SD 5.2mm) (**Table 10**). Dallan et al. and Gun et al. have provided endoscopic transoral views of the FA at the OP level [54, 55], however neither study have offered distance measurements to supplement the topographic anatomic dissection reports. To combine the distance knowledge where the FA closest point is from the pharyngeal wall and where

it is given off from the ECA means the surgeon will have a sound impression of how close the ECA is at that region thus may aid in avoiding sever haemorrhage from ECA injury.

The CNXII closest proximity to the pharynx corresponded to the point where the nerve made a turn toward the mouth having descended from the skull base. This level approximately corresponded to the inferior most part of the PPS near the GCH, posterior to the posterior edge of the hyoglossus muscle. The CNXII closest distance to the OP mucosa at this level was 9.5mm (SD 2.3mm) (**Table 9**). The nerve was 3.3 (SD 1.5mm) from the lateral wall of the pharyngeal constrictor muscle at this level (**Table 10**). Dallan et al., described the CNXII as it appeared in the endoscopic transoral view at the entrance to the mouth, where it was lateral to the hyoglossus muscle and associated with a concomitant vein [61]. These findings were then confirmed in a robotic transoral dissection of the two cadaveric specimens in the same study. The nerve is at risk of injury when BOT resections or radical tonsillectomy procedures need to be extended dissections infero-laterally to achieve adequate tumour margins. We hope the measurements given would be useful for the surgeon operating in this area. Taking into consideration the normal distances in the disease-free state the surgeon can plan to anticipate the nerve in the disease state taking into account the tumour size in preoperative imaging. Collaboration with a radiologist for preoperative planning may be valuable [61].

The depth to the LN was measured from the OP and lateral surface of pharyngeal constrictor muscle to the point where the nerve would make an 'L' shape turn having descended from the skull base, it turned anteriorly to past towards the mouth. We note that this turning point was the final portion of the LN in the PPS before entering the mouth.

The mean distance of the LN from the OP mucosa was 10.2mm (SD 3.1mm) and 3mm (SD 1mm) from the lateral surface of the pharyngeal wall (**Table 10**). Dallan et al., had shown in endoscopic dissections the position of the LN was inferior to the SGM distal attachment at the BOT [54]. Our dissections of coronally sectioned specimens from the posterior aspect confirmed this conclusion (**Figure 20**). The portion of this nerve than passes lateral to the medial pterygoid is somewhat protected from injury during TORS unless the muscle needs to be dissected as part of achieving an adequate oncologic margin. The LN is at risk of injury during TORS radical tonsillectomy at two possible positions. One position is at the region the nerve emerges to the floor of mouth anterior to the anterior border of the medial pterygoid muscle [55]. Second position is at the retromolar trigone before the nerve passes lateral to the posterior border of the medial pterygoid muscle.

Limitations of the study

The cadaver ages were rather senior in age (66 years to 94 years). The current growing number of tonsillar cancers are attributable to patients younger than this age range, especially HPV positive cancers [82, 83]. It is possible that the head and neck anatomy can change somewhat with advanced age. The cervical spine degeneration and shortening of the neck length may contribute to changes in vessel morphology. These factors would have affected the accuracy of some observations and measurements made in the PPS in our study compared to population of younger patients.

The measurements made on the axial plane may have some measurement error due to the axial plane was perceived with the measurer's eye of best fit. We hope obtaining a mean measurement value would have help reduce the error associated with this. Another way to improve this would be to use a calliper with a built-in water level to achieve a perfect horizontal plane measurement.

The study aimed at contributing for the knowledge base of transoral anatomy of the PPS. However, the transoral morphology was not explored in the study. Part of the reason for that was in order to make new deductions, we conserved the oropharyngeal mucosal surface and lateral surface of the pharyngeal wall. It would have strengthened the study to further dissect the coronally sectioned cadavers transorally once the measurements and observations were made from the posterior coronal plane. This method would have allowed us to gain more information regarding the anteriorly positioned vasculature of the mouth region that would be encountered in the first few stages of a TORS procedure. However, this would mean the scope of the study would have had to be expanded to the microsurgical anatomy of the mouth as well.

The study limited its findings to the PPS adjacent the oropharynx. The skull base anatomy adjacent the nasopharynx was largely not included in the measurements aspect of the study. Although the dissection did extend to this region somewhat, the skull base foramina level was left unexplored. The skull base component of the parapharyngeal space is undeniably complex and it is possible that TORS may play an important role in addressing the tumours of the skull base [84, 85]. We believe this could be an entirely new focused study for the future.

Our study did not correlate the gross anatomic dissection findings with radiological imaging. Radiological imaging such as CT and MRI play a critical role in the assessment of the head and neck

oncology patient. One way a study could expand to include these imaging information is by scanning the cadavers prior to dissection then correlating that anatomy with the dissection findings. Logistics of performing this task deemed too difficult at our institution due to unavailability of a CT scan on site for such studies.

Conclusions

The PPS at the BOT region was elaborated with proximity measurements from the BOT midline, midline vallecula and GCH. Considering the risk of injury to the LA at this region we provided the mean distance measurement to the PPS portion of the artery from three key anatomical landmarks stated. From the BOT midline the LA was 21mm (SD 3.8mm). LA is 23.6mm (SD 3.5mm) from the vallecula midline. From the GCH the LA is positioned 3.5mm (SD 1.6mm) superiorly.

The superior pole of the tonsil is a possible anatomical landmark that can be utilised to TORS of the PPS. We have provided mean proximity measurements of select PPS structures from this point on the axial plane, which may aid navigation of the PPS for surgeons. The ICA was 16.1mm (SD 4.3mm) from the superior pole of the tonsil. APA and aPA are 16.3mm (SD 7.4mm) and 10.1mm (SD 2.6mm) from here, respectively.

The SPM and SGM midpoints correlated to the tonsillar fossa region medially. The linear mean distances from the SPM and SGM provided in our study may benefit surgeons in conceptualising vicinity to vital select structures from these muscles during transoral PPS procedures. The SPM midpoint is very closely associated with the ICA. Form the SPM midpoint the ICA is located 2.1mm (1.6mm) posterolaterally. The CNIX is also closely associated with the midpoint of this muscle. It is 1.9mm (SD 1.6mm) form the SPM midpoint. The FA is 19.5mm (SD 3.2mm) inferior to the SPM midpoint. From the SGM midpoint the FA is 14.6mm (SD 3.9mm) inferiorly. The SGM midpoint was 5.5mm (3.4mm) from the ECA on the axial plan.

The distal attachments of the SPM and SGM represents a highly vascular area. Arterial branches to this area are supplied by the ECA directly, LA and FA. This area possibly could be conceptualised as a window: the SPM and SGM forming the superior border, the pharyngeal constrictor medially, the medial pterygoid muscle laterally, and the greater cornu of hyoid bone inferiorly.

The axial plane linear mean measurements provided from the OP mucosal wall and from the lateral surface of the pharyngeal constrictor muscle to select points of the PPS structures may help estimate dissection depth and help anticipate these PPS structures in transoral PPS surgery. From the oropharyngeal mucosa to the FA was 9.5mm (SD 3.4mm). Similarly, from the lateral surface of the pharyngeal constrictor muscle the artery was 6.7mm (4.1mm). CNXII was 9.1mm (SD 2.3mm) and

3.3mm (1.5mm) from the oropharyngeal mucosa and lateral surface of the pharyngeal constrictor muscle, respectively. The LN PPS portion was very close to the lateral surface of the pharyngeal wall near the GCH level. The nerve was 3.0mm (SD1.0) lateral to the lateral surface of the pharyngeal wall.

The ICA tortuosity can bring the vessel into proximity to the lateral surface of the pharyngeal wall. ICA tortuosity was present 38% (10 sides) of the specimen sides dissected. The linguofacial trunk was present in 19% of cases (5 sides). Evaluating these possible anatomical variations in preoperative images would be valuable to avoid major vascular injury.

References

1. Lingen MW. Chapter 16 Head and Neck. In: Kumar V, Abbas, A. K., Aster j. C. , editor. Robbins and Cotran Pathologic Basis of Disease 9th ed. Philadelphia: Elsevier Saunders; 2015. p. 727-48.
2. Khafif A, Segev Y, Kaplan DM, Gil Z, Fliss DM. Surgical management of parapharyngeal space tumors: a 10-year review. Otolaryngol Head Neck Surg. 2005;132(3):401-6.
3. Olsen KD. Tumors and surgery of the parapharyngeal space. Laryngoscope. 1994;104(5 Pt 2 Suppl 63):1-28.
4. National Cancer Registry Ireland. Cancer Trend No 33 HPV Associated Cancers. https://www.ncri.ie/news/article/hpv-associated-cancers-ireland-report-national-cancer-registry. Published 2017. Accessed September 23, 2018.
5. Hintze JM, O'Neill JP. Strengthening the case for gender-neutral and the nonavalent HPV vaccine. Eur Arch Otorhinolaryngol. 2018;275(4):857-65.
6. Chen R, Aaltonen LM, Vaheri A. Human papillomavirus type 16 in head and neck carcinogenesis. Rev Med Virol. 2005;15(6):351-63.
7. Gillison ML, Broutian T, Pickard RK, Tong ZY, Xiao W, Kahle L, et al. Prevalence of oral HPV infection in the United States, 2009-2010. JAMA : the journal of the American Medical Association. 2012;307(7):693-703.
8. Genden EM, O'Malley BW, Jr., Weinstein GS, Stucken CL, Selber JC, Rinaldo A, et al. Transoral robotic surgery: role in the management of upper aerodigestive tract tumors. Head Neck. 2012;34(6):886-93.
9. Viens LJ, Henley SJ, Watson M, Markowitz LE, Thomas CC, Thompson TD, et al. Human Papillomavirus-Associated Cancers - United States, 2008-2012. MMWR Morb Mortal Wkly Rep. 2016;65(26):661-6.
10. Australian Government Department of Health. Australian Immunisation Handbook. Human Papillomavirus (HPV). https://immunisationhandbook.health.gov.au/ vaccine-preventable-diseases/human-papillomavirus-hpv. Published 2018. Accessed September 23, 2018.
11. Lu B, Kumar A, Castellsague X, Giuliano AR. Efficacy and safety of prophylactic vaccines against cervical HPV infection and diseases among women: a systematic review & meta-analysis. BMC Infect Dis. 2011;11:13.

12. Brotherton JM, Fridman M, May CL, Chappell G, Saville AM, Gertig DM. Early effect of the HPV vaccination programme on cervical abnormalities in Victoria, Australia: an ecological study. Lancet. 2011;377(9783):2085-92.
13. Graham DM, Isaranuwatchai W, Habbous S, de Oliveira C, Liu G, Siu LL, et al. A cost-effectiveness analysis of human papillomavirus vaccination of boys for the prevention of oropharyngeal cancer. Cancer. 2015;121(11):1785-92.
14. Pasha D GJ. Otolaryngology Head and Neck Surgery Clinical Reference Guide Fourth Edition, Chapter 7, Pg 253- 334, San Diego Plural Publishing Inc 2014.
15. Lydiatt WM, Patel SG, O'Sullivan B, Brandwein MS, Ridge JA, Migliacci JC, Loomis AM, Shah JP. 2017. Head and Neck cancers-major changes in the American Joint Committee on cancer eighth edition cancer staging manual. CA Cancer J Clin 67:122-137.
16. Deschler DG, Moore MG, Smith RV, eds. Quick Reference Guide to TNM Staging of Head and Neck Cancer and Neck Dissection Classification, 4th ed. Alexandria, VA: American Academy of Otolaryngology–Head and Neck Surgery Foundation, 2014.
17. ClinicalTrials.gov [Internet]. Ferris R: National Library of Medicine (US). 2013 Jul 12-. Identifier NCT01898494, Transoral Surgery Followed By Low-Dose or Standard-Dose Radiation Therapy With or Without Chemotherapy in Treating Patients With HPV Positive Stage III-IVA Oropharyngeal Cancer; 2018 Aug 3 [cited 2018 Sep 23]. Available from: https://clinicaltrials.gov/ct2/show /study/NCT01898494?show_locs=Y#locn.
18. Bonner JA, Harari PM, Giralt J, Azarnia N, Shin DM, Cohen RB, et al. Radiotherapy plus Cetuximab for Squamous-Cell Carcinoma of the Head and Neck. N Engl J Med. 2006;354(6):567-78.
19. Bonner JA, Harari PM, Giralt J, Cohen RB, Jones CU, Sur RK, et al. Radiotherapy plus cetuximab for locoregionally advanced head and neck cancer: 5-year survival data from a phase 3 randomised trial, and relation between cetuximab-induced rash and survival. Lancet Oncol. 2010;11(1):21-8.
20. ClinicalTrials.gov [Internet]. Palma D, Nichols A: National Library of Medicine (US). 2012 May 2-. Identifier NCT01590355, A Phase II Randomized Trial for Early-stage Squamous Cell Carcinoma of the Oropharynx: Radiotherapy vs Trans-oral Robotic Surgery (ORATOR); 2018 Aug 18 [cited 2018 Sep 23]. Available from: https://clinicaltrials.gov/ct2/show/study/NCT01590355.

21. ClinicalTrials.gov [Internet]. Simon C: National Library of Medicine (US). 2016 Dec 6-. Identifier NCT02984410, Study Assessing The "Best of" Radiotherapy vs the "Best of" Surgery in Patients With Oropharyngeal Carcinoma (Best Of); 2018 Jul 17 [cited 2018 Sep 23]. Available from: https://clinicaltrials.gov/ct2/show/NCT02984410.
22. Nichols AC, Yoo J, Hammond JA, Fung K, Winquist E, Read N, et al. Early-stage squamous cell carcinoma of the oropharynx: radiotherapy vs. trans-oral robotic surgery (ORATOR)--study protocol for a randomized phase II trial. BMC Cancer. 2013;13:133.
23. Chen AY, Frankowski R, Bishop-Leone J, Hebert T, Leyk S, Lewin J, Goepfert H. 2001. The development and validation of a dysphagia-specific quality-of-life questionnaire for patients with head and neck cancer: the M. D. Anderson dysphagia inventory. Arch Otolaryngol Head Neck Surg 127:870-876.
24. Chu F, Tagliabue M, Giugliano G, Calabrese L, Preda L, Ansarin M. From transmandibular to transoral robotic approach for parapharyngeal space tumors. Am J Otolaryngol. 2017;38(4):375-9.
25. Yoo J, Dowthwaite SA, Fung K, Franklin J, Nichols A. 2013. A new angle to mandibular reconstruction: the scapular tip free flap. Head Neck 35:980-986.
26. New GB: Mixed tumors of the throat, mouth and face. J Am Med Assoc 75:732-736, 1920.
27. Work WP: Tumors of the parapharyngeal space. Trans Pac Coast Otoophthalmol Soc Annu Meet 45:79-82, 1964.
28. O'Malley BW, Jr., Weinstein GS, Snyder W, Hockstein NG. Transoral robotic surgery (TORS) for base of tongue neoplasms. Laryngoscope. 2006;116(8):1465-72.
29. Chung TK, Rosenthal EL, Magnuson JS, Carroll WR. Transoral robotic surgery for oropharyngeal and tongue cancer in the United States. Laryngoscope. 2015;125(1):140-5.
30. Lee SY, Park YM, Byeon HK, Choi EC, Kim SH. Comparison of oncologic and functional outcomes after transoral robotic lateral oropharyngectomy versus conventional surgery for T1 to T3 tonsillar cancer. Head Neck. 2014;36(8):1138-45.
31. Moore EJ, Olsen KD, Kasperbauer JL. Transoral robotic surgery for oropharyngeal squamous cell carcinoma: a prospective study of feasibility and functional outcomes. Laryngoscope. 2009;119(11):2156-64.
32. Weinstein GS, O'Malley BW, Jr., Snyder W, Sherman E, Quon H. Transoral robotic surgery: radical tonsillectomy. Arch Otolaryngol Head Neck Surg. 2007;133(12):1220-6.

33. O'Malley BW, Jr., Quon H, Leonhardt FD, Chalian AA, Weinstein GS. Transoral robotic surgery for parapharyngeal space tumors. ORL J Otorhinolaryngol Relat Spec. 2010;72(6):332-6.
34. Asher SA, White HN, Kejner AE, Rosenthal EL, Carroll WR, Magnuson JS. Hemorrhage after transoral robotic-assisted surgery. Otolaryngol Head Neck Surg. 2013;149(1):112-7.
35. Chia SH, Gross ND, Richmon JD. Surgeon experience and complications with Transoral Robotic Surgery (TORS). Otolaryngol Head Neck Surg. 2013;149(6):885-92.
36. Mandal R, Duvvuri U, Ferris RL, Kaffenberger TM, Choby GW, Kim S. Analysis of post-transoral robotic-assisted surgery hemorrhage: Frequency, outcomes, and prevention. Head Neck. 2016;38 Suppl 1:E776-82.
37. Bertolin A, Ghirardo G, Lionello M, Giacomelli L, Lucioni M, Rizzotto G. Lateral pharyngotomy approach in the treatment of oropharyngeal carcinoma. Eur Arch Otorhinolaryngol. 2017;274(6):2573-80.
38. Bozza F, Vigili M, Ruscito P, Marzetti A, Marzetti F. Surgical management of parapharyngeal space tumours: results of 10-year follow-up. Acta Otorhinolaryngol Ital. 2009;29(1):10-5.
39. van Hees T, van Weert S, Witte B, Rene Leemans C. Tumors of the parapharyngeal space: the VU University Medical Center experience over a 20-year period. Eur Arch Otorhinolaryngol. 2018;275(4):967-72.
40. Kucur C, Durmus K, Teknos TN, Ozer E. How often parapharyngeal space is encountered in TORS oropharynx cancer resection. Eur Arch Otorhinolaryngol. 2015;272(9):2521-6.
41. Lauretano AM, Li KK, Caradonna DS, Khosta RK, Fried MP. Anatomic location of the tongue base neurovascular bundle. Laryngoscope. 1997;107(8):1057-9.
42. Gross ND, Holsinger FC, Magnuson JS, Duvvuri U, Genden EM, Ghanem TA, et al. Robotics in otolaryngology and head and neck surgery: Recommendations for training and credentialing: A report of the 2015 AHNS education committee, AAO-HNS robotic task force and AAO-HNS sleep disorders committee. Head Neck. 2016;38 Suppl 1:E151-8.
43. Krishnan G, Mintz J, Foreman A, Hodge JC, Krishnan S. The acceptance and adoption of transoral robotic surgery in Australia and New Zealand. J Robot Surg. 2018. doi: 10.1007/s11701-018-0856-8

44. Richmon JD, Quon H, Gourin CG. The effect of transoral robotic surgery on short-term outcomes and cost of care after oropharyngeal cancer surgery. Laryngoscope. 2014;124(1):165-71.

45. Motz K, Chang HY, Quon H, Richmon J, Eisele DW, Gourin CG. Association of Transoral Robotic Surgery With Short-term and Long-term Outcomes and Costs of Care in Oropharyngeal Cancer Surgery. JAMA otolaryngology-- head & neck surgery. 2017;143(6):580-8.

46. Witschi E. Arrey & Tables (Witschi & Streeter) Washington DC: Federation of American Societies for Experimental Biology; 1962.

47. Sadler TW. Langman's Medical Embryology. 12th ed. Chapter 17. Philadelphia: Lippincott Williams & Wilkins 2012. p. 260-286.

48. Prades JM, Gavid M, Asanau A, Timoshenko AP, Richard C, Martin CH. Surgical anatomy of the styloid muscles and the extracranial glossopharyngeal nerve. Surg Radiol Anat. 2014;36(2):141-6.

49. Ozgur Z, Celik S, Govsa F, Aktug H, Ozgur T. A study of the course of the internal carotid artery in the parapharyngeal space and its clinical importance. Eur Arch Otorhinolaryngol. 2007;264(12):1483-9.

50. Cairney J. Tortuosity of the Cervical Segment of the Internal Carotid Artery. J Anat. 1924;59(Pt 1):87-96.

51. Ricciardelli E, Hillel AD, Schwartz AN. Aberrant carotid artery. Presentation in the near midline pharynx. Arch Otolaryngol Head Neck Surg. 1989;115(4):519-22.

52. McMinn RMH. Last's Anatomy Regional and Applied 9th ed. Chapter 6. London: Churchill Livingstone 1998. p. 421-575.

53. Yarlagadda BB, Grillone, G. A. . Anatomic Considerations in Transoral Robotic Surgery In: Grillone GA, Scharukh, J. , editor. Robotic Surgery of the Head and Neck : A Comprehensive Guide, New York Springer 2014. p. 13-27.

54. Dallan I, Seccia V, Muscatello L, Lenzi R, Castelnuovo P, Bignami M, et al. Transoral endoscopic anatomy of the parapharyngeal space: a step-by-step logical approach with surgical considerations. Head Neck. 2011;33(4):557-61.

55. Gun R, Durmus K, Kucur C, Carrau RL, Ozer E. Transoral Surgical Anatomy and Clinical Considerations of Lateral Oropharyngeal Wall, Parapharyngeal Space, and Tongue Base. Otolaryngol Head Neck Surg. 2016;154(3):480-5.

56. Rassekh CH, Weinstein GS, Loevner LA, O'Malley BW, Jr. Transoral robotic surgery for prestyloid parapharyngeal space masses. Operative Techniques in Otolaryngology-Head and Neck Surgery. 2013;24(2):99-105.
57. Ansarin M, Tagliabue M, Chu F, Zorzi S, Proh M, Preda L. Transoral robotic surgery in retrostyloid parapharyngeal space schwannomas. Case Rep Otolaryngol. 2014;2014:296025.
58. Ohtsuka K, Tomita H, Murakami G. Anatomy of the tonsillar bed: topographical relationship between the palatine tonsil and the lingual branch of the glossopharyngeal nerve. Acta Otolaryngol Suppl. 2002(546):99-109.
59. Lim CM, Mehta V, Chai R, Pinheiro CN, Rath T, Snyderman C, et al. Transoral anatomy of the tonsillar fossa and lateral pharyngeal wall: anatomic dissection with radiographic and clinical correlation. Laryngoscope. 2013;123(12):3021-5.
60. Wang C, Kundaria S, Fernandez-Miranda J, Duvvuri U. A description of the anatomy of the glossopharyngeal nerve as encountered in transoral surgery. Laryngoscope. 2016.
61. Dallan I, Seccia V, Faggioni L, Castelnuovo P, Montevecchi F, Casani AP, et al. Anatomical landmarks for transoral robotic tongue base surgery: comparison between endoscopic, external and radiological perspectives. Surg Radiol Anat. 2013;35(1):3-10.
62. Pfeiffer J, Ridder GJ. A clinical classification system for aberrant internal carotid arteries. Laryngoscope. 2008;118(11):1931-6.
63. Pfeiffer J, Becker C, Ridder GJ. Aberrant extracranial internal carotid arteries: New insights, implications, and demand for a clinical grading system. Head Neck. 2016;38 Suppl 1:E687-93.
64. Weibel J, Fields WS. Tortuosity, coiling, and kinking of the internal carotid artery. Ii. Relationship of morphological variation to cerebrovascular insufficiency. Neurology. 1965;15:462-8
65. Weibel J, Fields WS. Tortuosity, coiling, and kinking of the internal carotid artery. I. Etiology and radiographic anatomy. Neurology. 1965;15:7-18.
66. Deutsch MD, Kriss VM, Willging JP. Distance between the tonsillar fossa and internal carotid artery in children. Arch Otolaryngol Head Neck Surg. 1995;121(12):1410-2.
67. Wang C, Kundaria S, Fernandez-Miranda J, Duvvuri U. A description of arterial variants in the transoral approach to the parapharyngeal space. Clin Anat. 2014;27(7):1016-22.

68. Fagan J. Open Access Atlas of Otolaryngology, Head & Neck Operative Surgery Cape Town 2016. Available from: http://www.entdev.uct.ac.za/guides/open-access-atlas-of-otolaryngology-head-neck-operative-surgery/.
69. Cohen DS, Low GM, Melkane AE, Mutchnick SA, Waxman JA, Patel S, et al. Establishing a danger zone: An anatomic study of the lingual artery in base of tongue surgery. Laryngoscope. 2016.
70. Moore EJ, Janus J, Kasperbauer J. Transoral robotic surgery of the oropharynx: Clinical and anatomic considerations. Clin Anat. 2012;25(1):135-41.
71. Chan JY, Tsang RK, Eisele DW, Richmon JD. Transoral robotic surgery of the parapharyngeal space: a case series and systematic review. Head Neck. 2015;37(2):293-8.
72. Boyce BJ, Curry JM, Luginbuhl A, Cognetti DM. Transoral robotic approach to parapharyngeal space tumors: Case series and technical limitations. Laryngoscope. 2016;126(8):1776-82.
73. Duek I, Amit M, Sviri GE, Gil Z. Combined endoscopic transcervical-transoral robotic approach for resection of parapharyngeal space tumors. 2017(1097-0347 (Electronic)).
74. Pollei TR, Hinni ML, Moore EJ, et al. ANalysis of postoperative bleeding and risk factors in transoral surgery of the oropharynx. JAMA Otolaryngology–Head & Neck Surgery. 2013;139(11):1212-8.
75. Son EL, Underbrink MP, Qiu S, Resto VA. The surgical plane for lingual tonsillectomy: an anatomic study. J Otolaryngol Head Neck Surg. 2016;45:22.
76. Miller SC, Nguyen SA, Ong AA, Gillespie MB. Transoral robotic base of tongue reduction for obstructive sleep apnea: A systematic review and meta-analysis. Laryngoscope. 2017;127(1):258-65.
77. Gudis D, Newman JG, Leahy K. Transoral Robotic Surgery: A Novel Technique to Treat Eagle Syndrome. 2011. p. P157-P.
78. Paraskevas GK, Raikos A, Lazos LM, Kitsoulis P. Unilateral elongated styloid process: a case report. Cases journal. 2009;2:9135.
79. Won SY. Anatomical considerations of the superior thyroid artery: its origins, variations, and position relative to the hyoid bone and thyroid cartilage. Anat Cell Biol. 2016;49(2):138-42.

80. Mata JR, Mata FR, Souza MC, Nishijo H, Ferreira TA. Arrangement and prevalence of branches in the external carotid artery in humans. Ital J Anat Embryol. 2012;117(2):65-74.

81. Kamil RJ, Gonik NJ, Lee JS, Shifteh K, Smith RV. Transoral resection of stylopharyngeus calcification: a unique manifestation of a stylohyoid complex syndrome. Ann Otol Rhinol Laryngol. 2015;124(2):158-61.

82. Nasman A, Attner P, Hammarstedt L, Du J, Eriksson M, Giraud G, et al. Incidence of human papillomavirus (HPV) positive tonsillar carcinoma in Stockholm, Sweden: an epidemic of viral-induced carcinoma? Int J Cancer. 2009;125(2):362-6.

83. Gillison ML, Broutian T, Pickard RK, Tong ZY, Xiao W, Kahle L, et al. Prevalence of oral HPV infection in the United States, 2009-2010. JAMA : the journal of the American Medical Association. 2012;307(7):693-703.

84. Kim GG, Zanation AM. Transoral robotic surgery to resect skull base tumors via transpalatal and lateral pharyngeal approaches. Laryngoscope. 2012;122(7):1575-8

85. Carrau RL, Prevedello DM, de Lara D, Durmus K, Ozer E. Combined transoral robotic surgery and endoscopic endonasal approach for the resection of extensive malignancies of the skull base. Head Neck. 2013;35(11):E351-8.

Appendix 1

A research oral presentation related to the current study presented by the author

Stylopharyngeus and styloglossus muscles as key anatomical landmarks for transoral robotic surgery of the parapharyngeal space. Australian Society of Otolaryngology Head and Neck Surgery 68th Annual Scientific Meeting, Perth, Western Australia, Australia. 9th to 11th March 2018.

Aims: To explore the utility of the stylopharyngeus muscle (SPM) and styloglossus muscle (SGM) as anatomical landmarks for transoral robotic surgery of the parapharyngeal space (PPS). To measure distances from the midpoints of SPM and SGM as a reference point to select PPS arteries.
Methodology: Thirteen formalin fixed cadaveric head and neck specimens were dissected on both sides with a surgical microscope. The specimens were first dissected coronally to gain access to the pharynx and parapharyngeal spaces (PPS). The SPM and SGM was dissected on its entirety. The relationship of the midpoint of the SPM and SGM relative to the internal carotid artery (ICA), external carotid artery (ECA), lingual artery (LA) and facial artery (FA) was observed.
Results: The SPM distal attachment was found at the superior and middle constrictor junction. This region corresponded to the tonsillar fossa. The glossopharyngeal nerve was found on the posterior-inferior aspect of SPM. The distal attachments of SPM and SGM were supplied by braches of the FA and LA. The ICA was 2.1mm and 6.8mm from the SPM and SGM midpoints, respectively. FA found inferiorly at 19.5mm and 14.6mm from the SPM and SGM midpoints, respectively. Similarly the LA was found further inferior to these reference points.
Conclusion: The ICA is closely associated with the SPM midpoint. The FA and LA are found inferior to the SPM and SGM midpoints. These two muscles act as a barrier between the relatively safe prestyloid space and the poststyloid place which contain the key vascular structures of the PPS. The distal attachments of these muscles represent a highly vascular area. The SPM and SGM can be a useful anatomical landmark for orientation and estimation of depth to key neurovasculature within the PPS during TORS.

Appendix 2

Research poster presentations related to the current study presented by the author

Pasan Waidyasekara, Athanasios Raikos, Allan Stirling, Peter Jones, Samuel Dowthwaite. *An anatomical correlations and morphometric study between the oropharyngeal muscosa, the lateral surface of the pharyngeal constrictor muscle and key parapharyngeal space neurovasculature for transoral robotic lateral oropharyngectomy.* Australian Society of Otolaryngology Head and Neck Surgery 68th Annual Scientific Meeting, Perth, Western Australia, Australia. 9th to 11th March 2018.

Aim: To deduce correlations and provide depth measurements to key parapharyngeal space (PPS) neurovasculature from the oropharyngeal mucosa (OPM) and the lateral surface of the pharyngeal constrictor muscle (LSPCM) to facilitate transoral robotic lateral oropharyngectomy.

Methodology: Thirteen formalin fixed cadaveric head and neck specimens were dissected on both side with a surgical microscope. The specimens were first dissected coronally to gain access to the pharynx and parapharyngeal space (PPS). Using a calliper, measurements were made from OPM and LSPCM to key anatomical structures on the axial plane. For each measurement the mean distance was determined across all dissected sides.

Results: The facial artery (FA) closest distance to the LSPCM was 6.7mm. This position corresponded medially to the tonsillar fossa. The hypoglossal nerve (CNXII) was in close proximity to the LSPCM at the inferior PPS. The distance from the OPM to CNXII at this location was 9.1mm. The lingual artery (LA) origin at the external carotid artery (ECA) was 14.44mm and 11.6mm from the OPM and LSPCM, respectively. The SPM and SGM midpoints were 16.6mm and 17.3mm from the OPM and LSPCM, respectively.

Conclusion: The mean distance measurements from the OPM and LSCM are useful for depth approximation and anticipation of PPS neurovasculature during transoral robotic lateral oropharyngectomy. The FA and its branches can be anticipated lateral to the tonsillar fossa. The CNXII is at risk of injury during oropharynx resections at the lateral pharyngeal wall and valleculla. The depth to the CNXII measurements in the study may aid to avoid injury.

Pasan Waidyasekara, Athanasios Raikos, Allan Stirling, Peter Jones, Samuel Dowthwaite. *An anatomical study correlating the tonsillar fossa with the adjacent parapharyngeal space for transoral robotic surgery.* Australian Society of Otolaryngology Head and Neck Surgery 68th Annual Scientific Meeting, Perth, Western Australia, Australia. 9th to 11th March 2018.

Aim: To improve our understanding of the inside-to-outside anatomy for transoral robotic surgery (TORS) radical tonsillectomy through cadaveric dissection and morphometric measurements.
Methodology: Thirteen formalin fixed cadaveric head and neck specimens were dissected on both sides with a surgical microscope. The specimens were first dissected coronally to gain access to the pharynx and parapharyngeal spaces (PPS). Within the PPS the internal carotid artery (ICA) was dissected. Similarly the external carotid artery (ECA) and its branches were dissected. Corrolations were made with the tonsillar fossa. Stylopharyngeus muscle (SPM) and styloglossus muscle (SGM) was dissected and its midpoints was used as a reference point. Distance measurements were made from the tonsillar fossa apex (TFA) to the aforementioned PPS structures with a calliper.
Results: The ICA was a mean distance of 16.1mm from the TFA. ICA tortuosity was present in 10 sides (38%). The tortuosity of ICA diverged the ascending pharyngeal artery (APA) medially close to the TFA in some cases. The APA was 16.3mm from the TFA. The ECA was a mean distance of 20.3mm from the TFA. The ascending palatine arterty (aPA) branched off the facial artery in 81% and was 10.1mm from the TFA. The midpoints of the SPM and SGM correlated to the tonsillar fossa region on the axial plane. The SPM and SGM midpoints was a mean distance of 17.6 and 17.5mm from the TFA, respectively. The aPA was the main artery in the space between these two muscles.
Conclusion: The anatomical correlations and distance measurements made in our study from the TFA are useful for safe dissection during TORS radical tonsillectomy. The ICA tortuosity should alert the surgeon for possible close encounter of ICA and APA at TFA. Careful attention to the aPA is warranted when dissecting and transecting SPM and SPM.

Pasan Waidyasekara, Athanasios Raikos, Allan Stirling, Peter Jones, Samuel Dowthwaite. *An anatomical study of the parapharyngeal space adjacent the base of tongue to facilitate transoral robotic surgery*. Australian Society of Otolaryngology Head and Neck Surgery 68th Annual Scientific Meeting, Perth, Western Australia, Australia. 9th to 11th March 2018.

Aim: To provide anatomical correlations and proximity measurements between the base of tongue (BOT) region and the adjacent parapharyngeal space neurovasculature for transoral robotic BOT resections.

Methodology: Thirteen formalin fixed cadaveric head and neck specimens were dissected on both sides with a surgical microscope. The specimens were first dissected coronally to gain access to the pharynx and parapharyngeal spaces (PPS). Anatomical corralations and distance measurements were made from the following landmarks: foramen cecum of BOT, vallecula and greater cornu of hyoid (GCH) bone's posterior end. At the inferior end of the PPS, the external carotid artery (ECA), the lingual artery (LA), facial artery (FA), Lingual nerve (LN), glossopharyngeal nerve (CNIX), and hypoglossal nerve (CNXII) was dissected for correlation and mean distance measurements from the landmarks.

Results: The PPS portion of LA and FA was 21mm and 27.4mm from the foramen cecum of BOT, respectively. From the midline valleculla LA and FA was 23.6mm and 35.4mm, respectively. The point where CNIX pierce the constrictor muscle correlated to the level of the foramen cecum of BOT. A linguofacial trunk was present in 5 sides (21%). The LA exit point at the PPS correlated to the pharyngoepiglottic fold. The LA was 3.5mm superior to the GCH posterior end.

Conclusion: The PPS portion of LA and FA position can be estimated during TORS of BOT from the mean distance measurements and oropharyngeal correlations provided in this study. Thus risk of neurovascular complications can be minimised when operating at the valleculla and lateral pharyngeal wall.

Pasan Waidyasekara, Athanasios Raikos, Allan Stirling, Peter Jones, Samuel Dowthwaite. *Parapharyngeal Space Anatomy via the MidSagittal View: Layer by Layer Pictorial Essay and Potential Implications in TORS Approaches.* Australian Society of Otolaryngology Head and Neck Surgery 66th Annual Scientific Meeting, Melbourne, Australia. 6th to 8th March 2016.

Background: The parapharyngeal space is an area of the head and neck with immense clinical and surgical importance. It is bound superiorly by the skull base, inferiorly by the greater cornu of the hyoid bone; anteriorly by the pterygomandibular raphe; posteriorly by the carotid sheath; medially by the buccopharyngeal fascia; and laterally by the mandibular ramus, deep lobe of the parotid gland and the medial pterygoid muscle. The parapharyngeal space is frequently entered when resecting neoplasms of the tongue base, tonsil and parapharyngeal space. It has particular relevance with regards to operative planning for trans-oral robotic surgical cases. We aim to describe the topographical anatomy of the parapharyngeal space from a relatively novel vantage point.

Method: For the purpose of the study, we have dissected four hemisected cadaveric heads from the medial aspect in a layer-by-layer approach. First the pharyngeal mucosa, then the superior and middle constrictor muscles were dissected. Next the parapharyngeal adipose tissue were cleared. Photographs were taken before and after each step of dissection.

Results: The branches of the external carotid were identified. The course of the glossopharyngeal, vagus and hypoglossal nerves were recorded. These had a close relationship to the styloglossus and stylopharyngeus muscles.

Conclusions: The midsagittal specimens are suitable for further study of the parapharyngeal space. The styloglossus and stylopharyngeus muscles are key landmarks for describing the topographical anatomy with respect to the branches of the external carotid artery and the lower cranial nerves.